# Bachelorarbeit

Tobias Kathke

## Methodische Voruntersuchungen zur Vibroakustischen Simulation von Windenergieanlagen mit der Finite-Elemente-Methode (FEM)

# Tobias Kathke

# Methodische Voruntersuchungen zur Vibroakustischen Simulation von Windenergieanlagen mit der Finite-Elemente-Methode (FEM)

Bachelor-/Masterarbeit eingereicht im Rahmen der Bachelorprüfung

im Studiengang Maschinenbau/Entwicklung und Konstruktion
am Department Maschinenbau und Produktion
der Fakultät Technik und Informatik
der Hochschule für Angewandte Wissenschaften Hamburg

Erstprüfer/in: Prof. Dr.-Ing. habil. Frank Ihlenburg
Zweitprüfer/in: Prof. Dr.-Ing. Andreas Baumgart

Abgabedatum: 30.09.2016

# Zusammenfassung

**Tobias Kathke**

**Thema der Bachelorthesis**
Methodische Voruntersuchungen zur Vibroakustischen Simulation von Windenergieanlagen mit der Finite-Elemente-Methode (FEM)

**Stichworte**
Fluid-Struktur-Kopplung, Vibro-Akustik, Schall, Finite-Elemente-Methode, Abstrahlung, Impedanz, Robin-Randbedingung

**Kurzzusammenfassung**
In dieser Arbeit werden methodische Voruntersuchungen zur vibro-akustischen Simulation einer Windenergieanlage mittels der Finite-Elemente-Methode anhand einfacher Prinzipmodelle durchgeführt. Der Schwerpunkt liegt dabei auf der Umsetzung der Fluid-Struktur-Kopplung zwischen den vibrierenden Bauteilen des Antriebsstrangs und dem akustischen Umgebungsmedium (Luft), sowie der Untersuchung der akustischen Randbedingungen und dem Einfluss konstruktiver Maßnahmen auf den Schalldruck im akustischen Fluid.

**Tobias Kathke**

**Title of the paper**
Methodological Studies in Vibro-acoustic Simulation of Wind Turbines with the Finite Element Analysis (FEA)

**Keywords**
Fluid-Structure Interaction, Vibro-Acoustics, Sound, Finite Element Analysis, Radiation, Impedance, Robin boundary condition

**Abstract**
In this line of work methodological studies in vibro-acoustic simulations of a wind turbine are held on the basis of simple principle models using the finite element analysis. The emphasis lies on the implementation of the fluid-structure interaction between the vibrating parts of the power train and the surrounding acoustical medium (air), as well as the analysis of the acoustic boundary conditions and the influence of constructive modifications on the sound pressure within the acoustic fluid.

**Widmung**

Diese Arbeit widme ich meiner verstorbenen Großmutter Ingrid Kathke, die mir das Studium, so wie ich es erleben durfte, ermöglicht hat.

**Danksagung**

Ein herzlicher Dank geht an meinen Betreuer Prof. Dr.-Ing. habil. Frank Ihlenburg für seinen stetigen Optimismus und seine nicht abreißende Begeisterung diesem Projekt gegenüber, die mir über so manchen Totpunkt hinweghalf. Durch seine Anregungen, die ich gerne aufgenommen habe, umfasst die Arbeit gewiss einige Seiten mehr, die der Struktur und dem Inhalt zugutegekommen sind.

# Contents

# List of Tables

# List of Figures

A

## List of Abbreviations

BEM          Boundary Element Method

DOF          Degree of Freedom

FE           Finite Element

FEA          Finite Element Analysis

FEM          Finite Element Method

PDE          Partial Differential Equation

PML          Perfectly Matched Layer

RAM          Random Access Memory

RMS          Root Mean Square

SPL          Sound Pressure Level

SPL(A)       A-weighted Sound Pressure Level

## Nomenclature

| | | |
|---|---|---|
| $a$ | Acceleration $[m \cdot s^{-2}]$ | |
| $A$ | Area $[m]$ | |
| $A_n$ | Normal admittance $[m^3 \cdot N^{-1} \cdot s^{-1}]$ | |
| $B$ | Bulk modulus $[N \cdot m^2]$ | |
| $B'$ | Bulk modulus of a plate $[N \cdot m]$ | |
| $c$ | Speed of sound $[m \cdot s^{-1}]$ | |
| $c_B$ | Bending wave speed of sound $[m \cdot s^{-1}]$ | |
| $c_j$ | Damping of mode $j$ $[m \cdot s^{-1}]$ | |
| $c_L$ | Longitudinal speed of sound $[m \cdot s^{-1}]$ | |
| $C$ | Damping matrix $[kg \cdot s^{-1}]$ | |
| $C_s$ | Structure damping matrix $[kg \cdot s^{-1}]$ | |
| $C_f$ | Fluid damping matrix $[kg \cdot s^{-1}]$ | |
| $E$ | Young's modulus $[Pa]$ | |
| $f$ | Frequency $[Hz]$ | |
| $f$ | Volume load $[N \cdot m^{-3}]$ | |
| $F$ | Force $[N]$ | |
| $F_f$ | Applied force in fluid $[N]$ | |
| $F_J$ | Modal force $[N]$ | |
| $F_s$ | Applied force on structure $[N]$ | |
| $G$ | Flexibility matrix $[m \cdot N^{-1}]$ | |
| $\tilde{G}$ | Residual flexibility matrix $[m \cdot N^{-1}]$ | |
| $G_s$ | Interpolation Matrix $[m^2]$ | |
| $h$ | Thickness $[m]$ | |
| $h_\lambda$ | Elements per wave length $[-]$ | |
| $i$ | Mode [-] | |
| $I$ | Area moment of inertia $[m^4]$ | |
| $j$ | Mode [-] | |
| $k$ | Wavenumber $[m^{-1}]$ | |
| $k_B$ | Bending wavenumber $[m^{-1}]$ | |
| $k_j$ | Stiffness of mode $j$ $[N \cdot m^{-1}]$ | |
| $K$ | Stiffness matrix $[N \cdot m^{-1}]$ | |
| $K_s$ | Structure stiffness matrix $[N \cdot m^{-1}]$ | |
| $K_f$ | Fluid stiffness matrix $[N \cdot m^{-1}]$ | |

| | |
|---|---|
| $L_i$ | Sound pressure level $[dB]$ |
| $L_t$ | Total sound pressure level $[dB]$ |
| $L(A)$ | A-weighted sound pressure level $[dB]$ |
| $m$ | Number of modes $[-]$ |
| $m$ | Mass $[kg]$ |
| $m'$ | Mass per unit length $[kg \cdot m^{-1}]$ |
| $m''$ | Area mass $[kg \cdot m^{-2}]$ |
| $m_j$ | Mass of mode $j$ $[kg]$ |
| $M$ | Molar matrix $[kg]$ |
| $M_{mol}$ | Molar mass $[kg \cdot mol^{-1}]$ |
| $M_s$ | Structure mass matrix $[kg]$ |
| $M_f$ | Fluid mass matrix $[kg]$ |
| $n$ | Normal vector $[-]$ |
| $n$ | Total number of modes $[-]$ |
| $N$ | Number of modes $[-]$ |
| $n_f$ | Normal vector fluid $[-]$ |
| $n_f$ | Number of nodes of the fluid domain $[-]$ |
| $n_s$ | Normal vector structure $[-]$ |
| $n_s$ | Number of nodes of the solid domain $[-]$ |
| $p$ | Acoustic pressure $[Pa]$ |
| $\dot{p}$ | First derivative of acoustic pressure $[Pa \cdot s^{-1}]$ |
| $\ddot{p}$ | Second derivative of acoustic pressure $[Pa \cdot s^{-2}]$ |
| $p_{absorbed}$ | Absorbed acoustic pressure $[Pa]$ |
| $p_{incident}$ | Incident acoustic pressure $[Pa]$ |
| $p_0$ | Static pressure $[Pa]$ |
| $p_{reflected}$ | Reflected acoustic pressure $[Pa]$ |
| $p_t$ | Total pressure $[Pa]$ |
| $p_\Gamma$ | Acoustic pressure at boundary $\Gamma$ $[Pa]$ |
| $q$ | Transformation variable of modal pressure $[Pa]$ |
| $\dot{q}$ | First derivative of the transformation variable of modal pressure $[Pa \cdot s^{-1}]$ |
| r | Radius $[m]$ |
| $r_\Gamma$ | Reflection ratio $[-]$ |
| $R$ | Coupling matrix $[N \cdot m^{-1}]$ |
| $R$ | Gas constant $[J \cdot mol^{-1} \cdot K^{-1}]$ |
| $R$ | Residual vector matrix $[m]$ |
| $R$ | Radius $[m]$ |

| | | |
|---|---|---|
| $S$ | Surface area $[m^2]$ | |
| $t$ | Time $[s]$ | |
| $t$ | Surface load $[Pa]$ | |
| $T$ | Period $[s]$ | |
| $T_s$ | Interpolation matrix $[m^3]$ | |
| $T_0$ | Static temperature $[K]$ | |
| $u$ | Displacement $[m]$ | |
| $\dot{u}$ | Velocity $[m \cdot s^{-1}]$ | |
| $\ddot{u}$ | Acceleration $[m \cdot s^{-2}]$ | |
| $u_f$ | Displacement of fluid $[m]$ | |
| $u_i$ | Knot displacement $[m]$ | |
| $u_n$ | Normal displacement $[m]$ | |
| $u_s$ | Displacement of the structure $[m]$ | |
| $v$ | Acoustic particle velocity $[m \cdot s^{-1}]$ | |
| $v_n$ | Normal acoustic particle velocity at boundary $\Gamma$ $[m \cdot s^{-1}]$ | |
| $v_{n,f}$ | Normal acoustic fluid particle velocity $[m \cdot s^{-1}]$ | |
| $v_{n,s}$ | Normal acoustic particle velocity of the structure surface $[m \cdot s^{-1}]$ | |
| $v_0$ | Static particle velocity $[m \cdot s^{-1}]$ | |
| $v_t$ | Total particle velocity $[m \cdot s^{-1}]$ | |
| $v_\Gamma$ | Acoustic particle velocity at boundary $\Gamma$ $[m \cdot s^{-1}]$ | |
| $V$ | Volume $[m^3]$ | |
| $w$ | Test function $[Pa]$ | |
| $x$ | Mode contribution $[-]$ | |
| $x_H$ | Higher mode contribution $[-]$ | |
| $x_L$ | Lower mode contribution $[-]$ | |
| $y_i$ | Modal knot displacement $[m]$ | |
| $\dot{y}_i$ | Modal knot velocity $[m \cdot s^{-1}]$ | |
| $\ddot{y}_i$ | Modal knot acceleration $[m \cdot s^{-2}]$ | |
| $Z$ | Acoustic impedance $[Ns \cdot m^{-3}]$ | |
| $Z_n$ | Normal acoustic impedance $[Ns \cdot m^{-3}]$ | |
| $Z_n$ | Specific acoustic impedance $[Ns \cdot m^{-3}]$ | |
| $\alpha$ | Parameter for constant damping $[s^{-1}]$ | |
| $\beta$ | Parameter for constant damping $[s]$ | |
| $\varepsilon_v$ | Elastic strain $[m]$ | |
| $\kappa$ | Heat capacity ratio $[-]$ | |
| $\lambda$ | Wave length $[m]$ | |

| | | |
|---|---|---|
| $\lambda_B$ | Bending wave length $[m]$ | |
| $\mu$ | Poisson's ratio $[-]$ | |
| $\rho$ | Acoustic density $[kg \cdot m^{-3}]$ | |
| $\rho_f$ | Static density of acoustic fluid $[kg \cdot m^{-3}]$ | |
| $\rho_0$ | Static density $[kg \cdot m^{-3}]$ | |
| $\rho_t$ | Total density $[kg \cdot m^{-3}]$ | |
| $\omega$ | Angular speed $[s^{-1}]$ | |
| $\omega_j$ | Angular speed of mode $j$ $[s^{-1}]$ | |
| $\Gamma$ | Boundary $[m^2]$ | |
| $\Gamma_a$ | Boundary with absorbing elements $[m^2]$ | |
| $\Gamma_D$ | Dirichlet boundary $[m^2]$ | |
| $\Gamma_i$ | Impedance boundary $[m^2]$ | |
| $\Gamma_n$ | Neumann boundary $[m^2]$ | |
| $\Gamma_r$ | Radiation boundary $[m^2]$ | |
| $\Gamma_R$ | Robin boundary $[m^2]$ | |
| $\Delta_i$ | Attenuation factor $[dB]$ | |
| $\Phi_i$ | Test function $[-]$ | |
| $\Phi_j$ | Test function $[-]$ | |
| $\Phi_j$ | Mode shape $[-]$ | |
| $\Phi_j^L$ | Left mode shape $[-]$ | |
| $\Omega$ | Forcing frequency $[Hz]$ | |
| $\Omega$ | Acoustic domain $[m^3]$ | |
| $\Omega_f$ | Fluid acoustic domain $[m^3]$ | |
| $\Omega_{max}$ | Highest forcing frequency $[Hz]$ | |
| $\Omega_{min}$ | Lowest forcing frequency $[Hz]$ | |
| $\Omega_s$ | Structure acoustic domain $[m^3]$ | |

# 1    Motivation

Wind turbines are a common sight on Northern Germany's landscape, especially in East Frisia along the coastline due to the rather flat land and strong winds. A cycling tour from the town of Norden to the Jade Bight showed in a spectacular kind of way how disturbing, or more precisely noisy, these wind turbines can be. Although they were never too loud, they are indeed accompanying every sound in the region by a monotone noise. For this reason, every improvement on the sound radiation is welcome and could help to establish wind turbines even in underdeveloped regions like the south of Germany.

Because of my studies at the University of Portsmouth on the south coast of England and the circumstance that I never wrote an academic work and accordingly any other kind of important paper in English, I used the opportunity to train my language skills and write this thesis in English instead of German.

## 1.1    Background of the thesis

This thesis is a pre-work for the vibro-acoustic subproject within the upcoming research project X-Energy; a cooperation between the University of Applied Sciences HAW Hamburg and the wind turbine manufacturer Suzlon Ltd.

Since previous approaches to reduce the acoustic emissions of a wind turbine are primarily related to the aero-acoustic optimization of the rotor blades, the research of power train-related noise emission by means of vibro-acoustics is an almost unexplored territory [13]. Measured frequency spectra reveals a reason for this new direction of research, as a majority of corresponding frequencies are coming from the driveline components (generator and gearbox). The rotor blades are just the end of the acoustic path of the noise source via the drive shaft and hub.

For this reason, the sound radiating parts of the power train shall be analysed and improved regarding their acoustic emissions with the aid of the finite elements analysis (FEA). During the research project X-Energy a detailed vibro-acoustical model of the power train will be created, enhanced and later validated with a large-scale plant.

## 1.2    Tasks and objectives

The social acceptance of wind energy turbines also depends on their acoustic emissions. The vibro-acoustic simulation provides a helpful tool to analyse and influence these emissions during the development and design phase of new wind turbines. Therefore, the fluid-structure interaction (FSI) of the vibrating parts of the power train and the surrounding acoustic medium, e.g. air, plays a dominant role and needs to be realised.

In this line of work methodological studies to this objective are being executed with the use of the finite element software ANSYS.  In a first step an appropriate verification model from the literature is being recreated in the simulation in order to justify the acoustic radiation of the vibrating model. Afterward different solution methods and boundary conditions are tested in order to see their influence on the structure-acoustical system and its solution.

This is followed by a simple principle model for the fluid-structure interaction of the power train and the surrounding medium. A variation of mass, stiffness and damping is being applied in order to improve the acoustic radiation of the structure and its emission within the fluid by constructive modifications.

In a last step this model will be changed to resemble a more typical power train.

As results, the modal characteristics of the model (eigenmodes of the structure and fluid, influence of the fluid on structure modes, etc.) and the frequency responses of the structure and fluid are documented and analysed.

# 2 Theoretical Introduction

All acoustic problems have in common that they can be broken down into three sub-problems. That is to say excitation, dispersion and radiation. The excitation leads to the introduction of vibrational energy into a structure. The properties of the structure determine the dispersion of the wave and the transport of energy from the excitation source to the surroundings. The distribution of vibrational energy on a structure always causes the radiation of sound into the surrounding medium (e.g. air) [19].

Sound is a vibration that propagates as a typically audible mechanical wave of pressure $p$ and displacement $u$. While a technical fluid reacts only on changes of volume by changes in pressure, a solid also resists changes of its shape. Therefore, a separate description of airborne sound and structure-borne sound is needed. In the execution of this work sound is regarded as a time-harmonic vibration, as the considered acoustical sources behave also time-harmonic. Sound is normally characterized by a superposition of time-harmonic pure tones with different frequencies and amplitudes.

This section includes the theoretical fundamentals of sound excitation and its propagation in fluids and structures. It also describes the fluid-structure interaction as well as the boundary conditions needed for the analysis of the acoustic system, consisting of an acoustic medium and acoustic emission source. Finally, the analysis and solution methods and the acoustic output quantities are presented.

## 2.1 Airborne sound

Sound is characterized by small pressure fluctuations $p$ of the static pressure $p_0$ [21]. These fluctuations propagate through the medium, e.g. air, as sound waves and form the acoustic sound field. In fluids, sound propagates in longitudinal waves only, as shear strains cannot be sustained.

In the direction of propagation, the medium becomes denser and rarer. The changes in density $\rho$ and pressure require a periodic motion of fluid particles $v$ [21]. Therefore, the physical state of every point of the fluid volume can be characterized [16] by

$$p_t(x,t) = p_0 + p$$

$$\rho_t(x,t) = \rho_0 + \rho \qquad \qquad (\,2.1\,)$$

$$v_t(x,t) = v_0 + v$$

where $p, \rho, v$ describes the acoustic fluctuations, $p_0, \rho_0, v_0$ the static and $p_t, \rho_t, v_t$ the total value.

Due to very rapid temporal changes within the sound field it can be assumed that all sound processes underlie adiabatic behaviour, so that a sound field can be seen as a gas without thermal conduction [18]. Because of rather small changes of the dynamic components around the equilibrium point at their static components, the relationship between sound density and sound pressure can be linearised.

By considering the mass conservation

$$\delta\rho = -\rho_0\left(\frac{\delta V}{V_0}\right) \tag{2.2}$$

the relation between sound pressure and density can be described by the material law

$$p = \left(\frac{\partial p}{\partial\rho}\right)_0 \delta\rho = -(\kappa p_0)\left(\frac{\delta V}{V_0}\right) = -B\varepsilon_v = -B\,\mathrm{div}\,u \tag{2.3}$$

where $\kappa$ is the heat capacity ratio and $\left(\frac{\partial p}{\partial\rho}\right)_0$ describes the slope of the adiabatic curve, $B$ is bulk modulus and $\varepsilon_v$ is the elastic strain of the volume. Regarding a fluid volume element under external pressure in one direction
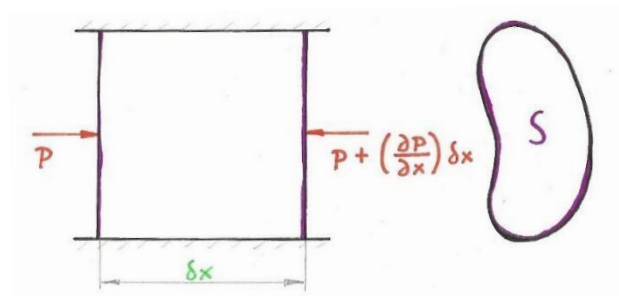


Figure 2.1: fluid element subject to a pressure gradient

the equilibrium results in

$$F = S\left[p - \left(p + \frac{\partial p}{\partial x}\delta x\right)\right] = -S\frac{\partial p}{\partial x}\delta x$$

$$F = ma$$

$$-S\frac{\partial p}{\partial x}\delta x = S\delta x\rho_0\frac{\partial v}{\partial t}$$

$$-\frac{\partial p}{\partial x} = \rho_0\frac{\partial v}{\partial t} \tag{2.4}$$

Expanded it to three directions results in the Euler equation

$$-\nabla p = \rho_0\frac{\partial v}{\partial t} \tag{2.5}$$

4

Combining equations ( 2.3 ) and ( 2.5 ) follows to the wave equation

$$\frac{\partial^2 p}{\partial x^2} + \frac{\partial^2 p}{\partial y^2} + \frac{\partial^2 p}{\partial z^2} = \left(\frac{\rho_0}{B}\right)\frac{\partial^2 p}{\partial t^2} \tag{2.6}$$

$$\Delta p = \frac{1}{c^2}\ddot{p} \tag{2.7}$$

The acoustic wave equation describes the acoustic response of the fluid. Planar waves represent one of the specific wave equation solutions for the one-dimensional wave propagation, spherical waves that for the three dimensional wave propagation.

The speed of sound $c$ is a constant which depends of the material and the absolute temperature. It describes the speed of propagation of the sound wave, whereas the particle velocity $v$ describes the movement of the particles during expansion and compression [18].

$$c = \sqrt{\frac{\rho_0}{B}} = \sqrt{\kappa\frac{R}{M_{mol}}T_0} \tag{2.8}$$

where $M_{mol}$ is the molar mass, $R$ is the gas constant and $T_0$ is the static temperature, e.g. room temperature in K. With the time-harmonic dependency of the sound pressure $p(x,t) = p(x)e^{-i\omega t}$ one gets the Helmholtz equation

$$\Delta p + k^2 p = 0 \tag{2.9}$$

where $k$ is the wave number. It describes the relationship between the circular frequency of the harmonic vibration and the speed of sound.

$$k = \frac{\omega}{c} \tag{2.10}$$

The wave length of the acoustic wave is

$$\lambda = \frac{2\pi}{k} = \frac{c}{f} \tag{2.11}$$

Figure 2.2 shows the relationship between the sound wave to the left and its progression through the sound field. The patterns of small particles at the lower right graph show regions of high and low density which correspond to high and low sound pressure. The upper right graph shows the spatial distribution of sound pressure for different points in time. The patterns are moving in course of time to the right. After the period $T$ the wave has moved by one wave length $\lambda$. The wave length is the distance between two antinodes in the distribution of sound pressure.
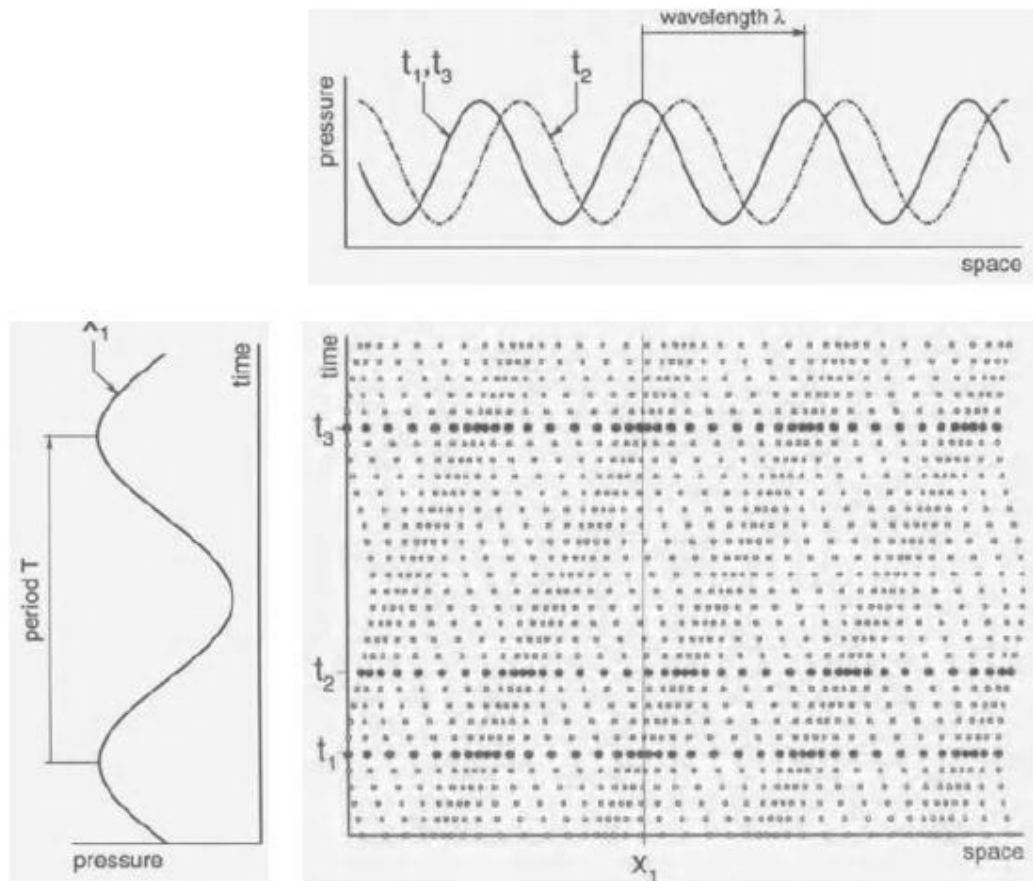
Figure 2.2: Illustration of sound wave, wave length and period [21]

## 2.2    Acoustic Boundary Conditions

To be able to find unique solutions of the Helmholtz equation ( 2.9 ) for a given domain $\Omega$ the boundary conditions at the border $\Gamma$ has to be known. There are three basic forms of natural constrains of the Helmholtz equation, namely the Dirichlet boundary condition, the Neumann boundary condition, and the impedance boundary condition.

This chapter describes the natural boundary conditions of the wave equation, as well as the acoustic boundary conditions used in FEM. By introducing the reflection at the border between two acoustic media, the boundary conditions can be differentiated between absorbing boundary conditions and reflecting boundary conditions. Figure 2.3 shows a general example of a fluid-structure interaction with different boundary conditions applied at the borders.
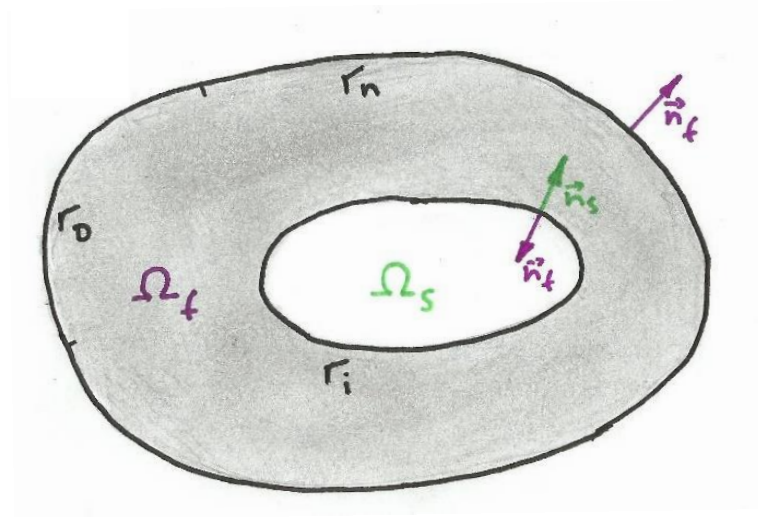
Figure 2.3: Fluid-Structure Interface with different boundary conditions

### 2.2.1 Sound-soft boundary (Dirichlet Boundary Condition)

The Dirichlet boundary or pressure boundary condition is a specification of the sound pressure $p$ at the border of the field area.

$$p = p_\Gamma \qquad \forall x: \in \Gamma_D \qquad\qquad (\,2.12\,)$$

The sound-soft boundary $p_\Gamma = 0$ is a special case of the Dirichlet boundary condition. It is used as an approximation of media transitions to an acoustic medium with much lower impedance, e.g. for a water basin covered by air [10].

### 2.2.2 Sound-hard boundary (Neumann Boundary Condition)

The Neumann boundary condition is the normal derivative of the sound pressure at the boundary. This corresponds to the specification of the normal component of the particle velocity $v_n$ at the border of the field area.

$$\nabla p \cdot n = \frac{\partial p}{\partial n} = -j\omega\rho_f v_n = \omega^2 \rho_f u_n \qquad\qquad \forall x: \in \Gamma_n \qquad\qquad (\,2.13\,)$$

where $u_n$ is the displacement in the normal direction. The sound-hard boundary $v_n = 0$ describes the natural boundary condition used in FEM (see ch. 3.1). It is a good approximation of a rigid boundary, such as a massive wall.

### 2.2.3 Robin Boundary Condition

For a plane wave the acoustic impedance $Z_n$ is defined by the relationship between the acoustic pressure and the normal component of the particle velocity. It is the resistance of an acoustic medium to the wave propagation.

$$Z_n = \frac{p}{v_n} \tag{2.14}$$

with the complex pressure amplitude $p = p_{incident} + p_{reflected}$. At fluid boundaries, the incident waves are partly absorbed and partly reflected depending on the relation between the specific acoustic impedances of the acoustic medium and the boundary. The reflection ratio $r_r$ is a technical measurable variable [10], which describes the ratio of reflected and incident acoustic pressure waves, it can be presented by the specific impedances of the regarded acoustic media at the boundary.

$$r_r = \frac{Z_2 - Z_1}{Z_2 + Z_1} = \frac{|p_r|}{|p_i|} \tag{2.15}$$

Sound-hard boundaries, such as rigid walls, have a reflection ratio $r_r = 1$, whereas open domains have a reflection ratio $r_r = 0$ and therefore no reflection at all. Unfortunately, the absence of reflection at open domains is only true when incoming waves are perpendicular to the surface of the boundary [14]. Figure 2.4 shows the reflection and absorption of an incoming wave at a wall with a rigid boundary as well as an open domain boundary. Depending on the size of the acoustic domain the reflection rate at the open domain boundary can be improved.
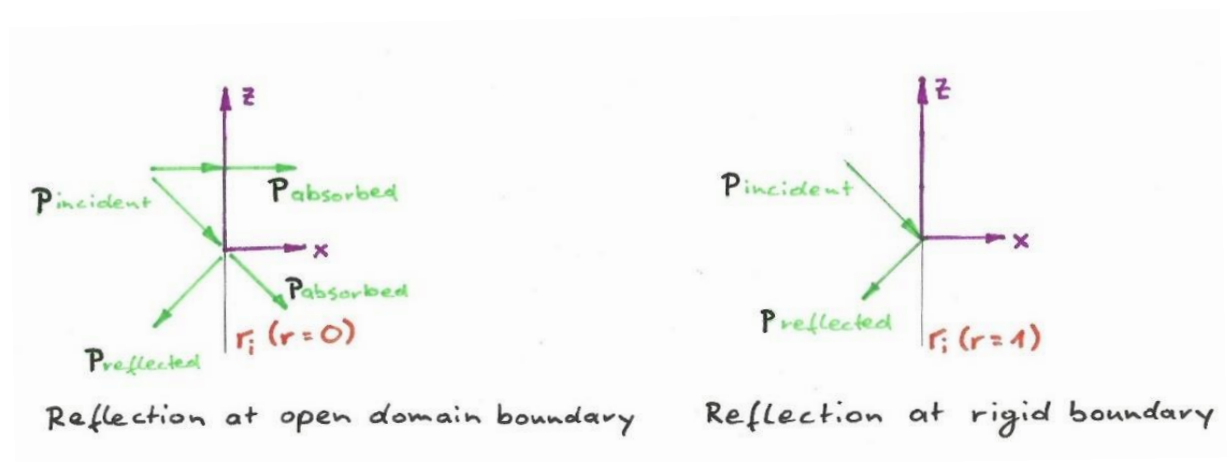


Figure 2.4: Transmission at a border with impedance boundary condition

In the far field pressure and particle velocity are in phase. The relationship can be expressed as

$$p = \rho_0 c v_n \qquad (2.16)$$

This leads to the characteristic sound impedance

$$Z_0 = \rho_0 c \qquad (2.17)$$

The admittance boundary is a special case of the Robin boundary condition, which is a weighted combination of the Dirichlet and Neumann boundary condition.

$$\nabla p \cdot n = \frac{\partial p}{\partial n} = -j\omega\rho_f\left(v_{n,f} - v_{n,s}\right) \qquad \forall x \in \Gamma_R \qquad (2.18)$$

with

$$v_{n,f} - v_{n,s} = A_n p = \frac{p}{Z_n} \qquad (2.19)$$

where $v_{n,f}$ is the normal velocity of the fluid particle on the boundary, $v_{n,s}$ is the normal velocity of the structure surface and $A_n$ is the normal admittance. Using the Euler equation ( 2.5 ) to change the particle velocity into pressure shows

$$\nabla p \cdot n = \frac{\partial p}{\partial n} = -j\omega\rho_f(A_n p) = -j\omega\rho_f\left(\frac{p}{Z_n}\right) = -\frac{\rho_0}{Z_n}\frac{\partial p}{\partial t} \qquad (2.20)$$

The density $\rho_0$ of the fluid can be replaced by the specific sound impedance of the fluid. This yields to the Robin boundary condition in terms of impedances.

$$\frac{\partial p}{\partial n} = -\frac{Z_0}{Z_n}\frac{1}{c}\frac{\partial p}{\partial t} = -\frac{1+r_r}{1-r_r}\frac{1}{c}\frac{\partial p}{\partial t} \qquad \forall x \in \Gamma_i \qquad (2.21)$$

Setting $Z_n = Z_0$ the radiation boundary condition [11] as a special case of the Robin Boundary Condition is

$$\frac{\partial p}{\partial n} = -\frac{1}{c}\frac{\partial p}{\partial t} \qquad \forall x \in \Gamma_r \qquad (2.22)$$

The radiation boundary is an open domain boundary and therefore shows no reflection at all, if the incident waves arrive in the normal direction to the boundary. At impedance boundaries, e.g. at the border of the FSI, the reflection is depending on the impedances of the two acoustic media and can be described by the reflection ratio.

9

### 2.2.4 Absorbing Elements (Infinite Elements)

Another method of absorbing outgoing acoustic pressure waves is to use infinite elements which partition the exterior of the outside of a spherical-shaped body. The pressure wave has to satisfy the Sommerfeld radiation condition, whereby the acoustic waves generated in the inside of the acoustic medium are outgoing, at infinity [3].

$$\lim_{r \to \infty} r \left[ \frac{\partial p}{\partial r} + \frac{1}{c} \frac{\partial p}{\partial t} \right] = \lim_{r \to \infty} r \left[ \frac{\partial p}{\partial r} - jkp \right] = 0 \qquad (2.23)$$

where $r$ is the distance from the origin.
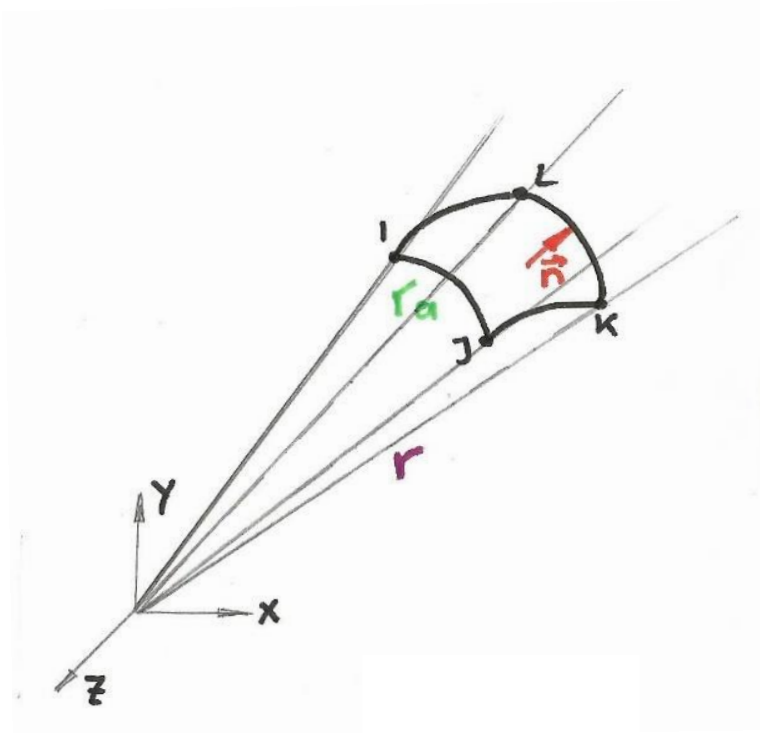


Figure 2.5: Schematic of a spherical infinite element

It is assumed that the sound generation in the acoustic domain, e.g. from an acoustic source or vibrating structure, is close to the origin. At large distances $r$ from the origin the acoustic response varies more in the radial direction than in directions that are perpendicular to the radial direction, which is characteristic of spherical spreading [14]. An equivalent notation of the Sommerfeld radiation condition is

$$\lim_{r \to \infty} r [p - \rho_0 c v_r] = 0 \qquad (2.24)$$

where $v_r$ is the acoustic particle velocity in the radial direction.

Equation ( 2.24 ) suggests that at large distances $r \to \infty$, the acoustic field resembles an outward-proceeding plane wave [3]. Rearranging this equation leads to the suggestion that at large distances $r$, the acoustic field resembles an outward-travelling plane wave. The impedance can then be described as

$$Z = \frac{p}{v_r}$$

( 2.25 )

While at infinite distances from the origin, the Sommerfeld radiation condition provides perfect absorption, the boundary condition has to be applied to an external surface of the acoustic domain in a finite element model [14]. Consequently, appropriate mass, stiffness and damping matrices, which satisfy the boundary condition (translated into a proper expression for a finite radius $r$), have to be implemented to an element attached to the exterior boundary of the acoustic domain.

## 2.2.5   Perfectly Matched Layers

Perfectly Matched Layers (PMLs) are artificial anisotropic materials that absorb all incident waves without any reflection, except those that are travelling tangentially to the PML interface [14]. The PML region acts as an infinite open domain and is attached to the acoustic medium.



Figure 2.6: Construction of the PML

Figure 2.6 shows a typical example for the construction of the PML enclosure. It can be seen that all edges of the bodies align with the coordinate system and a sound-soft Dirichlet boundary is applied on the border. Those conditions are of technical importance to the computational implementation within the FEM [3].
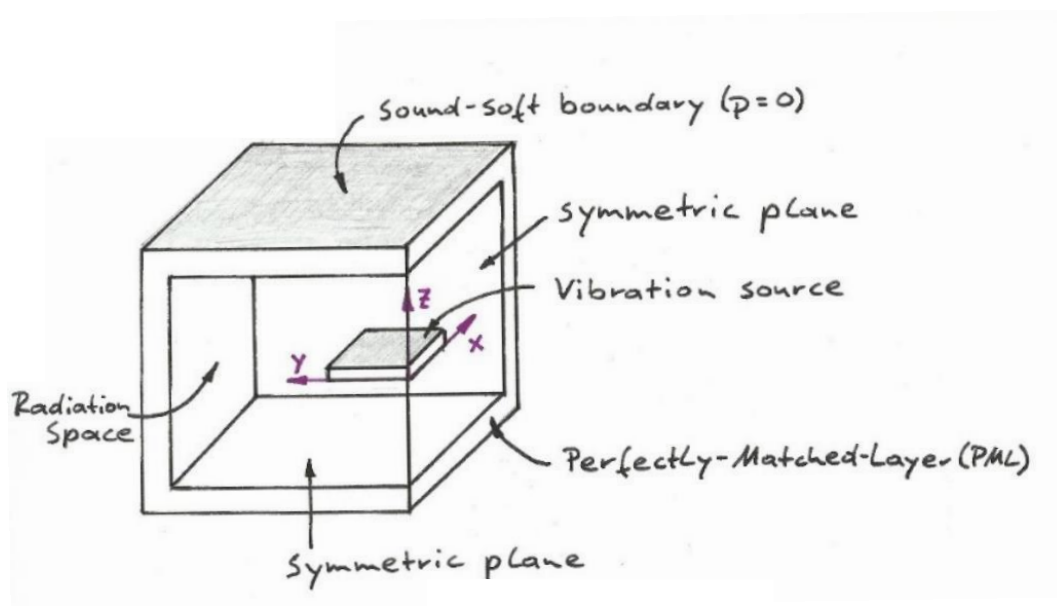
## 2.3 Structure-borne sound

A solid structure, e.g. a beam, plate, building, etc., reacts to outer loads by elastic deformation. As with airborne sound the vibration of the structure can be explained by continuous conversion of potential energy to kinetic energy of the involved masses. Because of the tri-axial state of stress every direction of movement has its own kind of wave [18]:

**Transverse bending wave**: Deflection is perpendicular to the direction of the wave propagation

**Transverse torsion wave:** Twisting of the beam sections

**Longitudinal strain wave:** Deflection along the beam axis

The most important kind of structure-borne wave for the radiation of sound into the surrounding medium is the transverse bending wave, as the deflection is perpendicular to the surface of the structure.

The main features of the bending wave can be obtained by regarding the bending wave equation of a beam without local forces.

$$\frac{\partial^4 v}{\partial x^4} - \frac{m'}{B}\omega^2 v = 0 \tag{2.26}$$

where $m'$ is the mass per unit length and $\omega$ is the angular speed. By inserting the particle velocity

$$v = v_0 e^{-jk_B x} \tag{2.27}$$

the bending wave number $k_B$ can be determined.

$$k_B{}^4 = \frac{m'}{B}\omega^2 \tag{2.28}$$

It is described by

$$k_B = \frac{\omega}{c_B} = \frac{2\pi}{\lambda_B} \tag{2.29}$$

The speed of sound in a structure can now be characterized by

$$c_B = \sqrt[4]{\frac{B}{m'}}\sqrt{\omega} = \sqrt[4]{\frac{EI}{\rho A}}\sqrt{\omega} \tag{2.30}$$

where $E$ is the Young's modulus, which describes the elasticity of a material, $A$ is the cross sectional area and $I$ is the area moment of inertia.

The bending wave length results in

$$\lambda_B = 2\pi \sqrt[4]{\frac{B}{m'} \frac{1}{\sqrt{\omega}}} = 2\pi \sqrt[4]{\frac{EI}{\rho A} \frac{1}{\sqrt{\omega}}}$$

(2.31)

In contrast to airborne sound, the wave of wave length $\lambda_B$ has a frequency depending speed of sound $c_B$. Similar to the bending wave of a beam, the bending wave length for a homogeneous plate can be written as

$$\lambda_B = 2\pi \sqrt[4]{\frac{B'}{m''} \frac{1}{\sqrt{\omega}}}$$

(2.32)

with

$$B' = \frac{E}{1 - \mu^2} \frac{h^3}{12}$$

(2.33)

and

$$m'' = \rho h$$

(2.34)

where $m''$ is the area density, $B'$ is the bending resistance of the plate, $h$ is the thickness of the plate and $\mu$ is the Poisson's ratio.

Neglecting $\mu^2 \ll 1$ the quotient $\frac{B'}{m''}$ can be simplified to

$$\frac{B'}{m''} = 12 \frac{\rho h}{E h^3} = \frac{12}{c_L^2 h^2}$$

(2.35)

where $c_L = \sqrt{\frac{E}{\rho}}$ is the speed of the longitudinal wave. The bending wave length can then be approximated to

$$\lambda_B \approx 1.35 \sqrt{\frac{h c_L}{f}}$$

(2.36)

and the structure-borne speed of sound to

$$c_B \approx 1.35 \sqrt{h c_L f}$$

(2.37)

## 2.4  Fluid-Structure Interaction

A typical example for fluid-structure interaction is the coupling of a thin solid shell structure to a relatively heavy fluid, as thin shell structures are easily excited by acoustic pressure when the ambient density of the surrounding medium is comparable to the structural density. In this case modelling the strong coupling FSI, meaning a bi-directional coupling, is indispensable. This is true for a fluid with a high density such as water, but is often omitted for fluid with relative low density like air; simplifying the considered problem to the *in vacuo* case (no acoustic FSI, as sound does not progress in a vacuum) or, if there is an interest in a point in the fluid domain, to the weak coupling case by treating the influence of the acoustic pressure to the structure as negligible. Figure 2.7 shows the difference of the two acoustic coupling cases.
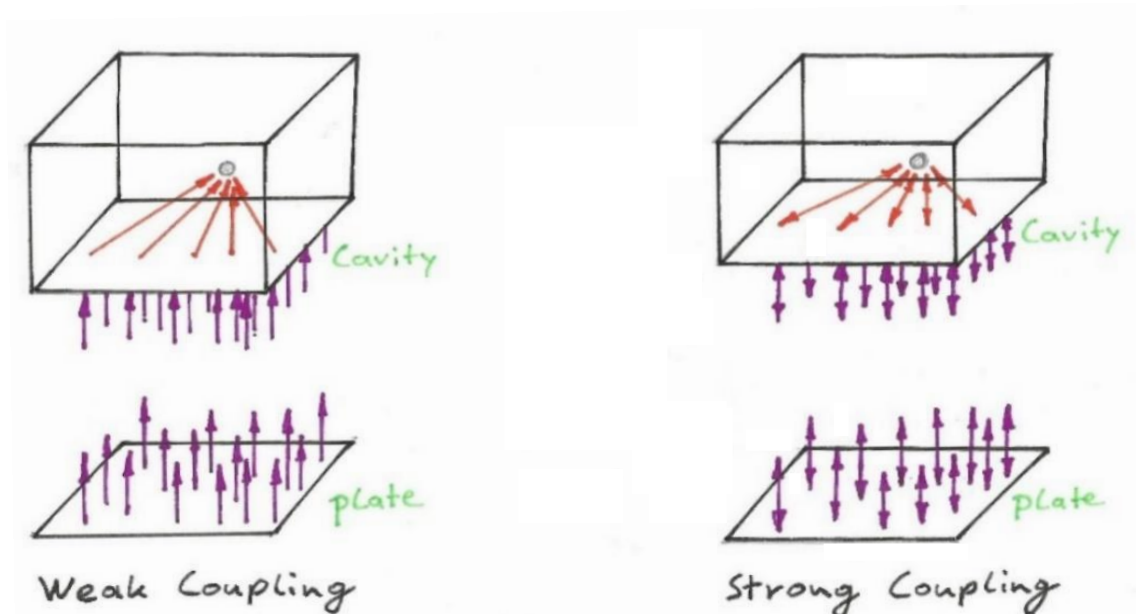


Figure 2.7: Coupling types between cavity and structure

For the bi-directional coupling between the vibration of the structure and the pressure response in the fluid, kinetic and kinematic coupling conditions have to be fulfilled [11]. The kinetic condition requires the normal force resultants of the fluid and the structure to be equal at every point on the interface between the boundaries ( 2.39 ), as seen in Figure 2.3. For an inviscid and therefore shear-free fluid the force equilibrium can be stated in the normal direction only. The kinematic condition requires the normal displacement components to be equal at all times ( 2.40 ).

$$\sigma \cdot n_s = -p \cdot n_f$$

$$n_s = n_f = n \qquad\qquad (\,2.38\,)$$

$$\sigma \cdot n = -p \cdot n \qquad\qquad (\,2.39\,)$$

$$u_s n = u_f n \qquad\qquad (\,2.40\,)$$

14

## 2.5 Perception of Sound

The human ear is a highly sensitive receiver capable of perceiving sound waves with frequencies be-tween 16 Hz and 20 kHz [8]. The limits of, in the field of vibro-acoustic interested, audible sound are not sharply specified, as the upper limits vary individually depending on the age of a person and other factors, such as noise exposure at work or habitual exposure to loud music [18].

Sound events with the same sound pressure but a different frequency are not considered equal in loudness. In order to evaluate the subjective effect of a sound event it is not enough to specify the objectively measurable sound pressure, rather the frequency-dependent sense of hearing must be considered [16]. The definition of volume is based on the subjective comparison of a sound event with the reference sound pressure $p_0 = 2 \cdot 10^{-5} Pa$ of an incident plane wave with the frequency of 1000 Hz.

This leads to the sound pressure level (SPL)

$$L_i = 20 \log\left(\frac{p}{p_0}\right) = 10 \log\left(\frac{p}{p_0}\right)^2 \qquad (2.41)$$

The perceived volume of a sound with the same loudness as a pure tone has the SPL $L$ with its own unit called phon. At the frequency of 1000 Hz the values for volume and SPL are identical. Measurements of pure tones depending on the frequency follows the curves of equal loudness found in Figure 2.8.
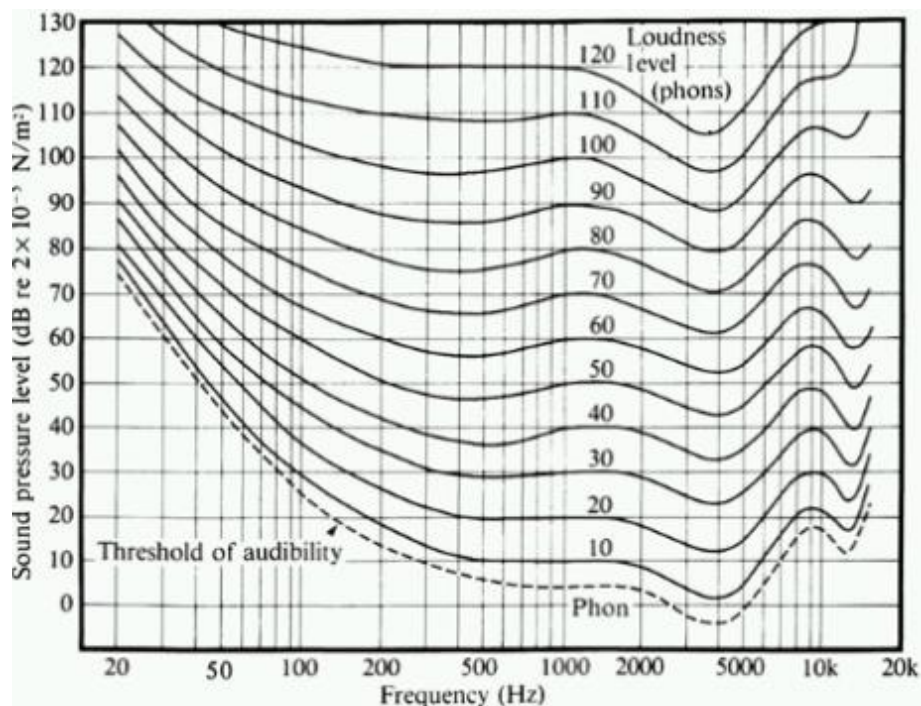


Figure 2.8: Fletcher-Munson curves of equal loudness [20]

The curve of the volume for just perceptible sound events is called hearing threshold. The volume level above a sound event is perceived as painful is called pain threshold. This value is in a range from 120 to 130 phon. Figure 2.9 shows the auditory sensation area between the two thresholds with the marked areas where music and voice related sound pressure and frequencies appear.
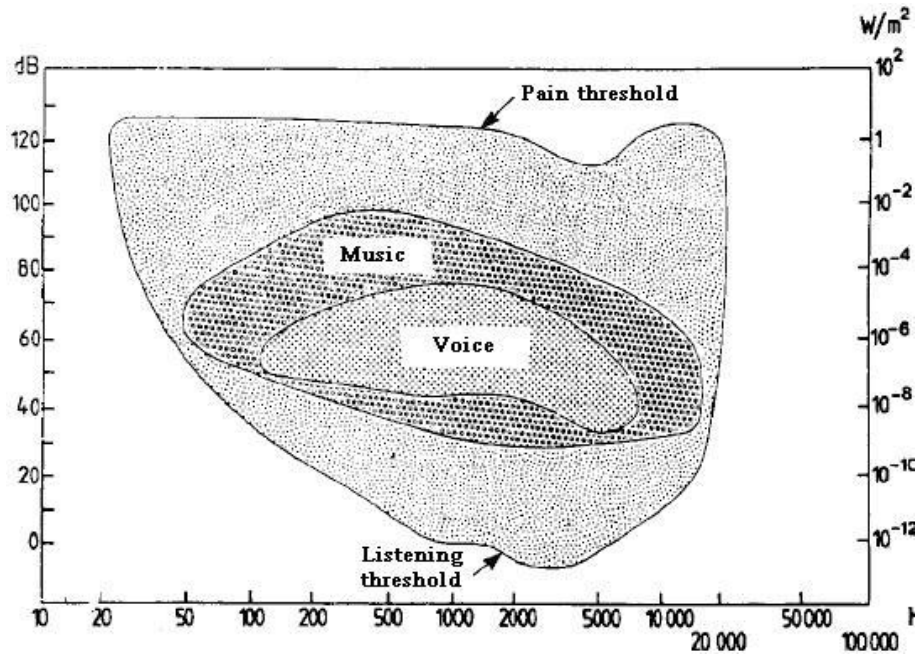


Figure 2.9: Auditory sensation area [22]

Table 2.1 shows the sound pressure and their corresponding SPLs along with some typical examples. Due to the logarithmic scale doubling the sound pressure causes an increase of 6 dB of the SPL, as well as a superposition of two equal loud sound events according to equation ( 2.41 ) an incline of 3 dB.

| Sound pressure $p(Pa, RMS)$ | Sound pressure level (SPL) $L(dB)$ | Situation/description |
|---|---|---|
| $2 \cdot 10^{-5}$ | 0 | Auditory threshold |
| $2 \cdot 10^{-4}$ | 20 | Forest with little wind |
| $2 \cdot 10^{-3}$ | 40 | Library |
| $2 \cdot 10^{-2}$ | 60 | Office |
| $2 \cdot 10^{-1}$ | 80 | Busy street in a city |
| $2 \cdot 10^{0}$ | 100 | Jackhammer, Siren |
| $2 \cdot 10^{1}$ | 120 | Start of jet aircrafts |
| $2 \cdot 10^{2}$ | 140 | Pain barrier |

Table 2.1: Classification of Sound Pressure and SPL (based on [18])

The total SPL can be calculated with

$$L_t = 10 \log \left( \sum_{i=1}^{n} 10^{L_i/10} \right)$$  ( 2.42 )

To represent the sensitivity of the human ear the sound level in the measurement and evaluation is often filtered. This reduces the weighting of the low frequencies and enhances the mid frequencies. Very often the A-filtered SPL is used, as it most resembles the human auditory sensation.

$$L(A) = 10 \log \left( \sum_{i=1}^{n} 10^{(L_i + \Delta_i)/10} \right)$$  ( 2.43 )

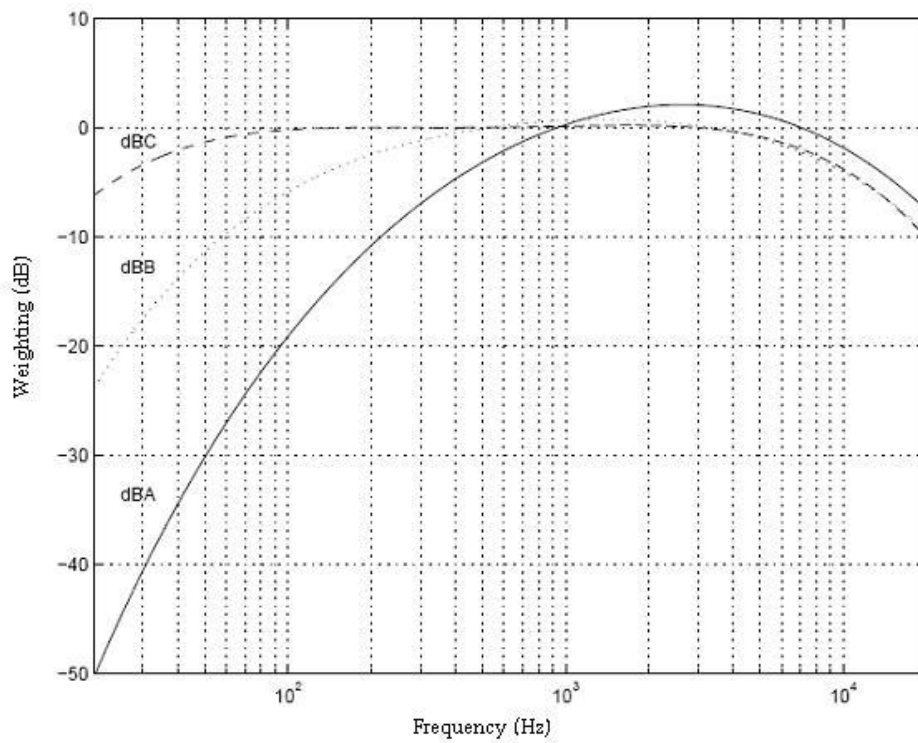where $\Delta_i$ is an attenuation factor according to the weighting in Figure 2.10.



Figure 2.10: A-,B-,C- weighted filter curves [22]

# 3     Finite Element Analysis

The finite element analysis (FEA) is a numerical method for finding approximate solutions to boundary value problems for partial differential equations. It can be used to calculate the response of a model by applying forcing functions, e.g. an acoustic source or mechanical forces. The to be analysed domain, e.g. a solid, a structure, a fluid, or a coupled fluid structure, is therefore partitioned into subdomains called finite elements whose corner points are called nodes.

In case of the fluid-structure interaction the physical unknowns $u$ and $p$ are approximated by nodal functions $u_h \approx u,\ p_h \approx p$

$$u_h(x,t) = \sum_{i=1}^{n_s} u_i(t)\, \varphi_i(x), \qquad p_h(x,t) = \sum_{i=1}^{n_f} p_i(t)\, \varphi_i(x) \tag{3.1}$$

where $u_i,\ p_i$ are unknown nodal values, $n_s$ is the number of nodes of the solid domain, $n_f$ is the number of nodes of the fluid domain and $\varphi_i$ are linear interpolants called testing functions. The summation extends over all nodes in the solid and fluid domain, separately for each one.

## 3.1     Governing Equations

The FE discretization procedure starts from the weak formulation of the partial differential equation (PDE). This formulation can be obtained by testing the PDEs using the Galerkin procedure. After the discretization of the weak formulations the coupling of the fluid and structure will be created.

### 3.1.1     Derivation of the variational formulations

For the finite element formulation of the acoustic fluid the Helmholtz equation ( 2.9 ) is multiplied by a testing function $w$ and integrated over the computational domain $\Omega_f$, whereby the stationary vector function $w$ satisfies the Dirichlet boundary condition.

$$\int_{\Omega_f} w(\nabla \cdot (\nabla p) + k^2 p)\, dV = 0 \tag{3.2}$$

$$\int_{\Omega_f} w \cdot \nabla \cdot (\nabla p)\, dV + \int_{\Omega_f} w \cdot k^2 p\, dV = 0$$

Using the Gauss integral theorem to integrate the first term yields the weak formulation

$$\int_{\Omega_f} \nabla w \cdot \nabla p\, dV - \int_{\Gamma} w\, \nabla p \cdot n\, dA - \int_{\Omega_f} w \cdot k^2 p\, dV = 0 \tag{3.3}$$

Rearranging and simplifying to

$$\int_{\Omega_f} \nabla w \cdot \nabla p \, dV - \int_{\Omega_f} w \cdot k^2 p \, dV = \int_{\Gamma} w \frac{\partial p}{\partial n} \, dA = - \int_{\Gamma} jw\omega\rho_f v_n dA \qquad (3.4)$$

Applying the natural boundary condition in FEM by setting a sound-hard boundary will simplify the term to

$$\int_{\Omega} \nabla w \cdot \nabla p \, dV - \int_{\Omega} w \cdot k^2 p \, dV = 0 \qquad (3.5)$$

Similar to the acoustic fluid the weak formulation of the structural vibration can be gathered by using the equilibrium ( 2.4 ) in terms of $\sigma$ and expand it into three dimensions. Multiplying this equilibrium by a stationary vector function $q$ and integrating it over the solid domain $\Omega_s$ equates

$$- \int_{\Omega} \nabla\sigma \cdot q \, dV + \int_{\Omega} \rho_s \ddot{u} \cdot q \, dV = 0 \qquad (3.6)$$

The weak formulation is gained by using the Gauss integral theorem to integrate the first term by parts

$$\int_{\Omega} \sigma : \nabla q \, dV - \int_{\Gamma} (\sigma \cdot n) \cdot q \, dA \int_{\Omega} \rho_s \ddot{u} \cdot q \, dV = 0 \qquad (3.7)$$

With $\sigma = C\varepsilon = CDu$, where $C$ is the solid material tensor and $D$ is the operator matrix

$$D = \begin{bmatrix} \frac{\partial}{\partial x} & 0 & 0 \\ 0 & \frac{\partial}{\partial y} & 0 \\ 0 & 0 & \frac{\partial}{\partial z} \\ \frac{\partial}{\partial y} & \frac{\partial}{\partial x} & 0 \\ \frac{\partial}{\partial z} & 0 & \frac{\partial}{\partial x} \\ 0 & \frac{\partial}{\partial z} & \frac{\partial}{\partial y} \end{bmatrix} \qquad (3.8)$$

and $\varepsilon(q) = Dq$ the tensor scalar $\sigma : \nabla q = \sigma(u) : \varepsilon(q)$ can be written as $\sigma : \nabla q = (Dq)^T C(Du)$, so that

$$\int_{\Omega} (Dq)^T C(Du) \, dV - \int_{\Gamma} (\sigma \cdot n) \cdot q \, dA \int_{\Omega} \rho_s \ddot{u} \cdot q \, dV = 0 \qquad (3.9)$$

### 3.1.2 Derivation of the Discrete Systems

The FEA is based on the discretisation of the weak form. The regarded system is divided into a number of elements with $n$ nodes. The acoustic pressure and weighting function $w$ can be approximated by using the Galerkin method to

$$p = \sum_{i=1}^{n} \varphi_i \, p_i \tag{3.10}$$

$$w = \sum_{j=1}^{n} \varphi_j w_j \tag{3.11}$$

where $\varphi_i$ are test functions. By inserting equation ( 3.10 ) and ( 3.11 ) the weak form ( 3.4 ) can be written as

$$w_i \int_{\Omega_f} \nabla\varphi_i \nabla\varphi_j \, dV \, p_j - k^2 w_i \int_{\Omega_f} \varphi_i\varphi_j \, dV \, p_j = j\rho_f w_i \omega \int_{\Gamma} \varphi_i\varphi_j v_n dA \tag{3.12}$$

for every combination of $i$ and $j$ within an element [10]. Replacing $k$ by equation ( 2.10 ) equals

$$w_i \int_{\Omega_f} \nabla\varphi_i \nabla\varphi_j \, dV \, p_j - \frac{\omega^2}{c^2} w_i \int_{\Omega_f} \varphi_i\varphi_j \, dV \, p_j = j\rho_f w_i \omega \int_{\Gamma} \varphi_i\varphi_j v_n dA \tag{3.13}$$

With $w_i = 1$ and by introducing $[M_f] = \frac{1}{c^2} \int_{\Omega_f} \varphi_i\varphi_j \, dV$ as the mass matrix, $[K_f] = \int_{\Omega_f} \nabla\varphi_i\nabla\varphi_j \, dV$ as the stiffness matrix, and $\{F_f\} = j\rho_f\omega \int_{\Gamma} \varphi_i\varphi_j v_n dA = \rho_f\omega^2 \int_{\Gamma} \varphi_i\varphi_j dA \, u_n$ as the load vector of the discrete system, the discretised system can be written as

$$(-\omega^2[M_f] + [K_f])\{p\} = \{F_f\} \tag{3.14}$$

By introducing the impedance boundary condition the discrete system of equation ( 3.13 ) is

$$w_i \int_{\Omega_f} \nabla\varphi_i \nabla\varphi_j \, dV \, p_j - \frac{\omega^2}{c^2} w_i \int_{\Omega_f} \varphi_i\varphi_j \, dV \, p_j + j\omega\rho_f w_i \int_{\Gamma_i} \varphi_i\varphi_j \frac{1}{Z_{n,j}} dA \, p_j$$
$$= \rho_f w_i \omega^2 \int_{\Gamma_n} \varphi_i\varphi_j dA \, u_n \tag{3.15}$$

where $\Gamma_n$ is the border of the Neumann boundary and $\Gamma_i$ is the border of the impedance boundary.

Equation ( 3.14 ) can now be expressed as

$$(-\omega^2[M_f] + j\omega[C_f] + [K_f])\{p\} = \{F_f\} \tag{3.16}$$

where $[C_f] = \rho_f \int_{\Gamma_i} \varphi_i \varphi_j \frac{1}{Z_{n,j}} dA$ is the damping matrix of the fluid.

Similar to the acoustic fluid the discretised system of the structure can be written as

$$(-\omega^2[M_s] + j\omega[C_s] + [K_F])\{u\} = \{F_s\} \tag{3.17}$$

where $[M_s] = \rho \int_{\Omega_s} \varphi_i \varphi_j \, dV$ is the mass matrix and $[K_s] = \int_{\Omega_s} \varphi_i D^T C D \varphi_j \, dV$ is the stiffness matrix. The load vector $\{F_s\} = [T_s]\{f\} + [G_s]\{t\}$ consists of the interpolation matrices $[T_s] = \int_{\Omega_s} \varphi_i \varphi_j \, dV$ for the inner forces and $[G_s] = \int_{\Gamma} \varphi_i \varphi_j \, dA$ for the outer forces, where $\{f\}$ is the vector of the volume forces and $\{t\}$ is the vector of the surface loads [10]. The structural damping can be respected by the proportional damping matrix $[C_s] = \alpha[M_s] + \beta[K_s]$ with $\alpha$ and $\beta$ as damping parameters.

### 3.1.3    Implementation of the FSI

Applying the coupling conditions ( 2.39 ) and ( 2.40 ) to the discretised weak formulations of the equations of motion for the structure and fluid equals

$$(-\omega^2[M_s] + j\omega[C_s] + [K_F])\{u\} - [R]\{p\} = \{F_s\} \tag{3.18}$$

$$(-\omega^2[M_f] + j\omega[C_f] + [K_f])\{p\} - \omega^2 \rho_0 [R]^T\{u\} = \{F_f\} \tag{3.19}$$

with $p = \omega^2 \rho_0 u$, where $[R]$ is the coupling matrix that take in account the surface area associated with each node on the fluid-structure interface. Written down as a linear system it is shown that the dynamic stiffness matrix is not symmetric.

$$\left(-\omega^2 \begin{bmatrix} M_S & 0 \\ \rho_0 R^T & M_F \end{bmatrix} + j\omega \begin{bmatrix} C_S & 0 \\ 0 & C_F \end{bmatrix} + \begin{bmatrix} K_S & -R \\ 0 & K_F \end{bmatrix}\right) \begin{Bmatrix} u \\ p \end{Bmatrix} = \begin{Bmatrix} F_s \\ F_f \end{Bmatrix} \tag{3.20}$$

By defying a transformation variable for the nodal pressure ( 3.21 ) the symmetric formulation of the linear system ( 3.22 ) can be obtained [4].

$$\dot{q} = j\omega q = p \tag{3.21}$$

$$\left(-\omega^2 \begin{bmatrix} M_S & 0 \\ 0 & -\dfrac{M_F}{\rho_0} \end{bmatrix} + J\omega \begin{bmatrix} C_S & -R \\ -R^T & -\dfrac{C_F}{\rho_0} \end{bmatrix} + \begin{bmatrix} K_S & 0 \\ 0 & -\dfrac{K_F}{\rho_0} \end{bmatrix}\right) \begin{Bmatrix} u \\ q \end{Bmatrix} = \begin{Bmatrix} F_s \\ \dfrac{j}{\omega\rho_0} F_f \end{Bmatrix} \tag{3.22}$$

## 3.2 Solution Methods for Frequency Response

While looking at the response of a vibrating system the frequency response is more of interest than its behaviour in time, as it clearly indicates the eigenfrequencies of a system and its response to it. The frequency response therefore records the magnitude and phase of the vibrating system as a function of frequency, e.g. in this work the frequency response of the amplitude of displacement or acoustic pressure is used to describe the behaviour of the system.

The solution used in the frequency response can be gained by the direct solution of the discrete system or the mode superposition method.

### 3.2.1 Direct Solution

The direct solution can be obtained by calculating the displacement and acoustic pressure of the linear system ( 3.20 ) or the symmetric equivalent ( 3.22 ) for every defined forcing frequency $\Omega$ within the requested frequency range $[\Omega_{min}:\Omega_{max}]$ [11].

Therefore, the displacement and acoustic pressure of the discrete system

$$(-\Omega^2[M] + i\Omega[C] + [K])\{u\} = \{f\} \tag{3.23}$$

can be computed by multiplying the inverse of the dynamic stiffness matrix on the left side with the force vector $\{f\}$.

$$\{u\} = \left[-\Omega^2[M] + j\Omega[C] + [K]\right]^{-1}\{f\} \tag{3.24}$$

Because of the dependency of the forcing frequency $\omega$, the inverse of the dynamic stiffness matrix has to be calculated at every sub-step. This leads to high computing times depending on the system's DOFs as well as the requested frequency range.

### 3.2.2 Mode Superposition

As an alternative to the direct approach, the solution of the harmonic response can be obtained by modal superposition. In a first step the natural frequencies and mode shapes are obtained from a modal analysis, which later characterises the dynamic response of the steady harmonic excitation [2].

The frequency response solution is searched as a superposition of eigenvectors $\Phi_i$. $\{u\}$ is

$$\{u\} = \sum_{i=1}^{N} \{\Phi_i\} y_i \tag{3.25}$$

where $N$ is the number of modes used in the computation and $y_i$ are modal coordinates of the real valued eigenvectors of the form $\Phi = \{u\}$, and $\Phi = \begin{Bmatrix} u \\ p \end{Bmatrix}$ for the coupled problem respectively. With $N \ll n$, the solution will be searched in form of the lower eigenvectors' superposition, whereby $n$ represents the system's number of modes.

Equation ( 3.23 ) can then be represented as

$$[M] \sum_{i=1}^{N} \{\Phi_i\} \ddot{y}_i + [C] \sum_{i=1}^{N} \{\Phi_i\} \dot{y}_i + [K] \sum_{i=1}^{N} \{\Phi_i\} y_i = \{f\} \tag{3.26}$$

and by pre-multiplying with the mode shape $\{\Phi_j\}^T$ as

$$\{\Phi_j\}^T [M] \sum_{i=1}^{N} \{\Phi_i\} \ddot{y}_i + \{\Phi_j\}^T [C] \sum_{i=1}^{N} \{\Phi_i\} \dot{y}_i + \{\Phi_j\}^T [K] \sum_{i=1}^{N} \{\Phi_i\} y_i = \{\Phi_j\}^T \{f\} \tag{3.27}$$

The orthogonality condition of the natural modes states that for $i \neq j$

$$\{\Phi_j\}^T [M] \{\Phi_i\} = 0 \tag{3.28}$$

$$\{\Phi_j\}^T [K] \{\Phi_i\} = 0 \tag{3.29}$$

and

$$\{\Phi_j\}^T [C] \{\Phi_i\} = 0 \tag{3.30}$$

if only Rayleigh or constant damping is allowed. Applying condition ( 3.28 ), ( 3.29 ) and ( 3.30 ) to equation ( 3.27 ) equals for $i = j$.

$$\{\Phi_j\}^T [M] \{\Phi_j\} \ddot{y}_j + \{\Phi_j\}^T [C] \{\Phi_j\} \dot{y}_j + \{\Phi_j\}^T [K] \{\Phi_j\} y_j = \{\Phi_j\}^T \{f\} \tag{3.31}$$

With the modal transformations of the mass and stiffness matrices

$$[\hat{M}] = \{\Phi_j\}^T [M] \{\Phi_j\} = [E] = \begin{bmatrix} 1 & & \\ & \ddots & \\ & & 1 \end{bmatrix}_{NxN} \tag{3.32}$$

$$[\hat{K}] = \{\Phi_j\}^T [K] \{\Phi_j\} = [\omega^2] = \begin{bmatrix} \omega_1^2 & & \\ & \ddots & \\ & & \omega_N^2 \end{bmatrix}_{NxN} \tag{3.33}$$

equation ( 3.31 ) can be written as

$$\left(-\Omega^2[\hat{M}] + j\Omega\{\Phi_j\}^T[C]\{\Phi_j\} + [\hat{K}]\right) y_j = \{\Phi_j\}^T\{f\} \tag{3.34}$$

$$\left(-\Omega^2[E] + j\Omega\{\Phi_j\}^T[C]\{\Phi_j\} + [\omega^2]\right) y_j = \{\Phi_j\}^T\{f\}$$

By multiplying the inverse of the modal transformed dynamic stiffness matrix on the left side with the modal transformed force vector $\{\hat{f}\}$ the modal coordinates $y_j$ can be estimated

$$y_j = \left(-\omega^2[\hat{M}] + j\omega[\hat{C}] + [\hat{K}]\right)^{-1}\{\hat{f}\} \tag{3.35}$$

The modal coordinates $y_j$ are then converted back into the geometric displacements $\{u\}$ by equation ( 3.25 ). For an accurate analysis of the driving frequency belt $\Omega \in [\Omega_{min}:\Omega_{max}]$ the solution should cover all modes with the associated frequencies $\omega \leq 1.5 \cdot \Omega_{max}$, as they characterise the frequency response [12]. The approximate solution generally shows a good convergence to the direct solution within the lower frequencies of the frequency belt. By increasing the number of modes $N$ to the system's number of modes $n$ the approximate solution equals the modal transformation of the direct solution. The main advantage of this approach lies within the reduced computational effort, as the system of equations is consistently trimmed with $N \ll n$.

For the mode-superposition in fluid-structure interaction, the symmetric formulation as shown above may not succeed in extracting all eigensolutions, therefore the unsymmetric formulation along with the unsymmetric eigensolver is being used [7].

Equation ( 3.31 ) is then replaced by

$$\{\Phi_j{}^L\}^T[M]\{\Phi_j\}\ddot{y}_j + \{\Phi_j{}^L\}^T[C]\{\Phi_j\}\dot{y}_j + \{\Phi_j{}^L\}^T[K]\{\Phi_j\}y_j = \{\Phi_j{}^L\}^T\{f\} \tag{3.36}$$

where $\{\Phi_j{}^L\}$ is the left mode shape of mode $j$ and $\{\Phi_j\}$ is the right mode shape of mode $j$.

**Residual Vectors**

When the applied loads excite the higher frequency modes of a structure the modally truncated solution will be imprecise. To improve the accuracy of the response additional modal transformation factors, called residual vectors, can be used [2]. The dynamic response $x$ can then be gained by superposition of the lower mode contributions $x_L$ by equation ( 3.1 ) and the higher mode contributions $x_H$, which can be represented as the combination of residual vectors.

$$\{x\} = \{x_L\} + \{x_H\} \tag{3.37}$$

The residual vectors $\{R\}$ can be expressed as

$$\{R\} = [\tilde{G}]\{f\} \tag{3.38}$$

with the residual flexibility matrix

$$[\tilde{G}] = \sum_{i=m+1}^{n} \frac{\{\Phi_j^L\}\{\Phi_j\}^T}{\omega_j^2} = [G] - \sum_{i=1}^{m} \frac{\{\Phi_j^L\}\{\Phi_j\}^T}{\omega_j^2} \tag{3.39}$$

where $[G]$ is the inverse matrix of the stiffness matrix $[K]$

$$[G] = \sum_{i=1}^{n} \frac{\{\Phi_j^L\}\{\Phi_j\}^T}{\omega_j^2} = \sum_{i=1}^{m} \frac{\{\Phi_j^L\}\{\Phi_j\}^T}{\omega_j^2} + \sum_{i=m+1}^{n} \frac{\{\Phi_j^L\}\{\Phi_j\}^T}{\omega_j^2} \tag{3.40}$$

**Restrictions of the Mode Superposition Method**

The mode superposition method is not supported if damping, apart from modal damping, proportional or Rayleigh damping is present [7]. In particular, if acoustic damped boundary conditions, fluid dynamics viscosity, perforated material, PML absorbing condition or infinite elements are defined. Consequently, absorbing boundary conditions are not supported in general.

## 3.3    Finite Elements for FSI (3D)

In order to solve a FSI problem the fluid and solid volumes are partitioned into finite elements. In case of the fluid the volume is divided into hexahedral or tetrahedral elements with one degree of freedom (DOF) per node. The solid domain can be meshed by volume elements with three DOFs or shell elements with 6 DOFs per knot. For the coupling between solid and fluid elements optional DOFs (corresponding to the translational DOFs of the structure) are being used within the fluid elements (for further information see ch. 8.1.2 or [5] and [6]).
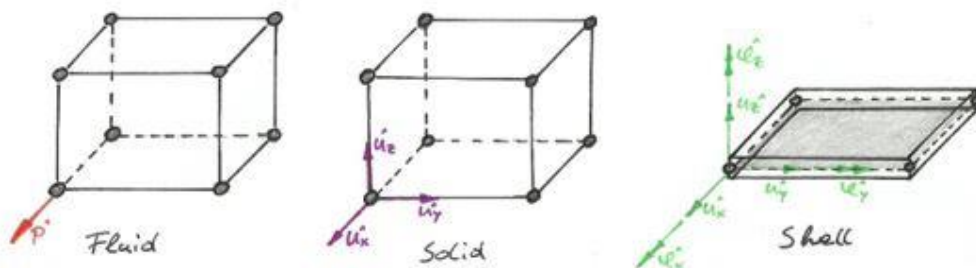


Figure 3.1: Hexahedral solid, shell and fluid element with nodal DOFs

# 4 Verification Examples

## 4.1 Rectangular Panel Backed on Closed Cavity

To demonstrate and validate the structural-acoustical coupling of the FSI between an acoustic medium and a structure it is common to take a look at a rectangular panel backed by a rectangular closed cavity, as it represents a typical sound radiating application where the response of a structure is influenced by the acoustic pressure on its surface and vice versa, e.g. thin walls in frame buildings or machine housings.
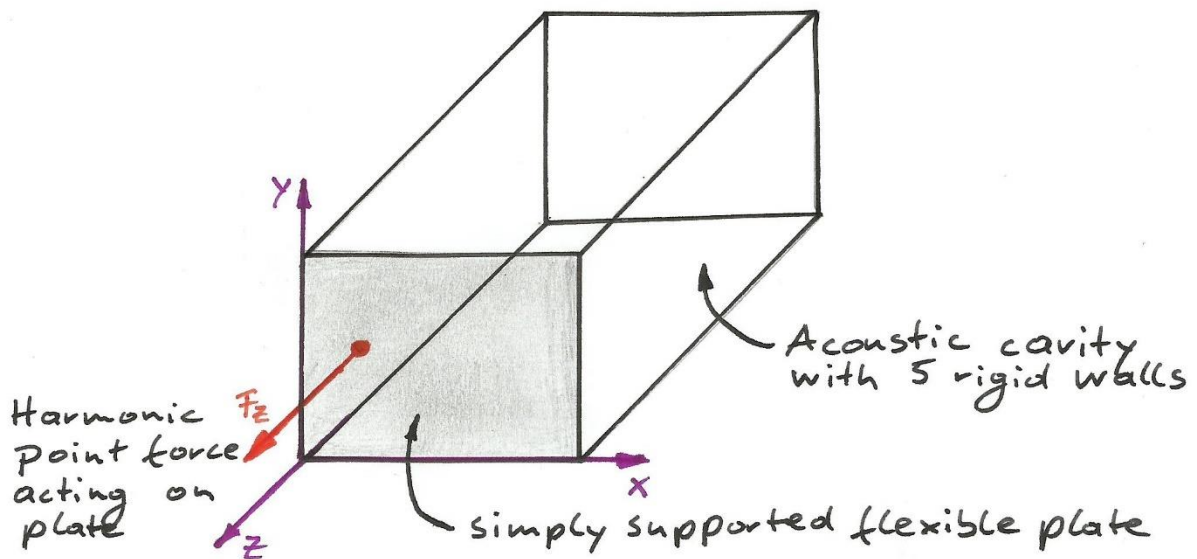


Figure 4.1: A closed acoustic cavity with an attached flexible plate

In this example the flexible plate is forced to swing at the point $(0.2, 0.3)$ m due to a time-harmonic force of 1N within the frequency range $\Omega = [0 : 250]s^{-1}$. The elastic panel has the dimensions $1m \cdot 1m$ and the thickness $h = 0.01\ m$. The panel is simply supported and coupled to an acoustic cavity with the dimensions $1m \cdot 1m \cdot 1m$. The remaining surfaces of the cavity are rigid walls, i.e. Neumann boundary conditions are applied. The acoustic fluid is water ($\rho_F = 1000\frac{kg}{m^3}, c_F = 1481\frac{m}{s}$) and the flexible plate is made from steel ($E = 210\ GPa,\ \rho_S = 7900\frac{kg}{m^3}, \nu = 0.3$).

The frequency response at the driving point is recorded and then compared with the work of M. Fischer and L. Gaul [17]. The flexible plate's applied mesh of the referred work consists of $20 \cdot 20$ shell elements with an element length $h_\lambda = 0.05m$. The same element length is applied to the acoustic cavity.

With the longitudinal speed of sound $c_L$ and the dominant driving frequency $\Omega$ the bending wave length can be determined

$$c_L = \sqrt{\frac{E}{\rho}} = \sqrt{\frac{210 \cdot 10^9 \frac{N}{m^2}}{7900 \frac{kg}{m^3}}} = 5155.80 \frac{m}{s}$$

$$\lambda_B \approx 1.35 \sqrt{\frac{hc_L}{\Omega}} = 1.35 \sqrt{\frac{0.01m \cdot 5155.80 \frac{m}{s}}{250 \, s^{-1}}} = 0.61m$$

With the element per wave length condition $\frac{\lambda_B}{h_\lambda} = 6 \dots 8$ the recommended element size can be estimated to

$$h_\lambda = \frac{\lambda}{8} = \frac{0.61m}{8} = 0.076m \qquad (4.1)$$

The chosen element length in the referred work $h_{\lambda,chosen} = 0.05m$ does fulfil the recommended element per wave length condition in equation ( 4.1 ).
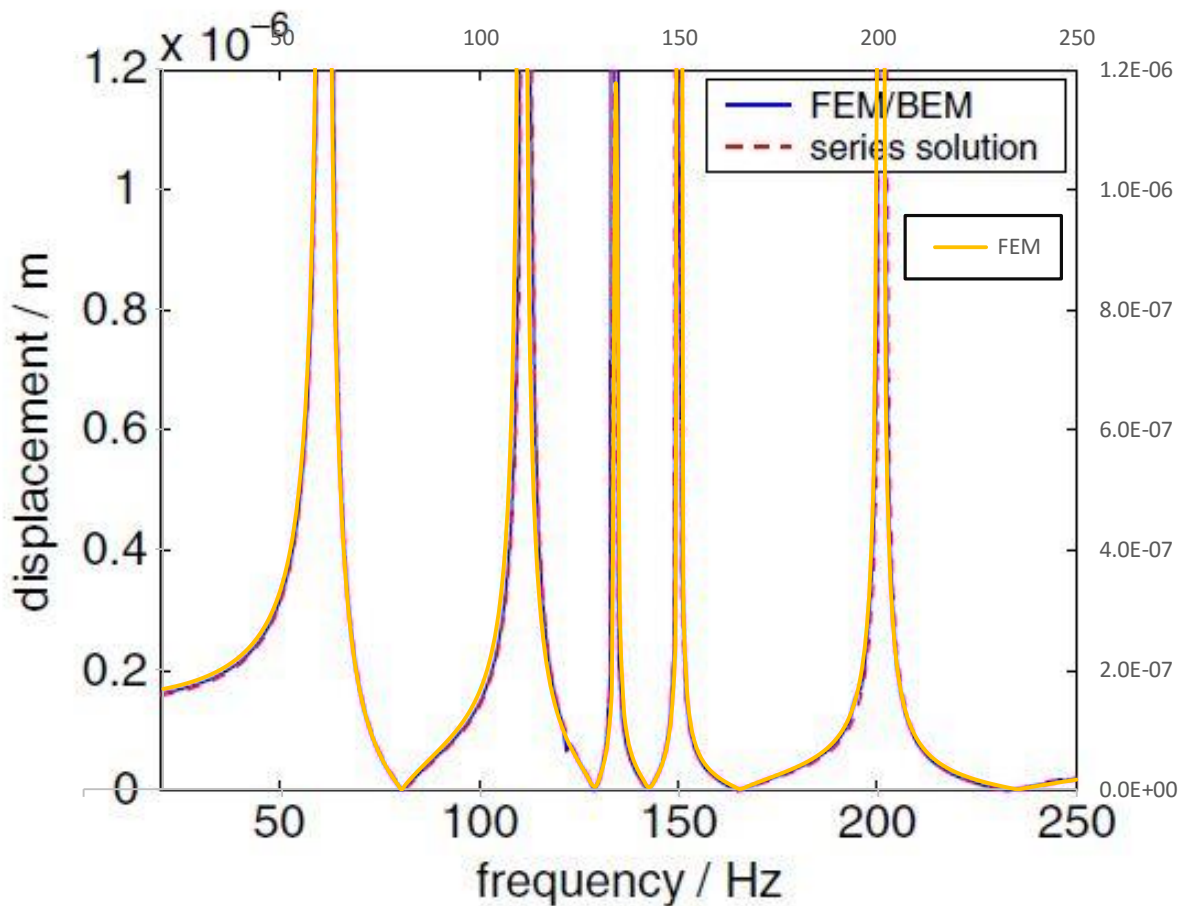


Figure 4.2: Frequency response at the driving point (after [17])

The frequency response of the graph in Figure 4.2 compares the FEM solution of ANSYS with the analytical Fourier series solution derived by Pretlove [1] and the FEM-BEM solution by M. Fischer and L. Gaul. All graphs show an appropriate correspondence to each other.

**Comparison of the solution methods**

The solution can be found by three different settings and two methods as described in chapter 3.2. Figure 4.3 affirms the similarity of the three graphs, but also shows a slight difference regarding the unsymmetric and symmetric matrix formulated solution using the direct method. The advantage of the symmetric matrix formulation lies in the lower computing time; however, the computing time of the mode-superposition method is considerably lower than using the direct solution.
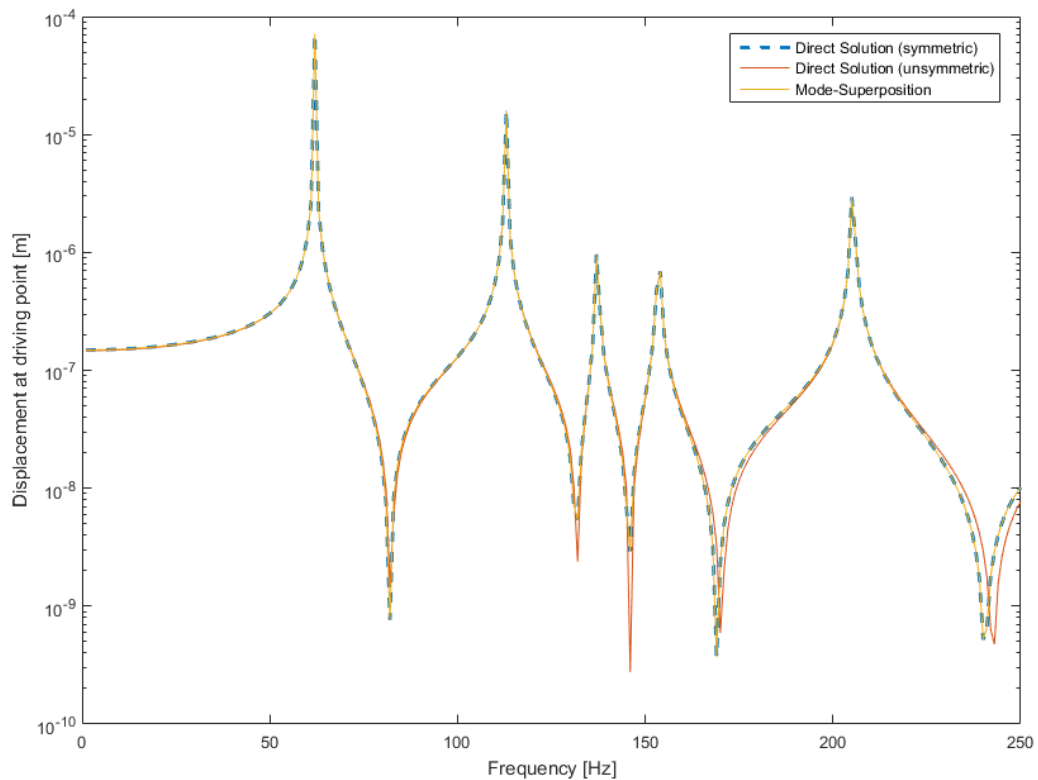


Figure 4.3: Comparison of the solution methods

| Solution method | Computing time |
|---|---|
| Direct solution with unsymmetric matrix formulation | 2h06' |
| Direct solution with symmetric matrix formulation | 1h42' |
| Modal-Superposition with unsymmetric matrix formulation | 41'36'' |

Table 4.1: Comparison of the computing times for the cavity-plate example

The computing times in Table 4.1 were achieved by using a laptop computer with four AMD A8-3520M processors with a frequency of 1600 Mhz and a RAM of 8 GB. The direct solution calculated the frequency range $\Omega = [0:250]s^{-1}$ in 250 steps for both matrix formulations. The modal superposition method used the first 200 modes of the system to calculate the solution.

**Acoustic pressure inside the cavity**

Carl Howard [14] has calculated the vibro-acoustic response of a simply supported rectangular plate backed to a cavity with rigid boundaries by mode-superposition of the plate's eigenfrequencies (after Leissa [15]) and the natural frequencies of the acoustic cavity (after Leo L. Beranek and István L. Ver [9]). A modified version of his script, attached in the appendix, uses the same dimensions and defined points as the academic example used above. It leads to roughly same results and offers the opportunity to measure the acoustic pressure at a point in the acoustic cavity. Figure 3.5 shows the acoustic pressure at the point $(0.2, 0.3, 0.5)$ m.
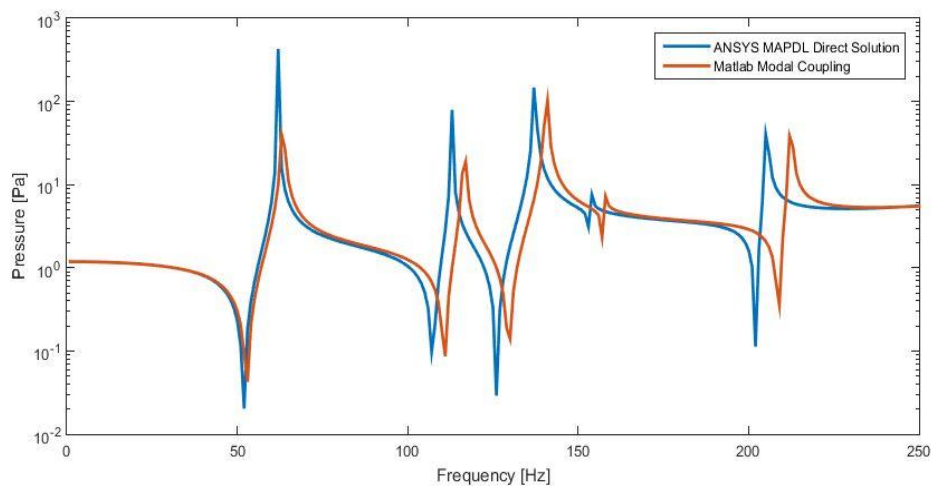


Figure 4.4: Acoustic pressure at $(0.2, 0.3, 0.5)$ inside the cavity

The results from the theoretical modal coupling do not precisely align with the results of the direct solution using FEM. This can be explained by a higher stiffness effect within the theoretical model, as all the eigenfrequencies are at higher frequencies as their corresponding modes using FEM.

**Influence of acoustic fluids**

As mentioned in chapter 2.4 the density of the used acoustic fluid characterises the influence of the FSI, as the modes are affected by the added mass and added stiffness effect of the coupled system. Figure 4.5 shows a comparison of four fluids with known speeds of sounds and densities (s. Table 4.2) to the displacement of the uncoupled plate.

Comparing the vibration modes to the eigenmodes of the uncoupled plate (*in vacuo* case) the effect of the acoustic cavity is particularly noticeable for mode shapes that have a non-zero average flux over the interface. In this case the stiffness effect of the cavity plays a dominant role [17], whereas the added mass effect of the acoustic fluid is dominant for mode shapes with zero average flux.
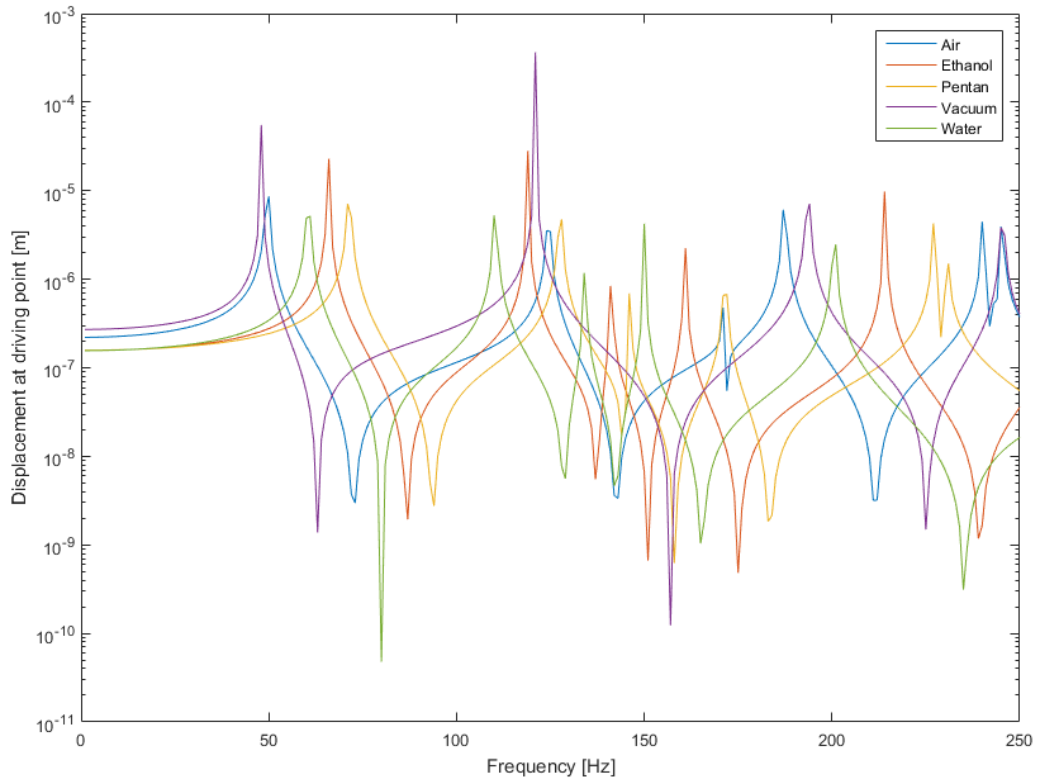


Figure 4.5: Comparison of acoustic fluids at driving point

| Fluid | Density $\rho\ (kg/m^3)$ | Speed of Sound $c\ (m/s)$ |
|---|---|---|
| Air | 1,21 | 343 |
| Ethanol | 790 | 1160 |
| Pentan | 621 | 1020 |
| Vacuum | 0 | 0 |
| Water | 1000 | 1481 |

Table 4.2: Used acoustic fluids for comparison of displacement at driving point

Figure 3.6 shows the first four mode shapes of the uncoupled plate (upper shapes) in comparison to their counterparts of the acoustic fluid water (lower shapes). It is recognisable that the first eigenfrequency's mode shape of the uncoupled plate at a frequency of 49 Hz can be found at a frequency of 134 Hz in the coupled system. Mode shapes with zero average flux over the interface can be found at frequencies below their uncoupled counterparts due to the added mass effect.

**Air**

| Mode (1,1) | Mode (1,2) | Mode (2,2) | Mode (3,1) |
|---|---|---|---|
| $f = 49Hz$ | $f = 122Hz$ | $f = 196Hz$ | $f = 245Hz$ |



**Water**

| Mode (1,1) | Mode (1,2) | Mode (2,2) | Mode (1,3) |
|---|---|---|---|
| $f = 134Hz$ | $f = 60Hz$ | $f = 111Hz$ | $f = 149Hz$ |
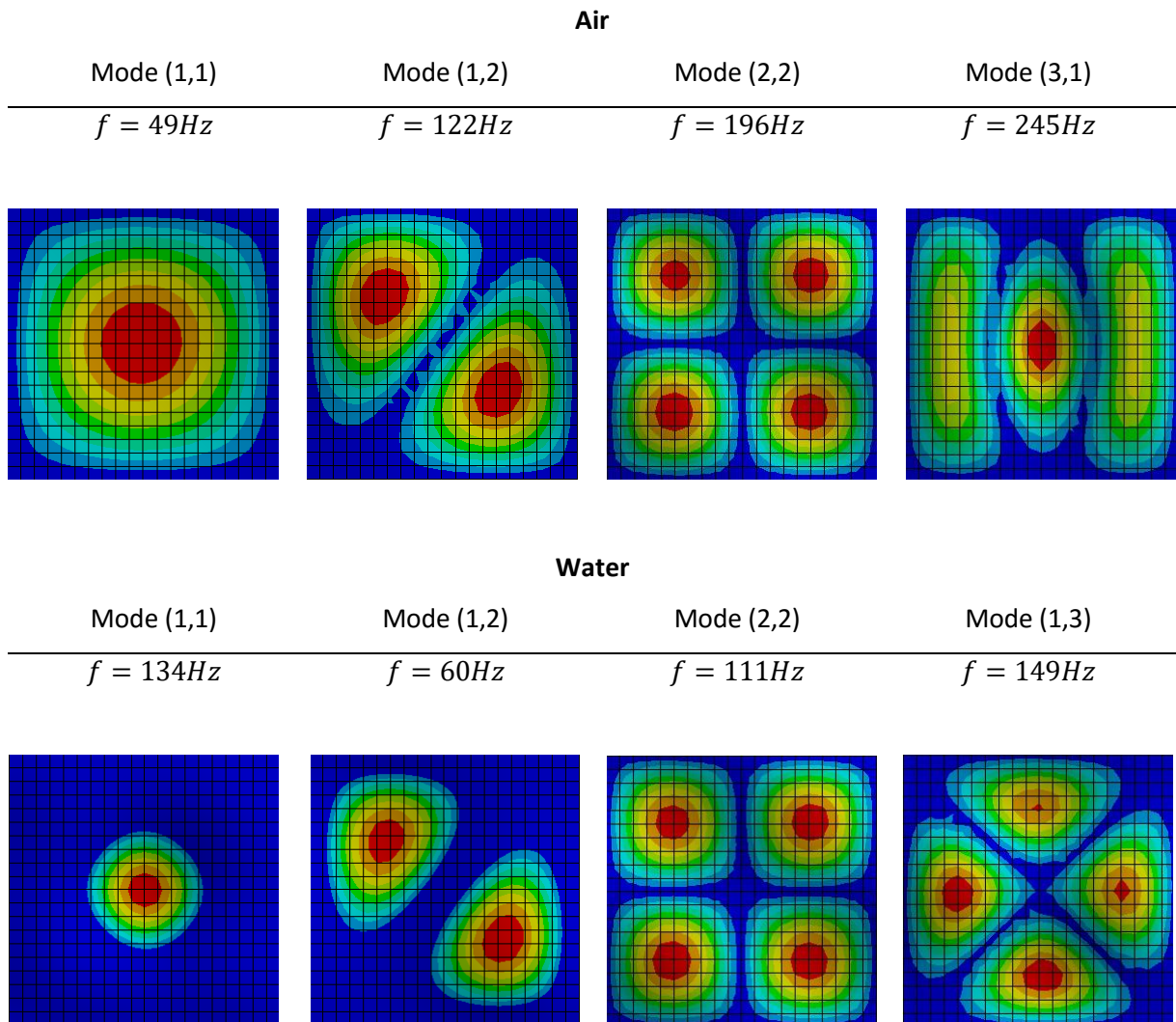


Figure 4.6: Comparison of the first four mode shapes

**Comparison of boundary conditions**

Figure 4.7 shows a comparison of the sound-hard boundary with the radiation boundary. One can see that the peaks of the curve with the radiation boundary are clearly reduced, as the reflection ratio compared to the reflecting Neumann curve is much lower. Figure 4.8 then shows the same setting with the acoustic fluid air and the *in vacuo* case. It thus can be shown that the influence of the reflection is not as huge as the acoustic fluid water and the influence of the absorbing boundary is not as high.
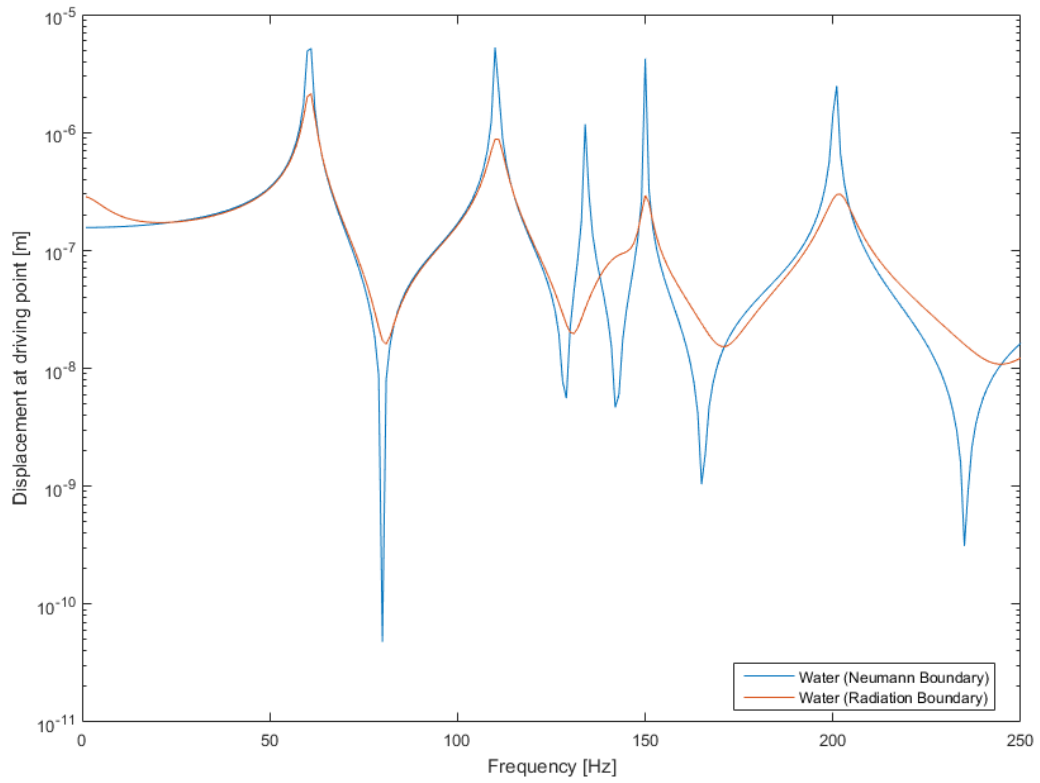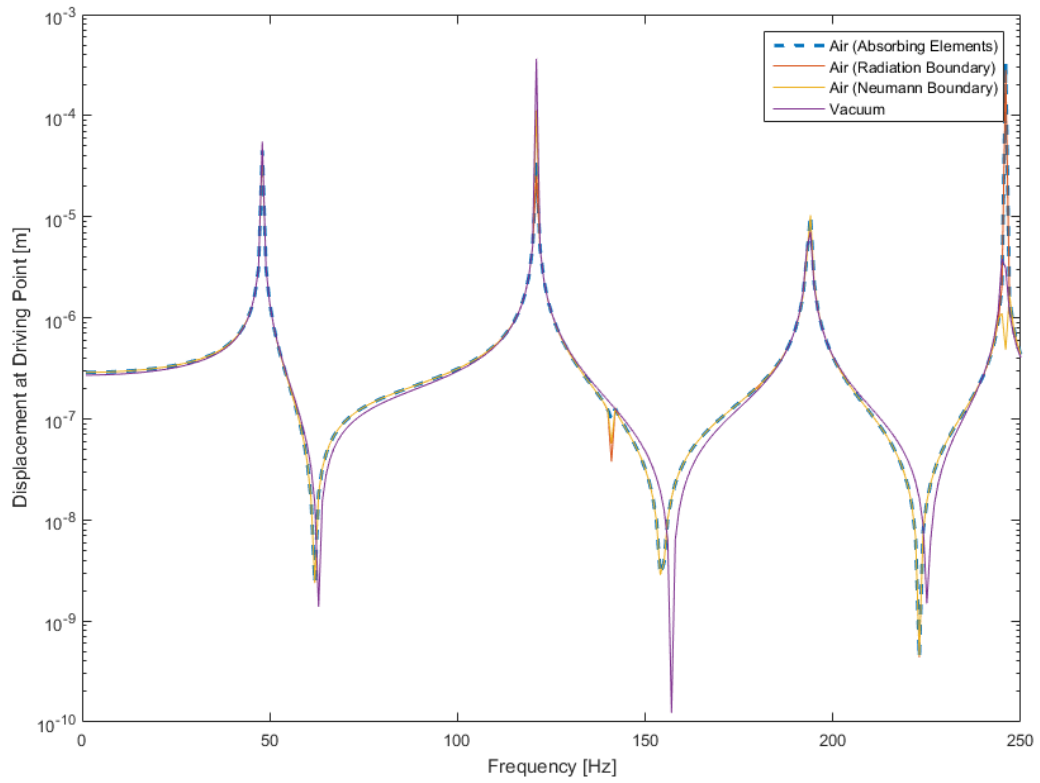
Figure 4.7: Driving point displacement different boundary conditions (water, rectangular cavity)
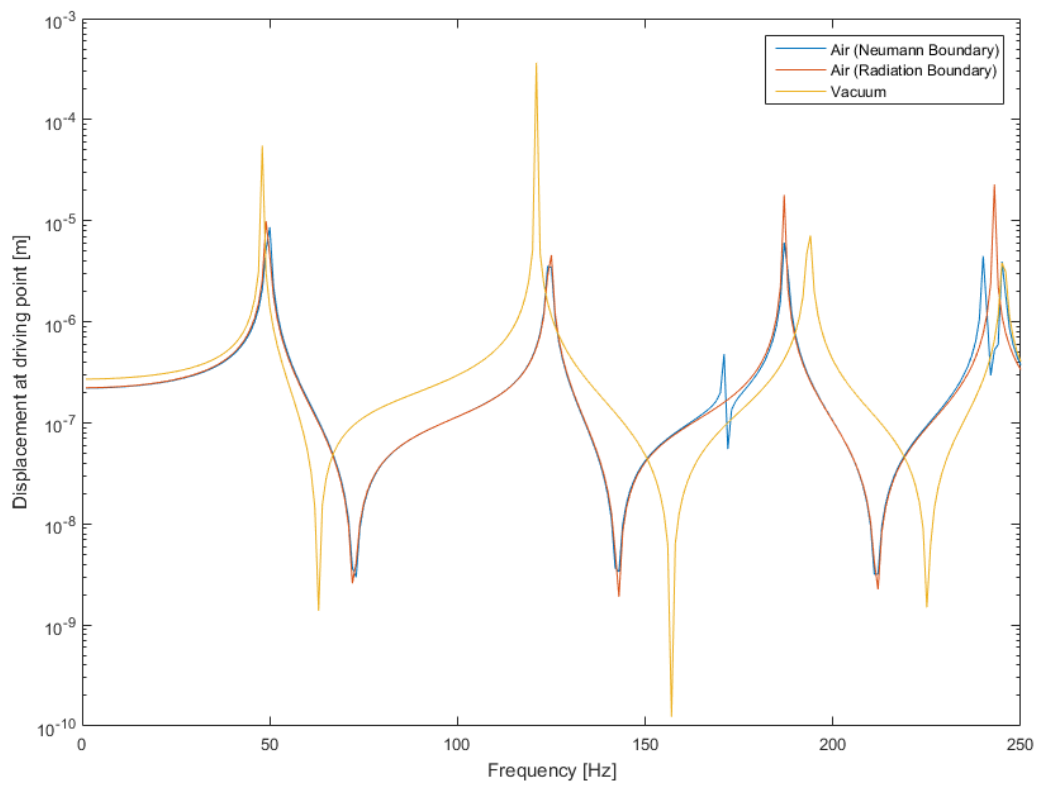


Figure 4.8: Driving point displacement with different boundary conditions (air, rectangular cavity)

32

## 4.2 Rectangular Panel on Hemisphere

To be able to compare the different absorbing boundary conditions with each other the plate described in chapter 4.1 is attached to a hemisphere with the radius $r = 1m$. The origin of the hemisphere lies at the centre of the plate at $(0.5, 0.5)m$. At the ground of the hemisphere impedance boundary conditions are applied, corresponding to the FSI and the attached open domain. In addition to the displacement at the driving point, the acoustic pressure at the point $(0.475, 0.675, 0.575)m$ is being recorded.
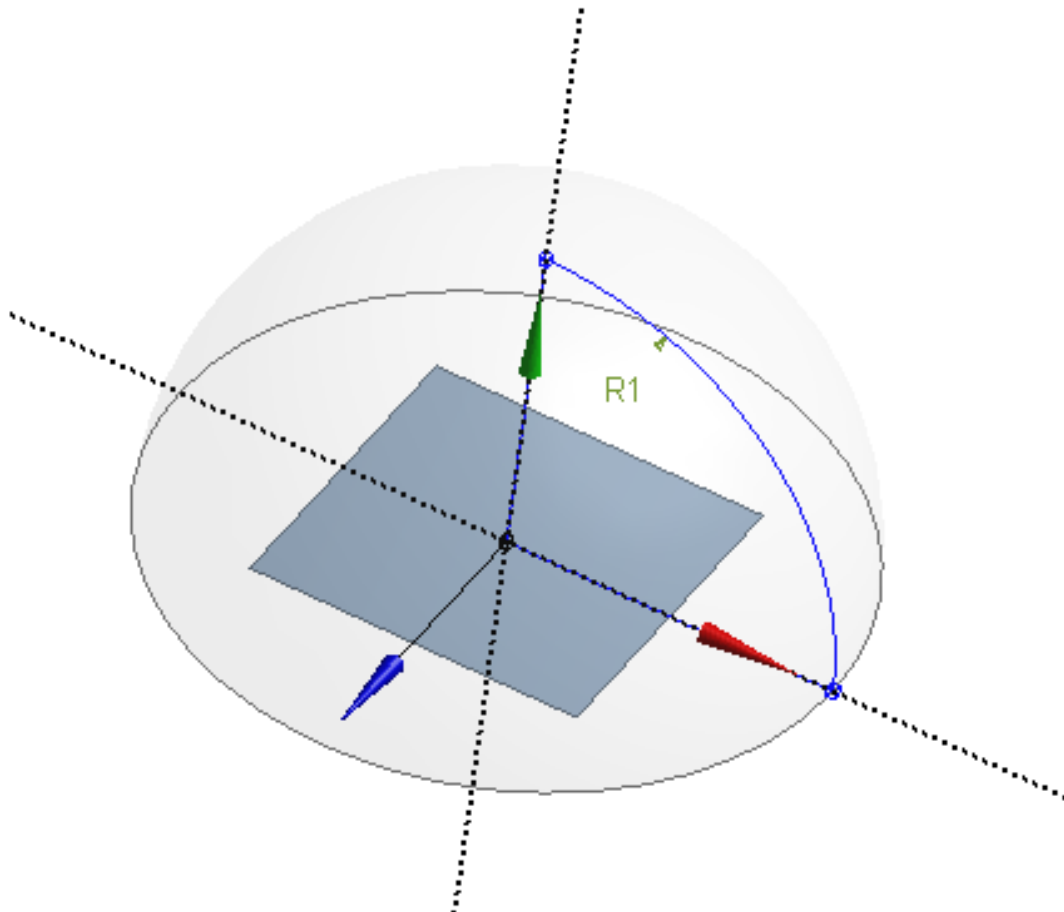


Figure 4.9: Plate backed on hemisphere cavity

Figure 4.10 and Figure 4.11 show the displacement of the driving point on the plane for different boundary conditions and the *in vacuo* case. Due to the cavity's different construction the response varies from the previous example, showing a more ideal behaviour for a plate swinging in an open domain. The stiffness of the coupled system does not influence the modes as strongly as in the previous example and so the added mass effect can now be clearly seen.

Figure 4.10: Driving point displacement with different boundary conditions (air, hemisphere)
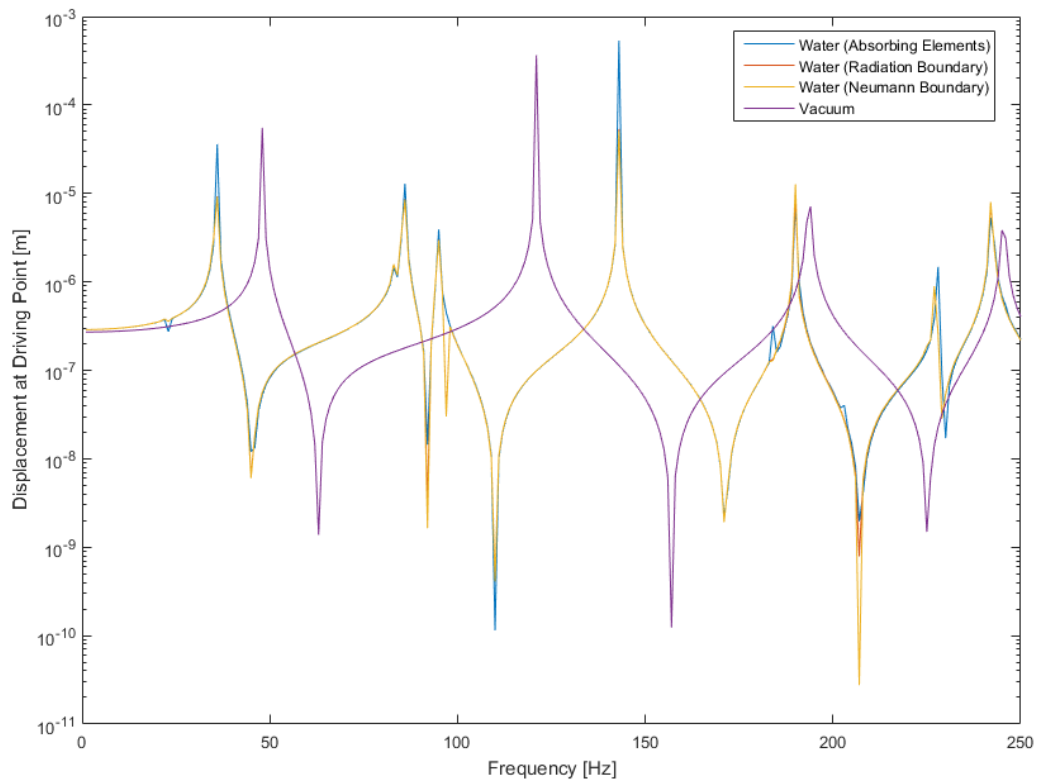


Figure 4.11: Driving point displacement with different boundary conditions (water, hemisphere)

The differences between the absorbing boundary conditions are negligible for the displacement of the driving point, but there are small deviations between the graphs of the radiation boundary and the infinite element boundary at the point in the acoustic cavity in Figure 4.12 and Figure 4.13. Although the radiation damping effect in air can not be seen at the driving point, there is a clear damping effect measuring the acoustic pressure at the point in the cavity. Peaks influenced by the reflection of the Neumann boundary condition are suppresed or reduced when using an absorbing boundary condition.
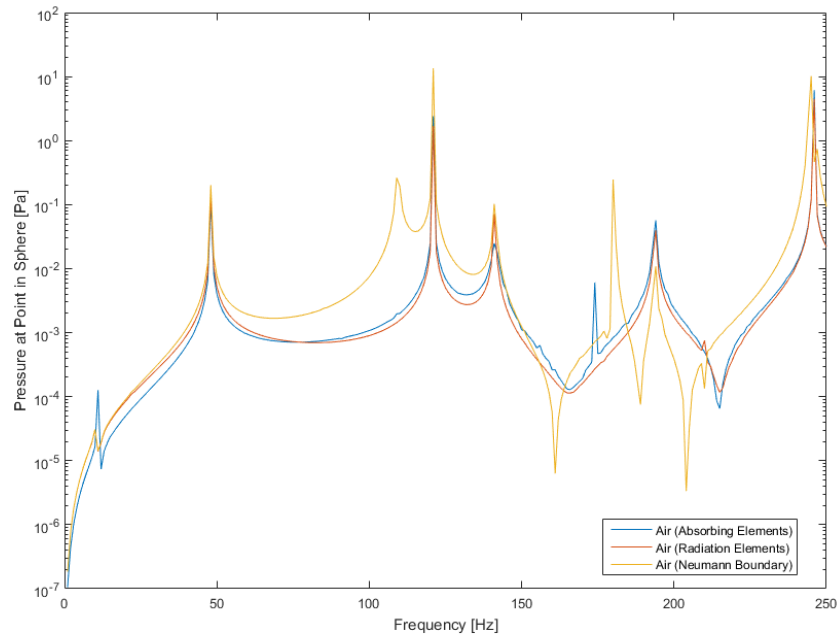


Figure 4.12: Acoustic pressure of $(0.475, 0.675, 0.575)$ with absorbing boundary conditions (air)
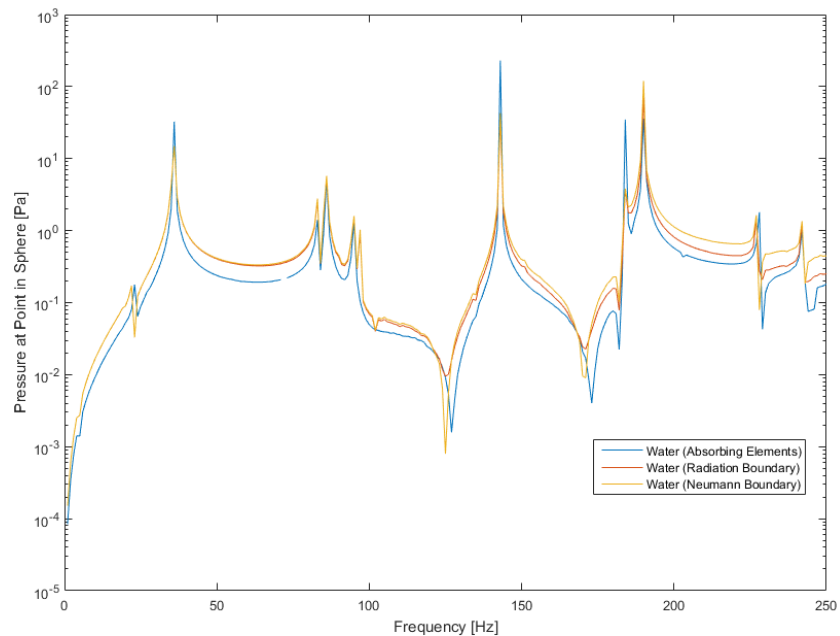


Figure 4.13: Acoustic pressure of $(0.475, 0.675, 0.575)$ with absorbing boundary conditions (water)

# 5  Application Case Studies

To show and analyse the FSI of the vibrating parts of the power train two principle models are being looked at. The first model regards the power train of the wind turbine as one cylindrical module lying in an acoustic medium. The second model treats the power train as a group of parts, showing the generator, the gear box, a brake and the main shaft in the same acoustic fluid. In both cases an outer shell does not exist, reducing the problem to the inner space of the wind turbine cabin.

## 5.1  Cylinder in Air

The model consists of a solid cylinder lying in the acoustic fluid air. The cylinder is forced to vibrate with the harmonic force $F = 1N$ within the frequency range $\Omega = [100: 2000]s^{-1}$ in the y-direction of the model. The cylinder is unsupported. At the outer border of the model the radiation boundary condition is applied, reducing the influence of the reflection within the model.
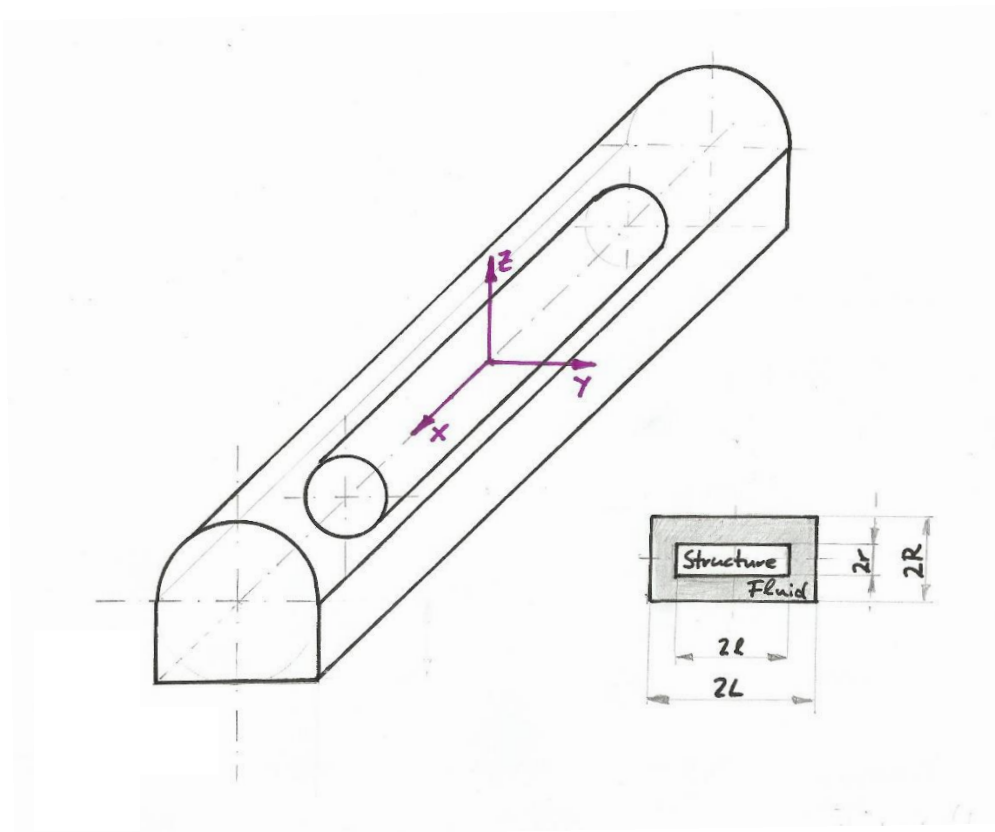


Figure 5.1: Principle model for the FSI of a wind turbine

The cylinder has a length of $2l = 2m$, a radius of $r = 0.25m$ and a thickness of $h = 0.01m$. The acoustic cavity filled with the acoustic fluid air (see Table 4.2) has a length of $2L = 2.5m$ and a radius $R = 0.5$m.

The dominant wave length of the acoustic fluid is

$$\lambda = \frac{c}{f} = \frac{343\frac{m}{s}}{2000\frac{1}{s}} = 0.1715m \tag{5.1}$$

With the element per wave length condition $\frac{\lambda}{h_{\lambda,air}} = 6 \dots 8$ the recommended element size of the fluid can be estimated to

$$h_{\lambda,air} = \frac{\lambda}{6} = \frac{0.1715m}{6} = 0.0286m \tag{5.2}$$

The dominant bending wave length of the cylindrical structure can be determined by

$$\lambda_B = 2\pi \cdot \sqrt[4]{\frac{B}{m'}} \cdot \frac{1}{\sqrt{\omega}} = 2\pi \cdot \sqrt[4]{\frac{5.002 \cdot 10^{16}\frac{kgmm^3}{s^2}}{61.037 \cdot 10^{-3}\frac{kg}{mm}}} \cdot \frac{1}{\sqrt{2\pi \cdot 2000\frac{1}{s}}} = 1686.41mm \tag{5.3}$$

$$B = E \cdot I = 2.1 \cdot 10^5 \frac{N}{mm^2} \cdot \frac{\pi}{64}(500^4 - 490^4)mm^4 = 5{,}002 \cdot 10^{13}\ Nmm^2$$

$$= 5{,}002 \cdot 10^{16}\frac{kgmm^3}{s^2}$$

$$m' = \rho \cdot A = 7850\frac{kg}{m^3} \cdot \frac{\pi}{4}(0.5^2 - 0.49^2)m^2 = 61.037\frac{kg}{m} = 61.037 \cdot 10^{-3}\frac{kg}{mm}$$

whereby the moment of inertia $I$ and the Area $A$ are related to an open cylinder. As the recommended element size of the structure is

$$h_{\lambda,structure} = \frac{1.68641m}{6} = 0.2812m \tag{5.4}$$

and the chosen element length is $h_{\lambda,structure,chosen} = 0.05m$ this simplification is not affecting the results. The model is calculated with the fluid element size $h_{\lambda,air} = 0.03m$ for frequencies under $f = 1000\ Hz$ and $h_{\lambda,air} = 0.05m$ for frequencies above. A constant damping ratio of $D = 0.002$ is applied.

Figure 5.2 shows the frequency response at $(0,0,0.25)m$ of the uncoupled cylinder. The bending modes of the cylinder are at a frequency of $f = 514\ Hz$, $f = 1068Hz$ and $f = 1594\ Hz$. The other peaks correspond to either bending modes of the closed cylinder's caps, extensional modes or radial shearing modes. As the bending modes in the normal direction of the applied harmonic force causes the highest radiation of sound into the acoustic medium they are the only modes being looked at during further investigations, showing the influence of mass, stiffness and damping variation on each of the corresponding modes.
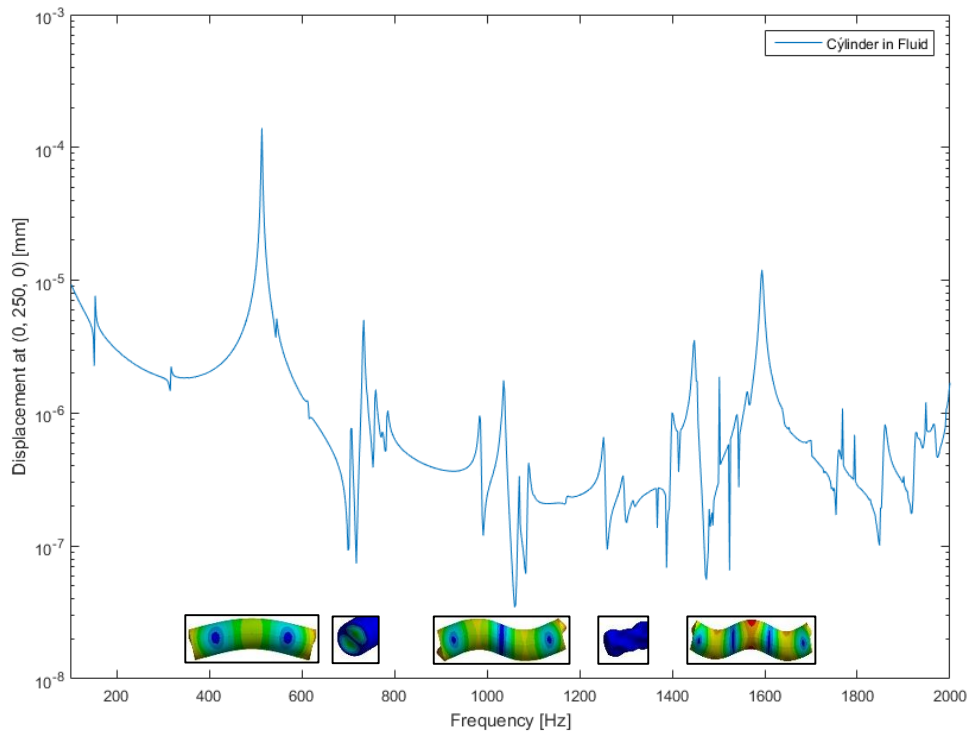
Figure 5.2: Displacement of the cylinder at (0, 250, 0) and corresponding mode shapes
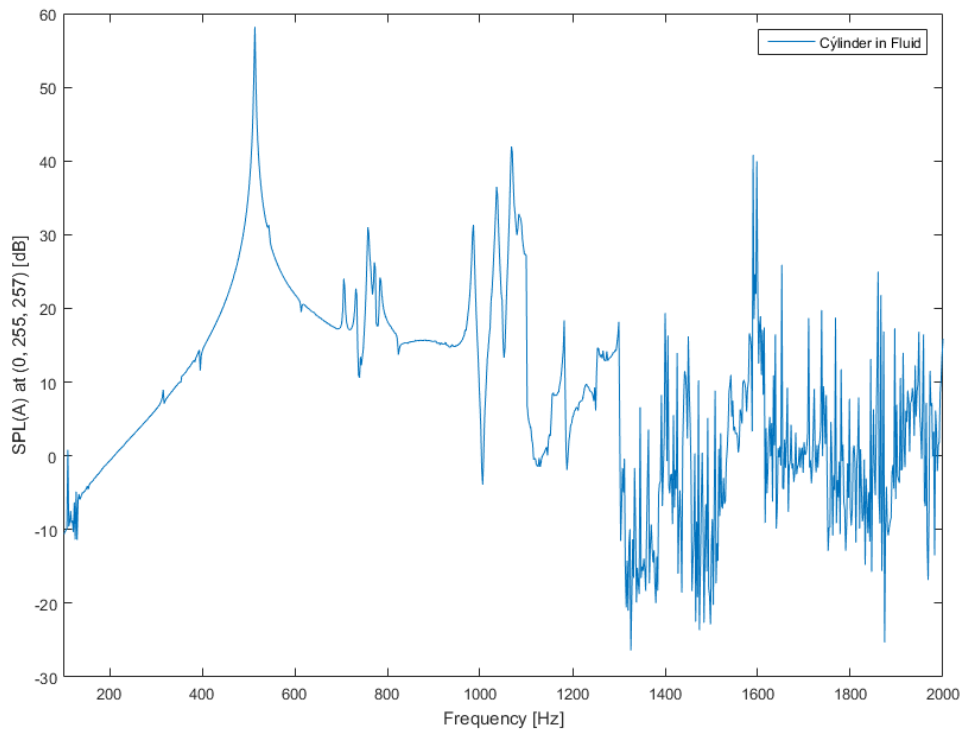


Figure 5.3: SPL(A) at (0, 255, 257)

### 5.1.1 Constructive Modifications

The behaviour of a discrete system can easily be changed by constructive modifications influencing the present mass, stiffness and damping characteristics. In most of the cases the adjustment of the eigenfrequency to a higher or lower frequency level plays a dominant role, depending on the working frequencies of a machine.

To influence the eigenfrequency of the structure in a first step the mass of the cylinder is augmented by a distributed mass, shared in equal parts on every knot of the system. In a next step the areas of the added mass are reduced to the areas of highest displacement at the eigenfrequencies. These concentrated mass areas are then replaced by point masses.

In a similar way the thickness of the system will be variated to show the influence of the system's stiffness. The thickness of the cylinder is then adjusted to the areas of highest displacement during the modes by the use of attached patches.

This is followed by the use of tuned mass dampers, which influence the behaviour of the dominant mode dramatically and can be used to reduce the radiated sound pressure, if well designed.

**Addition of an equally distributed mass**

The influence of the mass on a vibrating system plays a dominant role, e.g. a lighter system is easily excited to swing with a higher frequency than the corresponding heavy system. As the radiation of sound is influenced by the amplitude and frequency of the vibrating system, the acoustic pressure can be efficiently decreased by adding an equally distributed mass to the system. To adequately reduce the second and third mode a relatively heavy mass is needed.
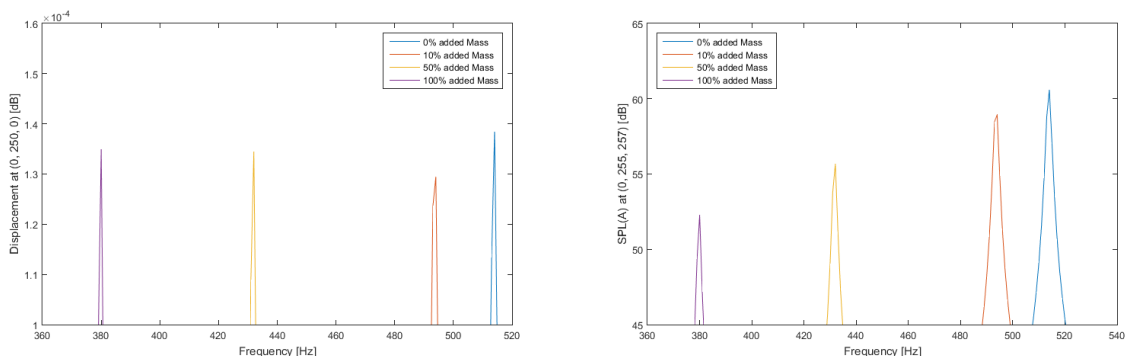


Figure 5.4: First Mode displacement at (0, 250, 0) and SPL(A) at (0, 255, 257) with added mass
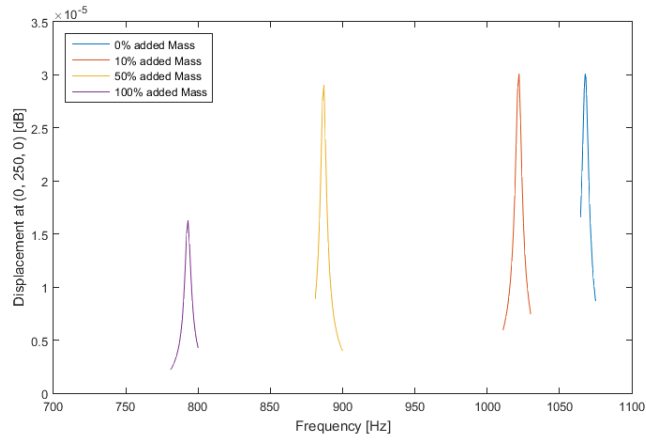
Figure 5.5: Second mode displacement at (-500, 250, 0) with added mass
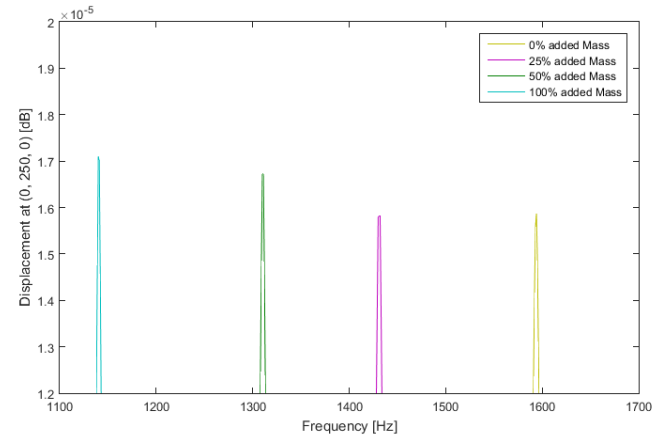


Figure 5.6: Third mode displacement at (0, 250, 0) with added mass
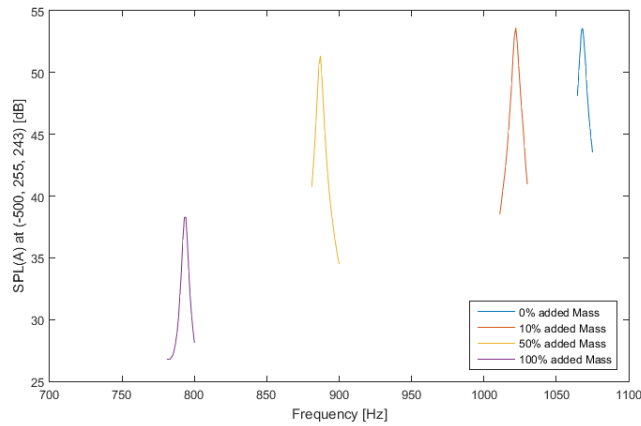


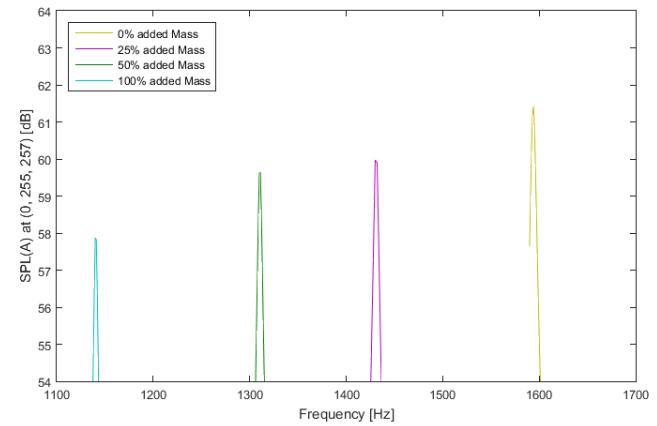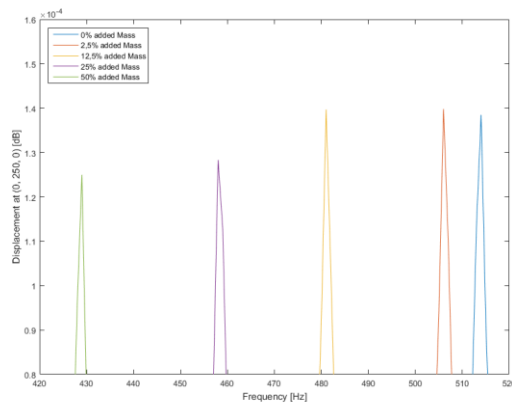Figure 5.7: Second mode SPL(A) at (-500, 255, 257) with added mass



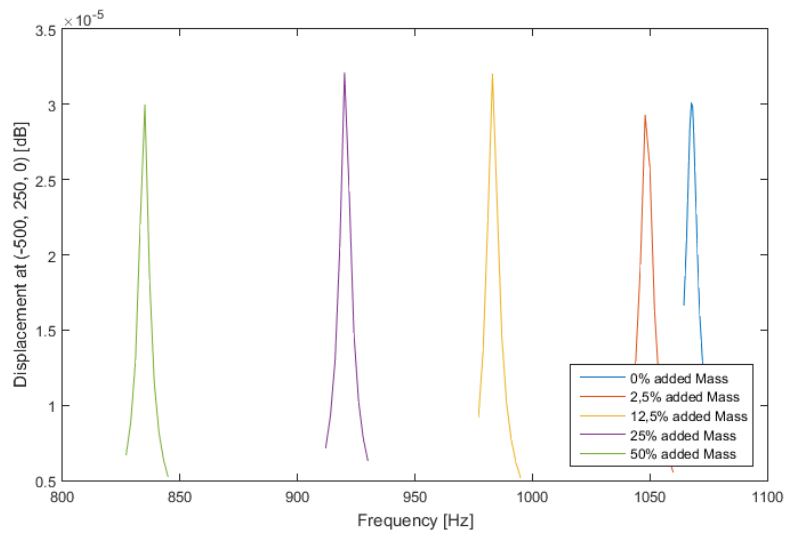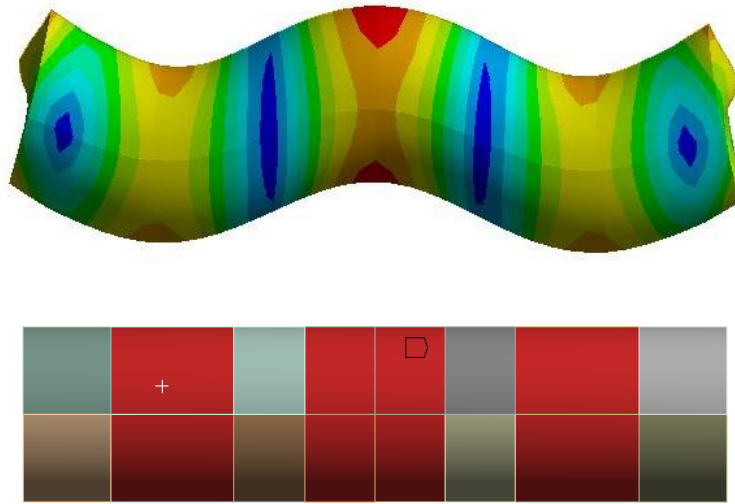Figure 5.8: Third mode displacement at (0, 255, 257) with added mass

**Distributed mass on selected area**

Adding an equally distributed mass on the areas of highest displacement shows nearly the same behaviour as adding the same mass onto the whole surface. Figure 5.9, Figure 5.12 and Figure 5.15 show the areas with the attached weight.
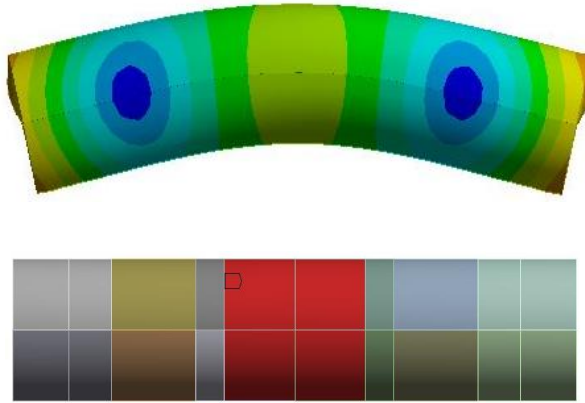


Figure 5.9: First mode and selected area



Figure 5.10: First mode displacement at (0, 250, 0) with area-wide mass
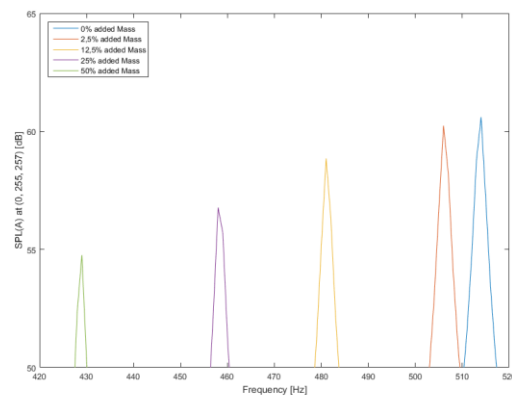


Figure 5.11: First mode SPL(A) at (0, 255, 257) with area-wide mass

41
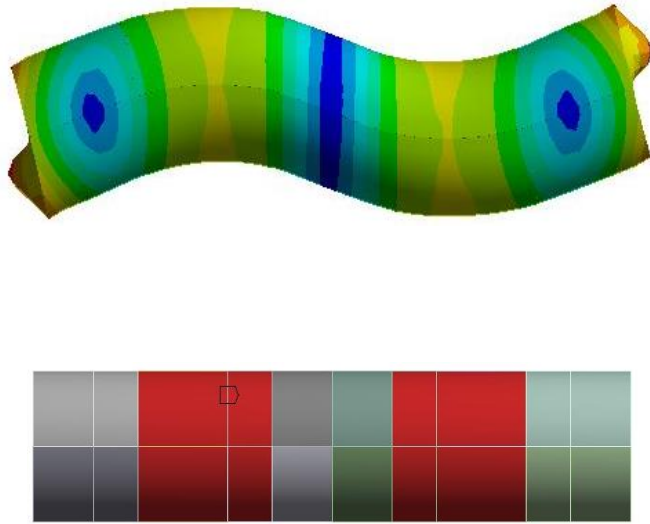
Figure 5.12: Second mode and selected area



Figure 5.13: Second mode displacement at (-500, 250, 0) with area-wide mass
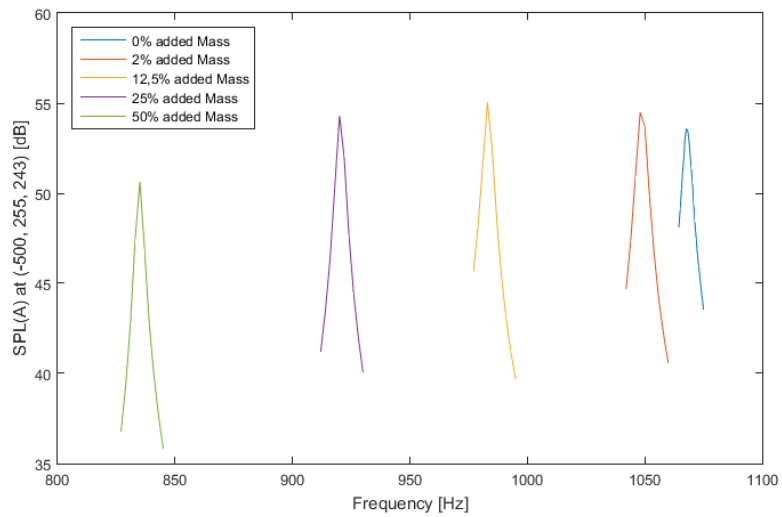


Figure 5.14: Second mode SPL(A) at (-500, 255, 243) with area-wide mass

Figure 5.15: Third mode and selected area
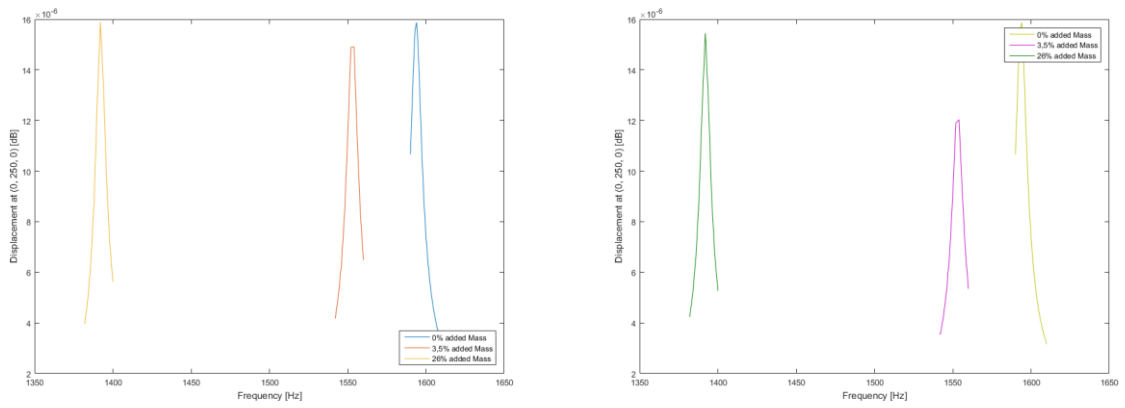


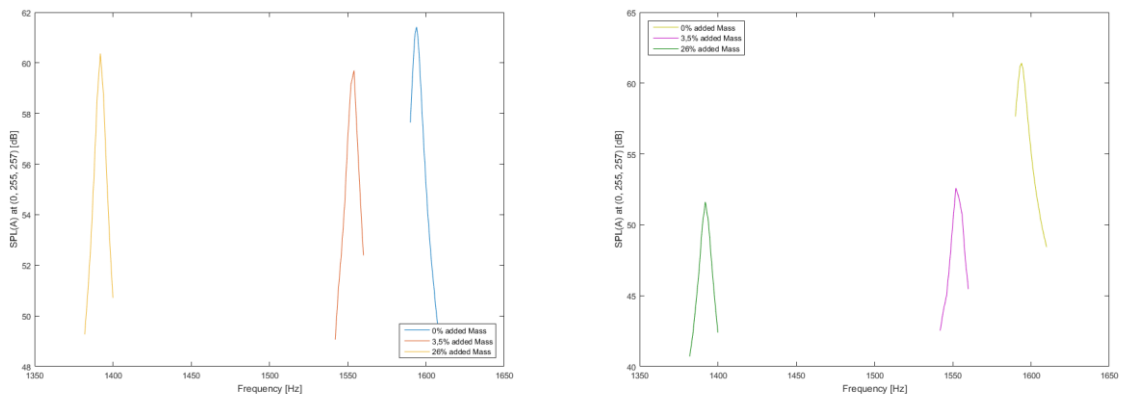Figure 5.16: Third mode displacement at (0, 250, 0) and (-500, 250, 0) with area-wide mass



Figure 5.17: Third mode SPL(A) at (0, 255, 257) and (-500, 255, 243) with area-wide mass

**Addition of point masses**

Adding point masses to the system can augment or reduce the radiation of sound into the surrounding medium, depending on the placement of the point masses onto the system. Figure 5.18, Figure 5.21 and Figure 5.24 show an example for point masses attached to the system optimised for the dominant modes of the system. The SPL(A) is trimmed with a higher value, as it is by the attachment of an equally distributed mass.
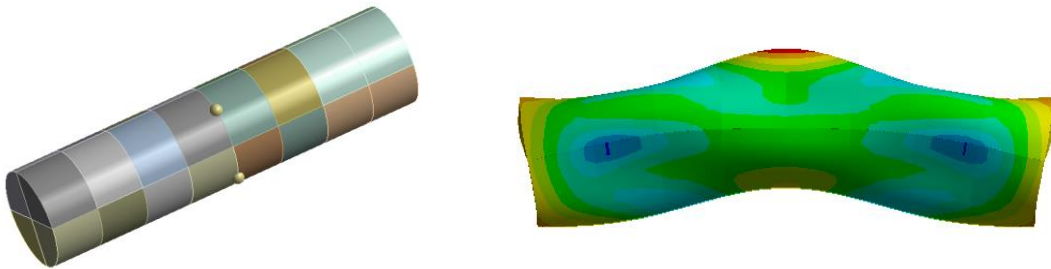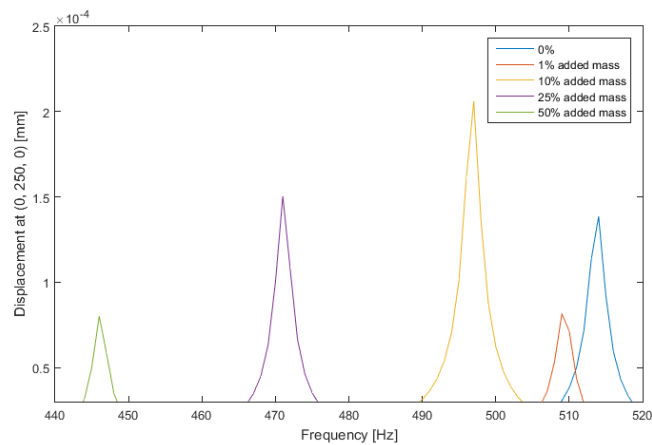


Figure 5.18: Attached point masses and influenced first mode shape



Figure 5.19: First displacement at (0, 255, 0) with added point masses
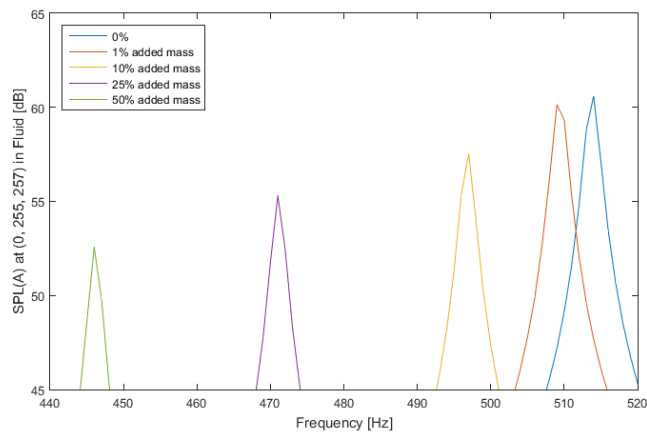


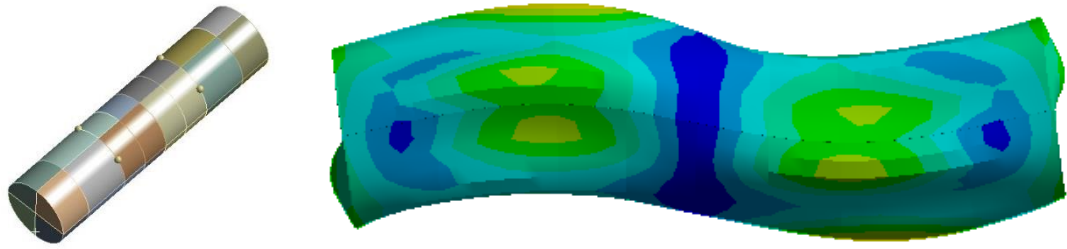Figure 5.20: First mode SPL(A) at (0, 255, 257) with added point masses

Figure 5.21: Attached point masses and influenced second mode shape
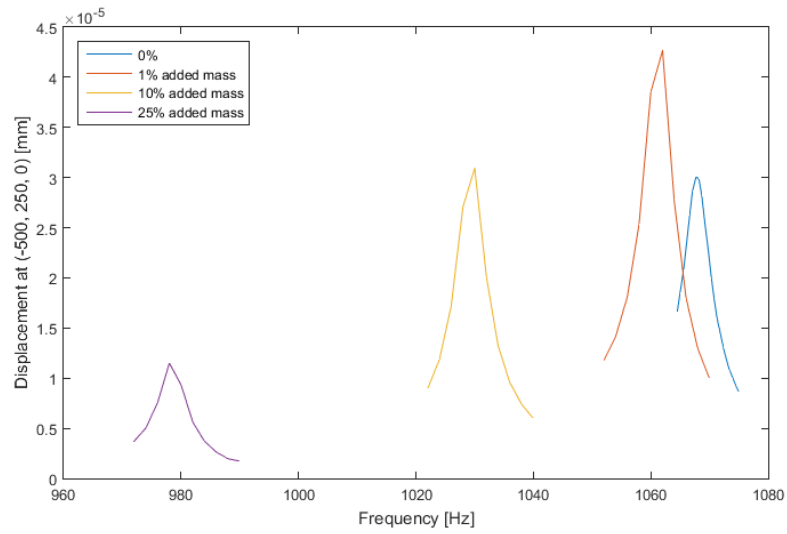


Figure 5.22: Second mode displacement at (0, 250, 0) with added point masses
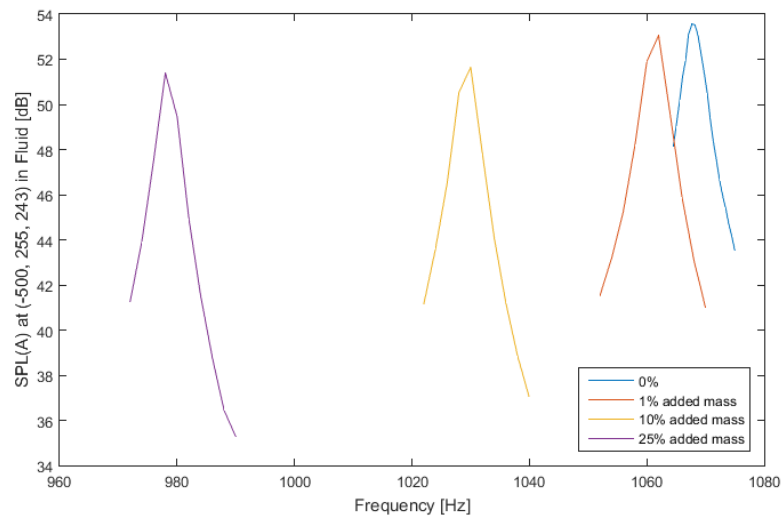


Figure 5.23: Second mode SPL(A) at (-500, 255, 257) with added point masses
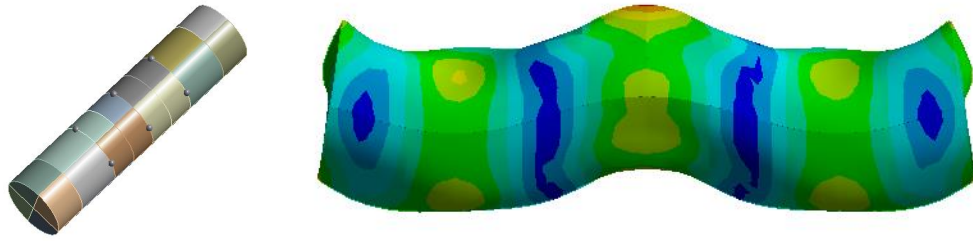
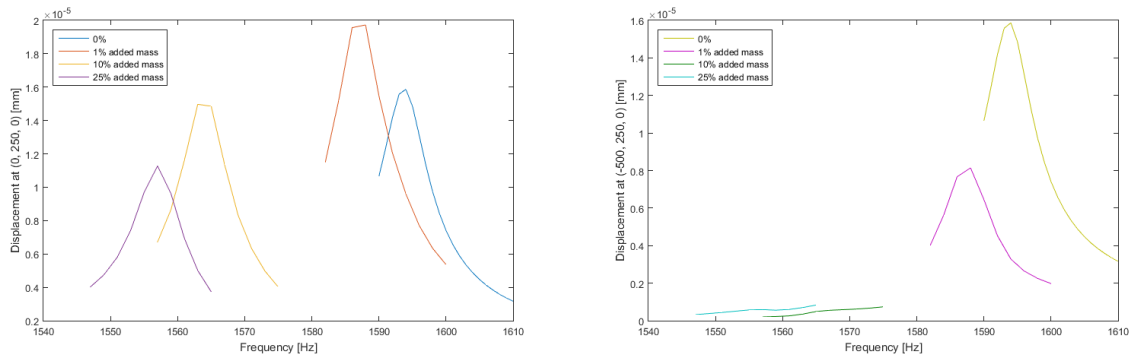Figure 5.24: Attached point masses and influenced third mode shape



Figure 5.25: Third mode displacement at (0, 250, 0) and (-500, 250, 0) with added point masses
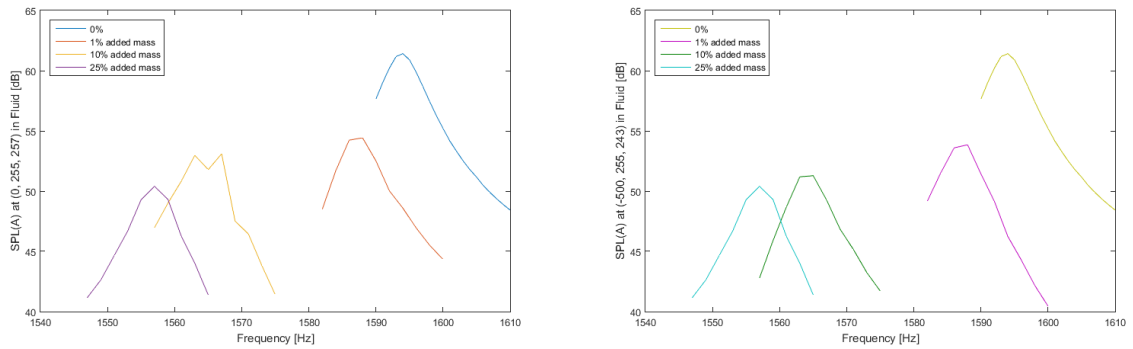


Figure 5.26: Third mode SPL(A) at (0, 255, 257) and (-500, 255, 243) with added point masses

**Variation of the thickness**

Varying the thickness of the system's outer shell results in a higher frequency due to the added stiffness effect. By increasing the weight of the system dramatically the damping effect shows an excellent reduction of the SPL for the mode shapes with a non-zero average flux over the interface (in this case the first and the third mode). The second mode first reacts by an added stiffness effect, but then changes to an added mass effect, reducing the frequency in a forceful way.
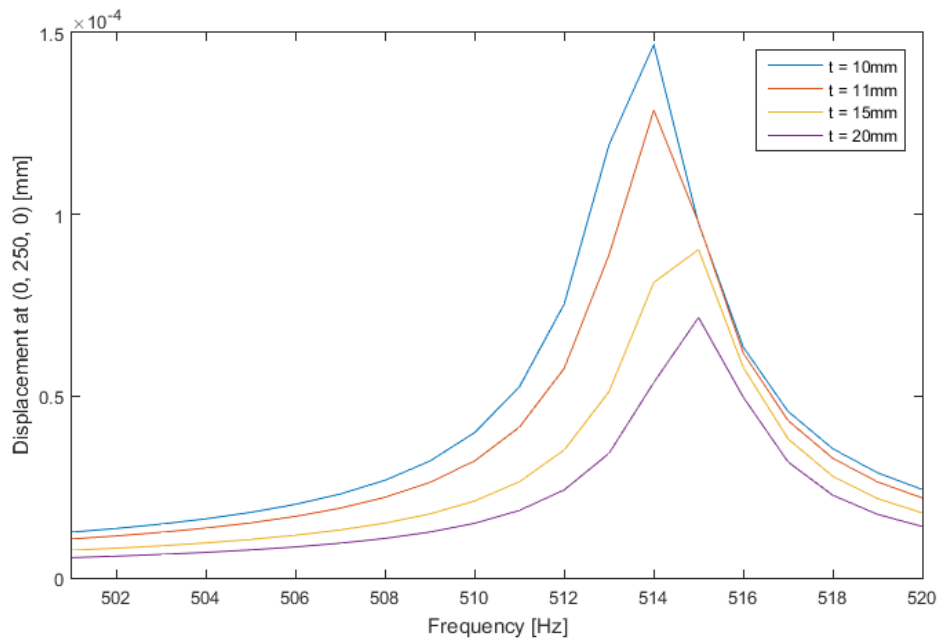


Figure 5.27: First mode displacement at (0, 250, 0) with added thickness
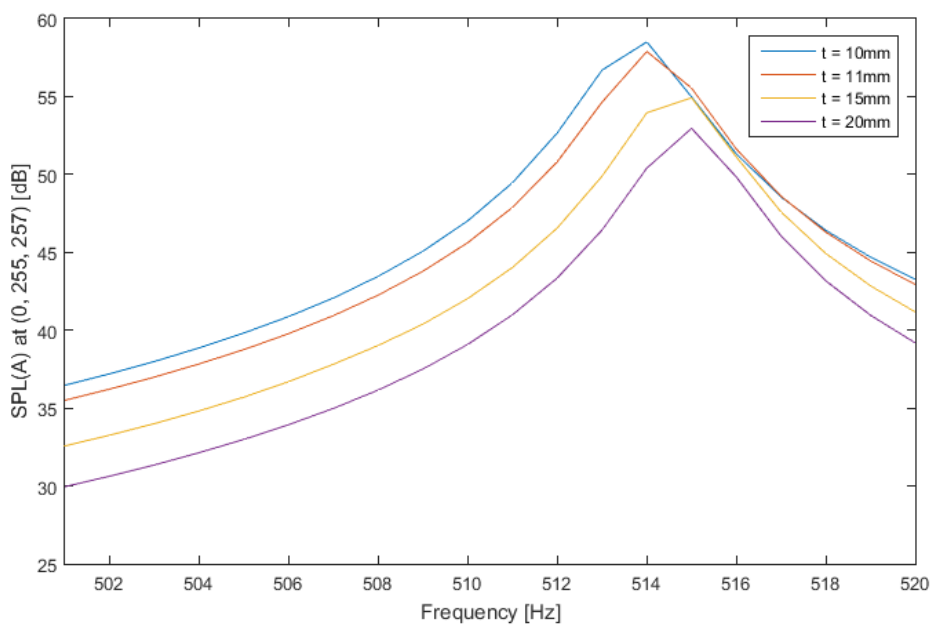


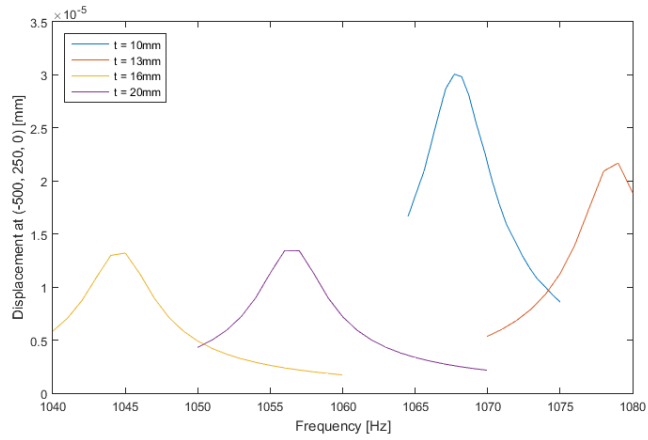Figure 5.28: First mode SPL(A) at (0, 255, 257) with added thickness

Figure 5.29: Second mode displacement at (-500, 250, 0) with added thickness
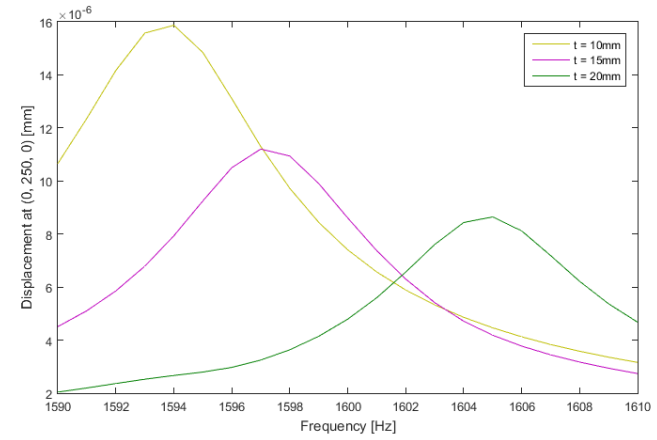


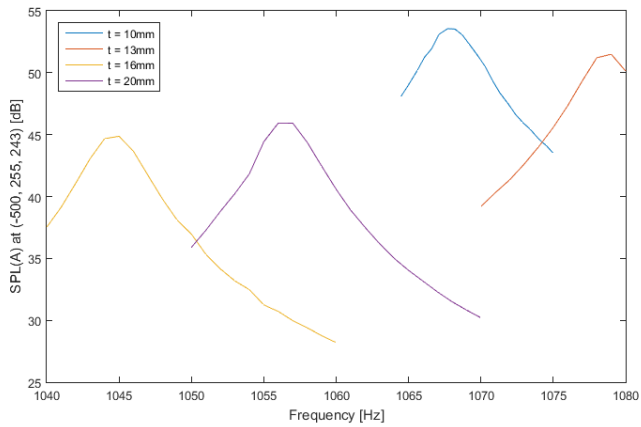Figure 5.30: Third mode displacement at (0, 250, 0) with added thickness



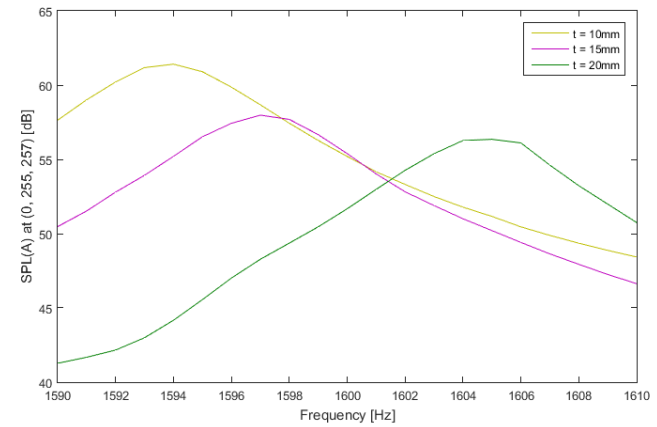Figure 5.31: Second mode SPL(A) at (-500, 255, 243) with added thickness



Figure 5.32: Third mode SPL(A) at (0, 255, 257) with added thickness

**Addition of patches**

To influence the modes directly, patches according to Figure 5.9, Figure 5.11 and Figure 5.15 are attached to the system in the regions of highest displacement. It is a good choice to reduce the sound pressure without heavily increasing the weight of the system. Figure 5.33 to Figure 5.36 show the displacement and SPL(A) for a patch with the same material as the original system; so it appears more along the lines of a variation of the outer shell thickness on selected areas. The added patches can be made from different materials, e.g. sound absorbing bitumen, butyl rubber materials or materials with higher modal damping values.

The damping of the radiated sound pressure is more efficient if the added masses are huge. In case of the second mode, the added thickness has to be larger than $t = 15mm$ to show any improvement on the radiated sound pressure at all. By augmenting the mass on the patches for the side peaks of the third mode (Figure 5.36, right graph), the radiation of sound pressure could be improved for the cases with a high middle peak's patch thickness $t_1$.
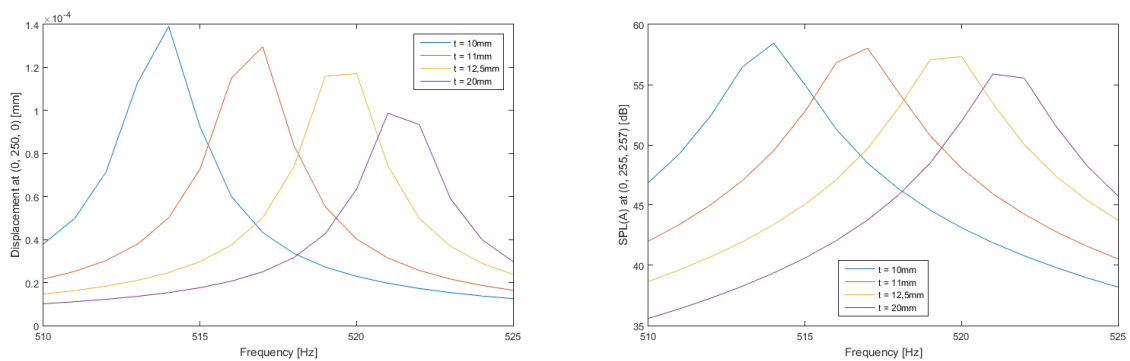


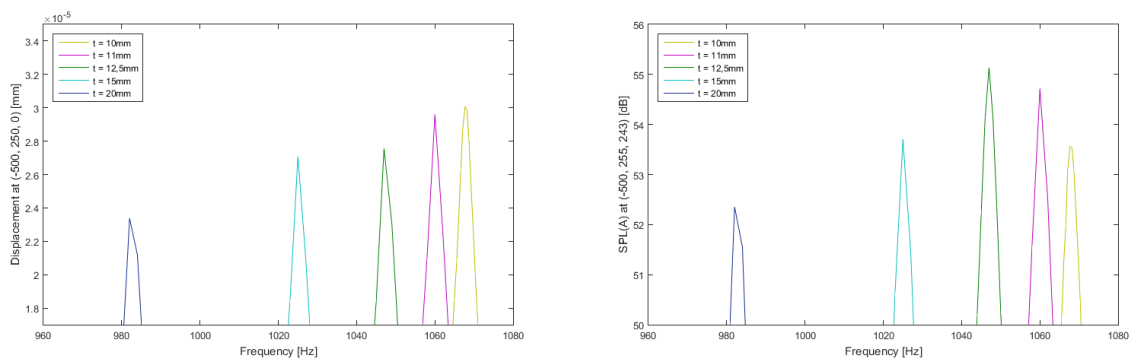Figure 5.33: First mode displacement at (0, 250, 0) and SPL(A) at (0, 255, 257) with patch



Figure 5.34: Second mode displacement at (-500, 250, 0) and SPL(A) at (-500, 255, 243) with patches
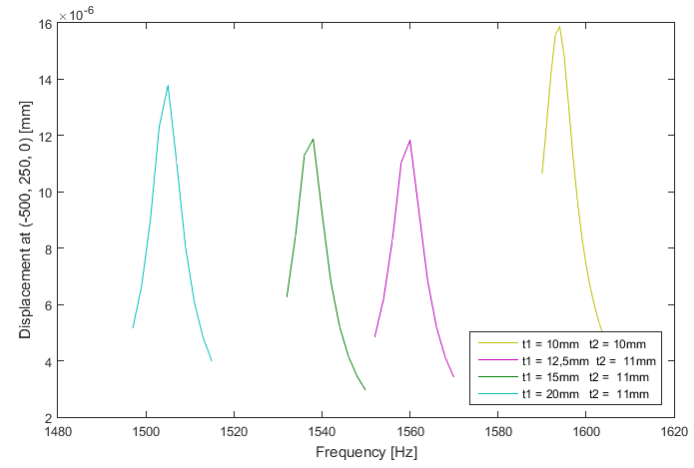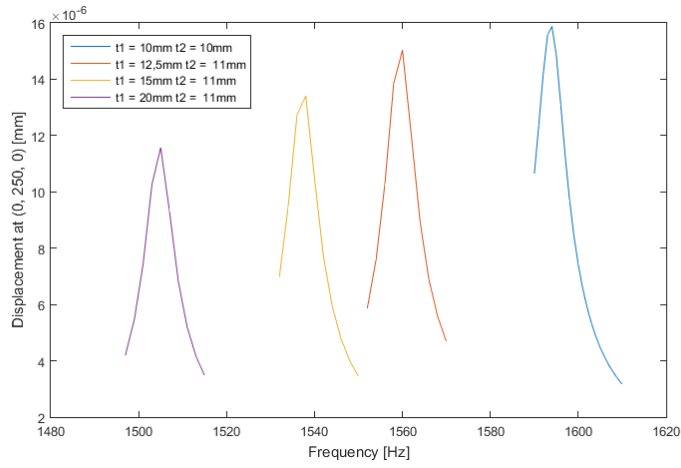
Figure 5.35: Third mode displacement at (0, 250, 0) and (-500, 250, 0) with added patches
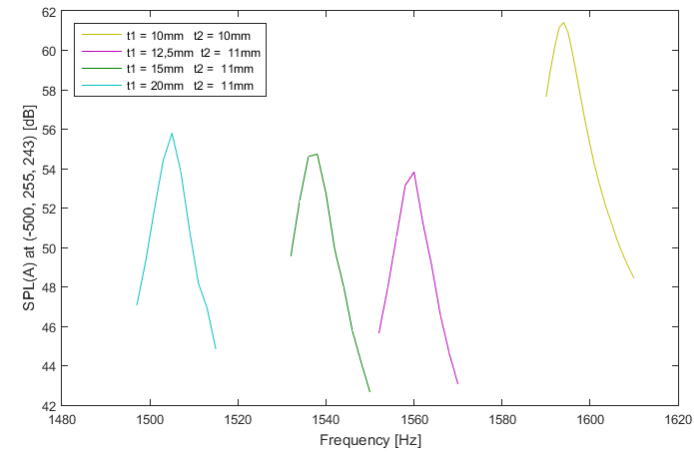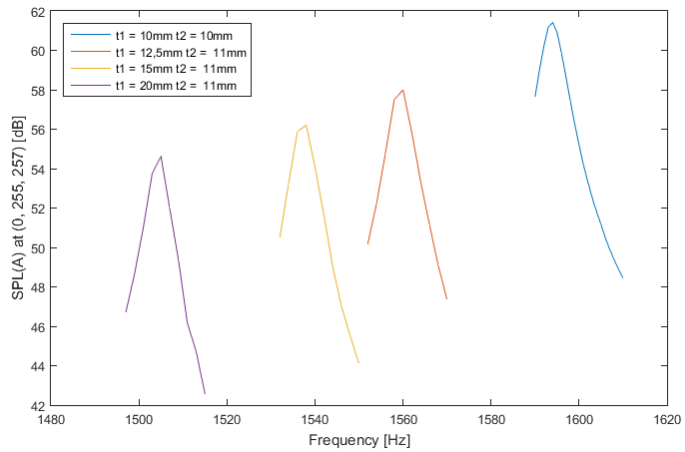


Figure 5.36: Third mode SPL(A) at (0, 255, 257) and (-500, 255, 243) with added patches

**Addition of a tuned mass damper**

Tuned mass dampers are used to reduce the vibration response of single dominant peaks. The tuned mass damper is a mass oscillator attached to the vibrating system, which is constructed to have the same eigenfrequency as the peak that is to be reduced. The dominant peak is reduced in an efficient way, but two additional peaks will occur to both sides of the peak, according to the stiffness and mass of the used tuned mass damper. Unfortunately, these peaks will radiate sound when excited, so a well-coordinated design of the tuned mass damper is necessary to not create a louder acoustic source.
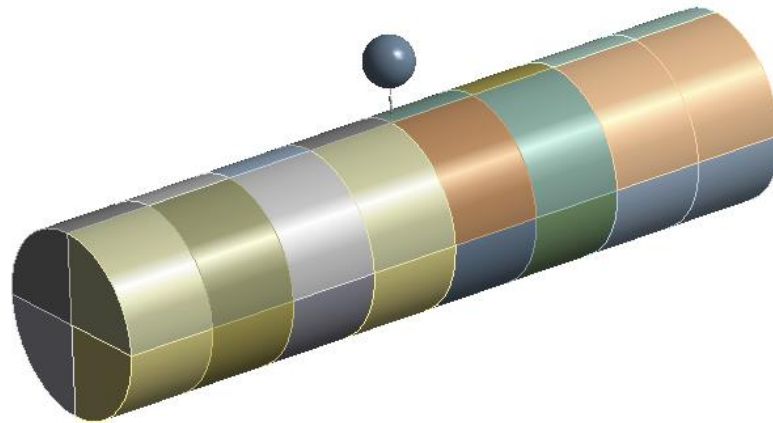


Figure 5.37: Tuned mass damper attached to the cylinder for the first and third mode

The displayed tuned mass damper in Figure 5.37 consists of a sphere with the mass $m$ and a spring with the stiffness $k$ balanced to the natural frequency $\omega$ of the dominant peak. Table 5.1 shows the parameters for each of the dominant modes within the frequency range.

| | Frequency of the mode shape Hz | | |
|---|---|---|---|
| | 514 | 1068 | 1594 |
| **Mass** kg | **Stiffness of the spring** N/m | | |
| 0,1 | $10430.4 \cdot 10^2$ | | |
| 1 | $10430.4 \cdot 10^3$ | $45030.31 \cdot 10^3$ | $100308.18 \cdot 10^3$ |
| 10 | $10430.4 \cdot 10^4$ | | |
| 100 | $10430.4 \cdot 10^5$ | | |

Table 5.1: Parameter for tuned mass damper

Figure 5.38 and Figure 5.39 show the first mode displacement and SPL(A) with tuned mass dampers of different masses. It can be shown that the created peak of dominated stiffness is converging to a frequency, whereas the mass dominated peak is lowering its frequency due to the added mass effect. By increasing the mass of the tuned mass damper the radiated SPL of the stiffness dominated peak is rising as well, whereas the SPL of the mass dominated peak is decreasing with the decline of the frequency.

Figure 5.42 shows an example of a badly coordinated tuned mass damper design, as the mass dominated peak's SPL(A) is higher than the SPL(A) of the original system. Adding a higher mass to the tuned mass damper could solve this problem, but this will lead to the increase of the second peak; which is almost on the same level as the dominant peak of the system without a tuned mass damper. Consequently, other constructive modifications should have priority.
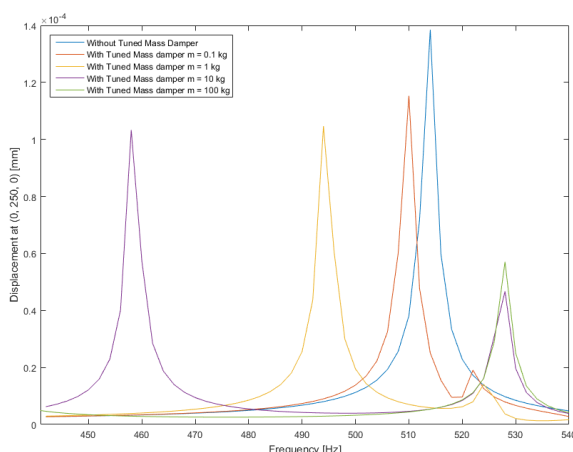


Figure 5.38: First mode displacement at (0, 250, 0) with added tuned mass damper
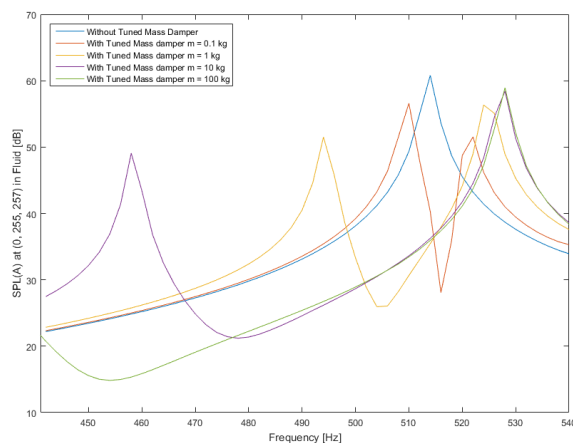


Figure 5.39: First mode SPLA at (0, 255, 257) with added tuned mass damper
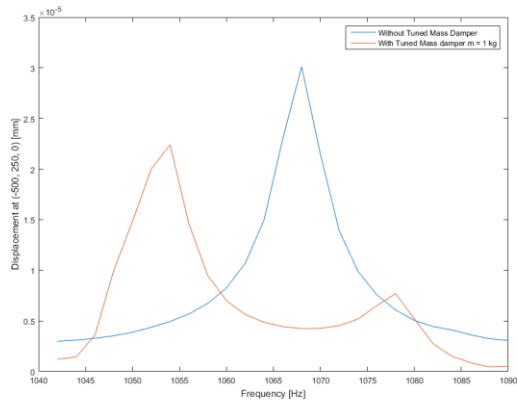
Figure 5.41: Second mode displacement at (-500, 250, 0) with tuned mass damper
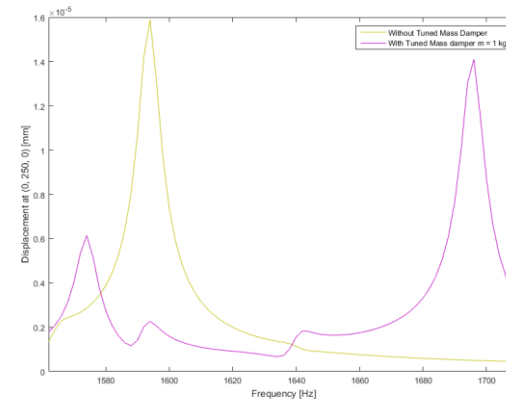


Figure 5.40: Third mode displacement at (0, 250, 0) with tuned mass damper
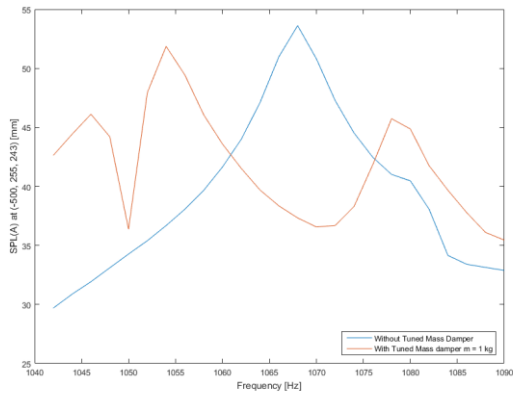


Figure 5.43: Second mode SPL(A) at (-500, 255 ,243) with tuned mass damper
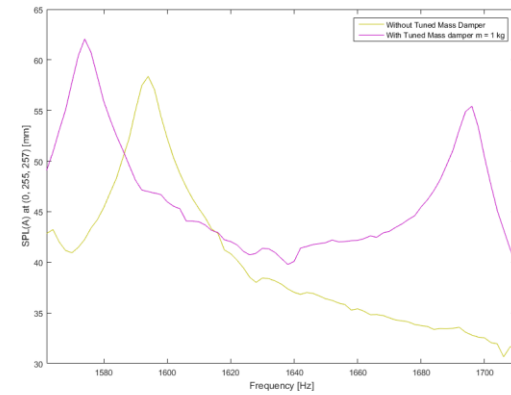


Figure 5.42: Third mode SPL(A) at (0, 255, 257) with tuned mass damper

## 5.2    Power Train in Air

The simplified model shows a power train (consisting of a gear box, a generator, a break, and a part of the main shaft) lying in the acoustic fluid air. The parts of the power train are forced to vibrate with the harmonic force $F = 1N$ within the frequency range $\Omega = [100: 2000]s^{-1}$ in the x-direction of the model. The model is unsupported and a constant damping ratio of $D = 0.002$ is used. At the outer border of the model the radiation boundary condition is applied.
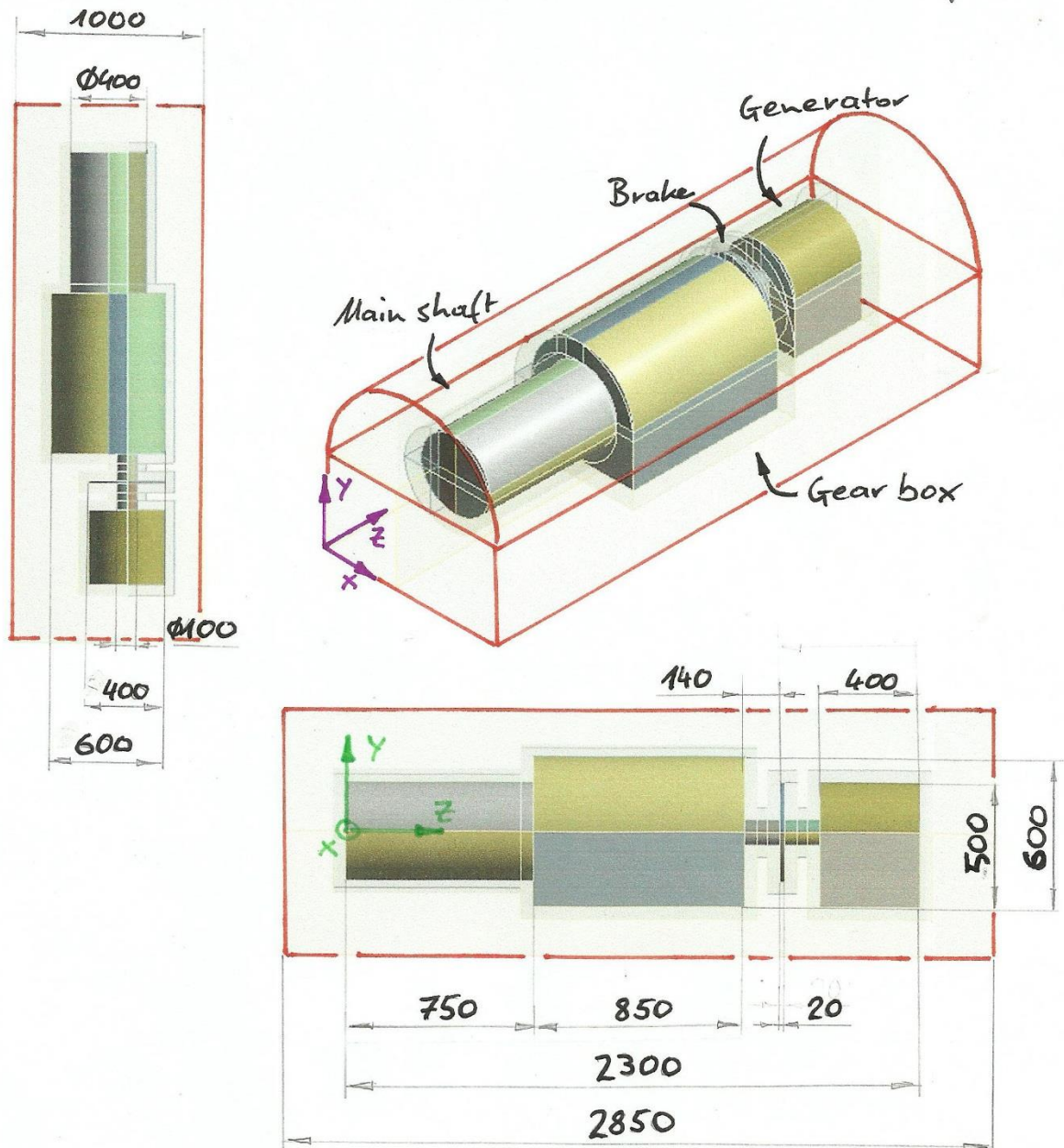


Figure 5.44: Power train in air

54
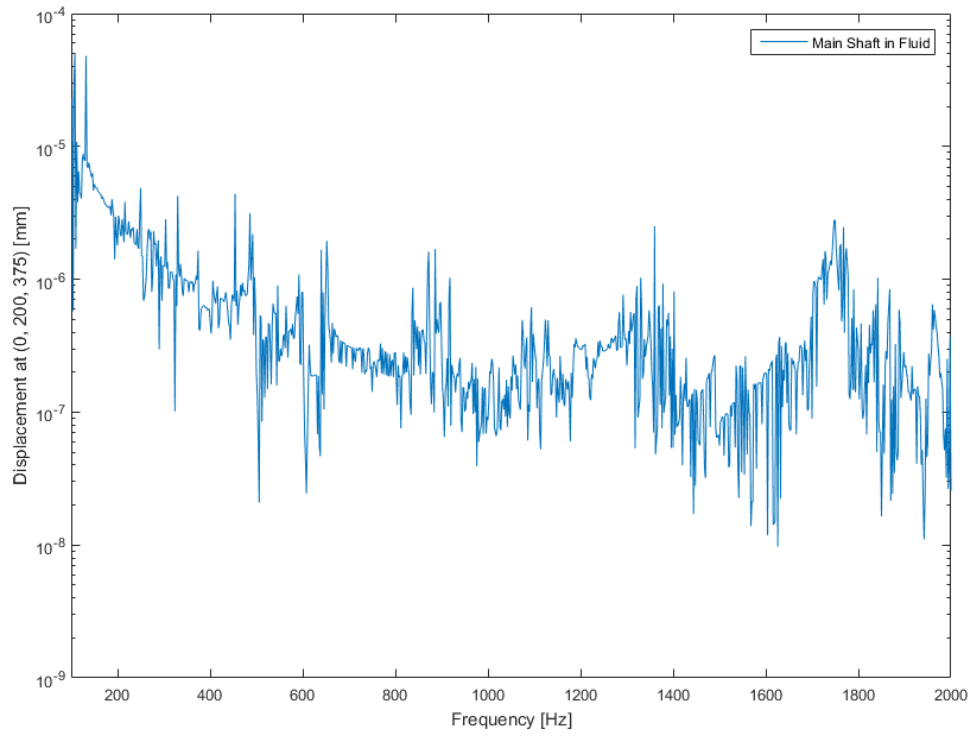
Figure 5.45: Main shaft displacement at (0, 200, 375)
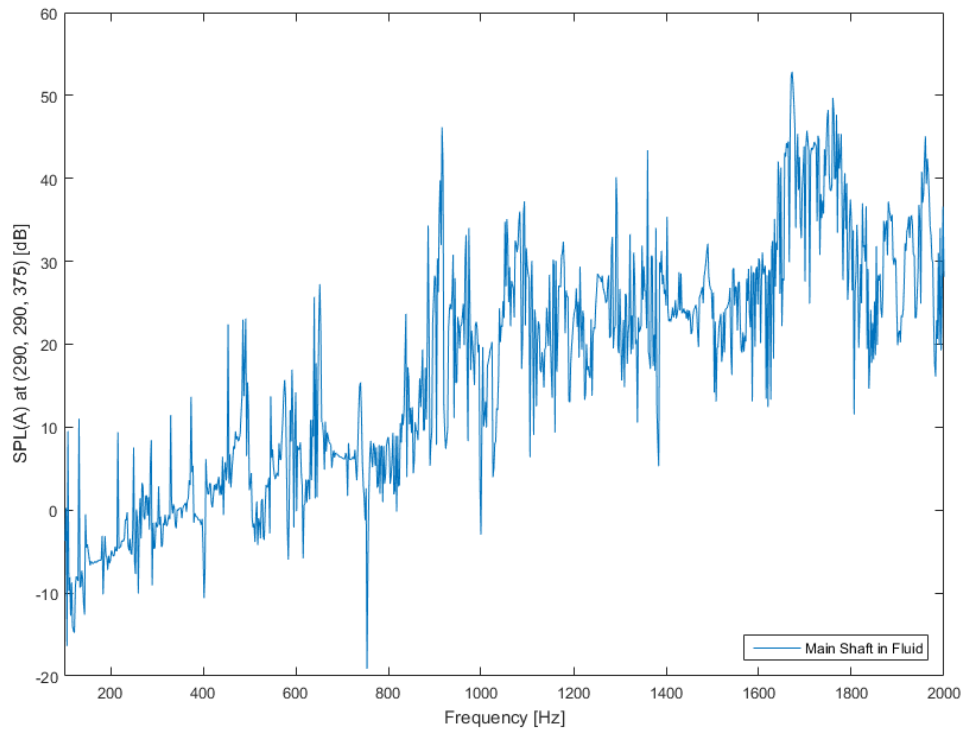


Figure 5.46: Main shaft SPL(A) at (290, 290, 375)
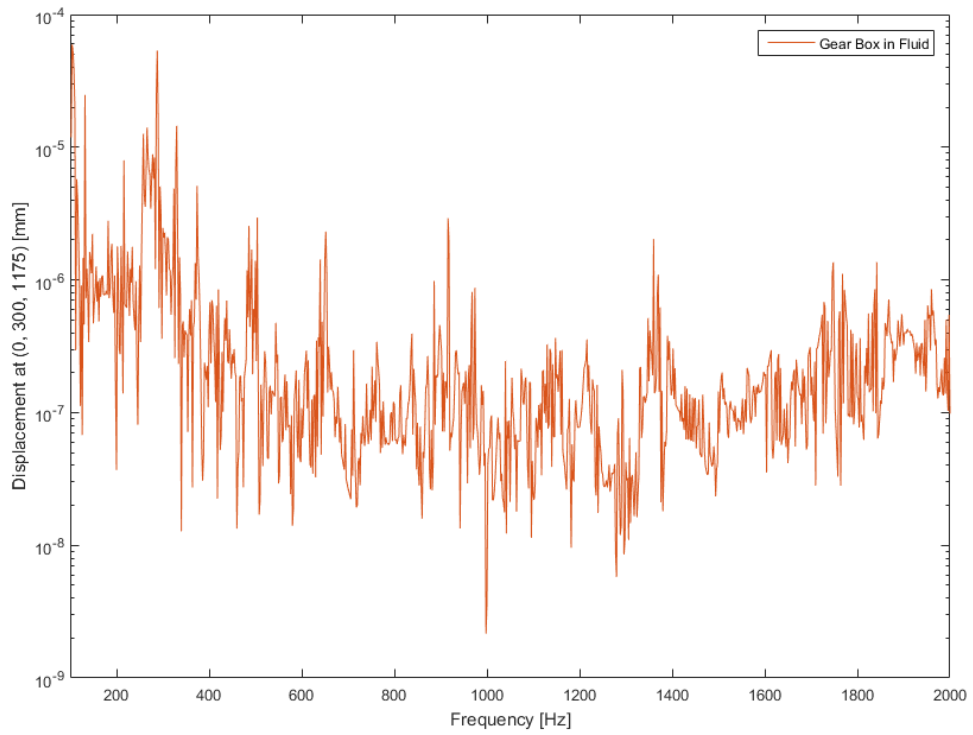
Figure 5.47: Gear box displacement at (0, 300, 1175)
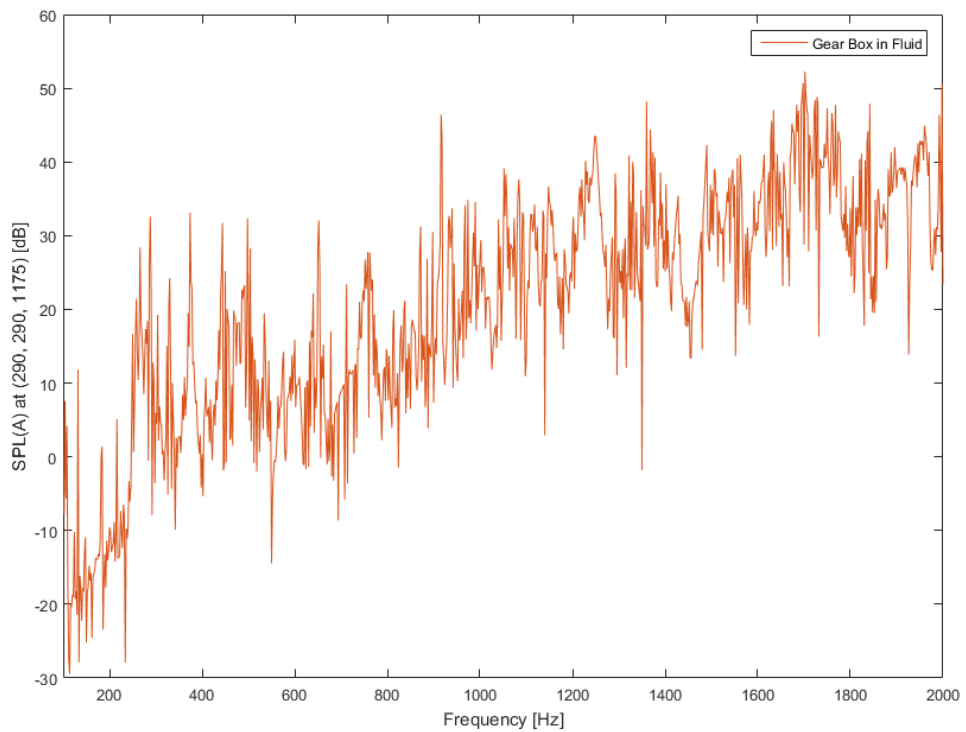


Figure 5.48: Gear Box SPL(A) at (290, 290, 1175)
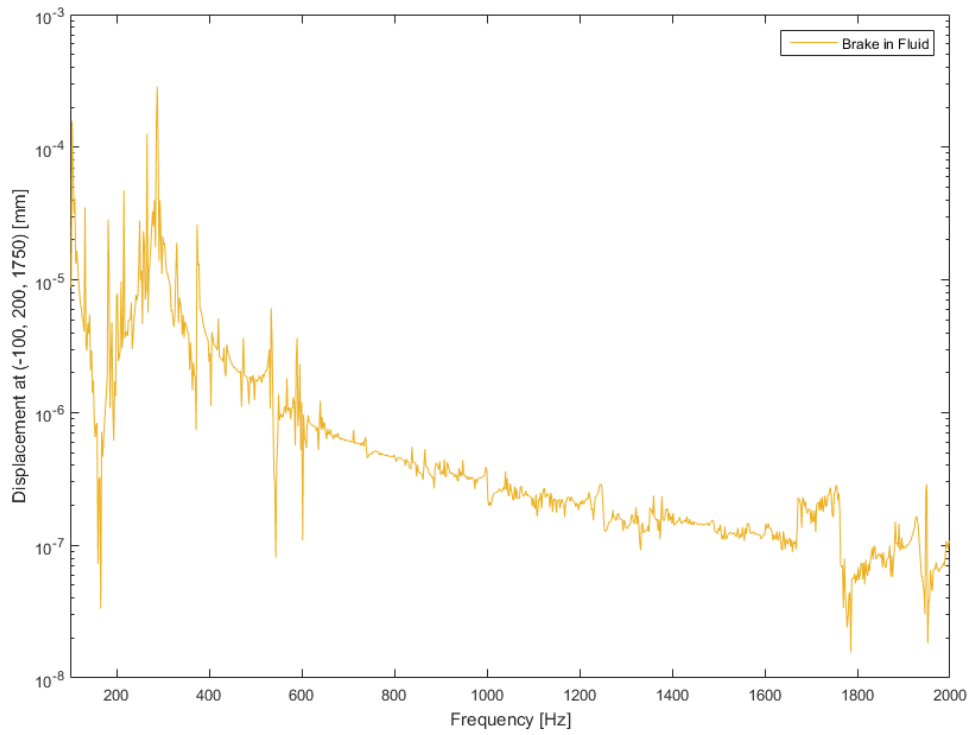
Figure 5.49: Brake displacement at (-100, 200, 1750)
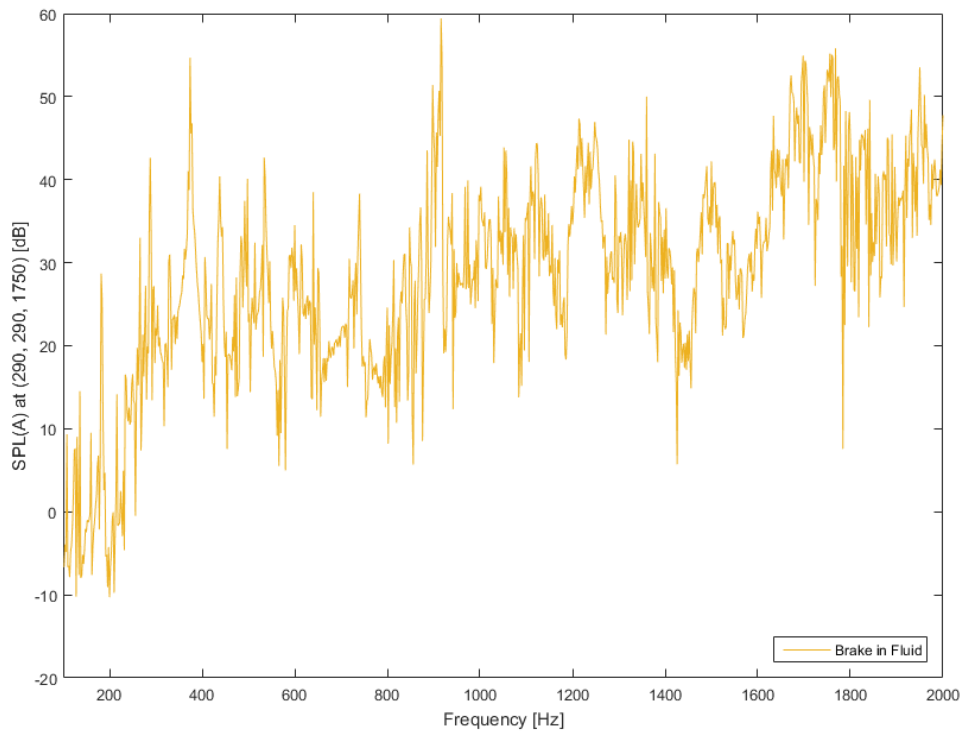


Figure 5.50: Brake SPL(A) at (290, 290, 1750)
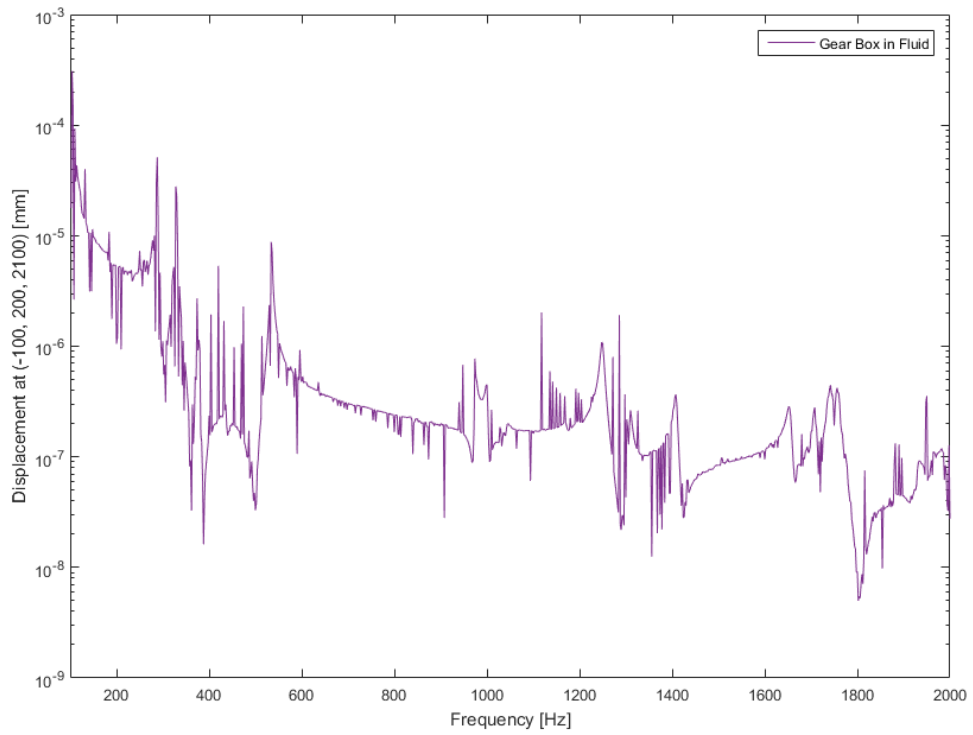
Figure 5.51: Generator displacement at (-100, 200, 2100)
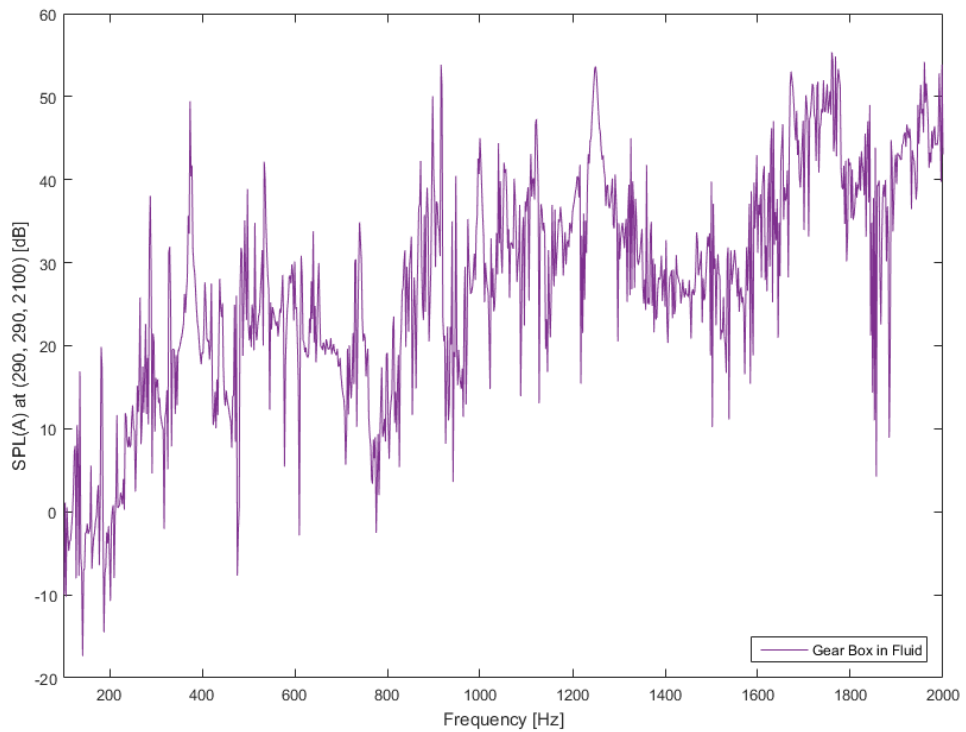


Figure 5.52: Generator SPL(A) at (290, 290, 2100)

## 5.2.1    Constructive Modifications

As the SPL augment along with the frequency, constructive modification of the mass is realised for the frequency of $f = 1766\ Hz$ as an example. At this frequency the generator of the power train shows some mode shapes. The modification is applied to the generator only.
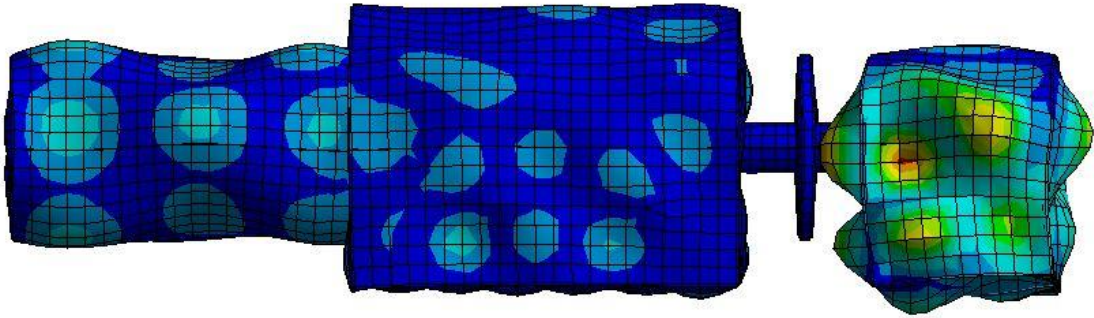


Figure 5.53: Displacement figure of the power train at 1766 Hz
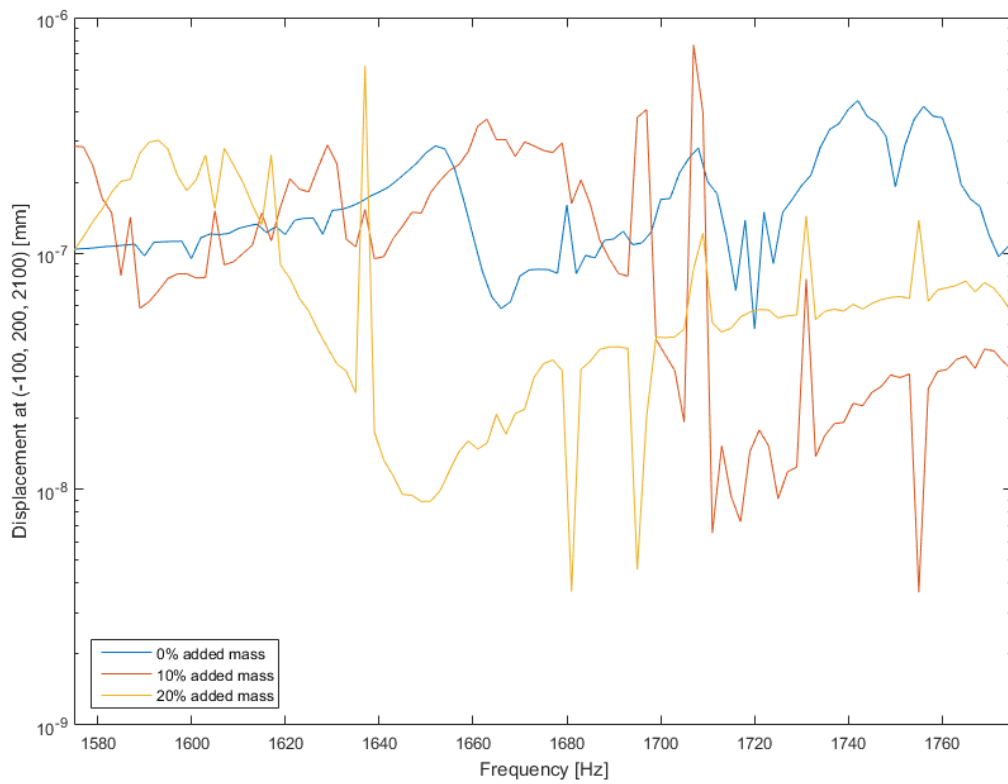


Figure 5.54: Generator displacement at (-100, 200, 2100) with added mass
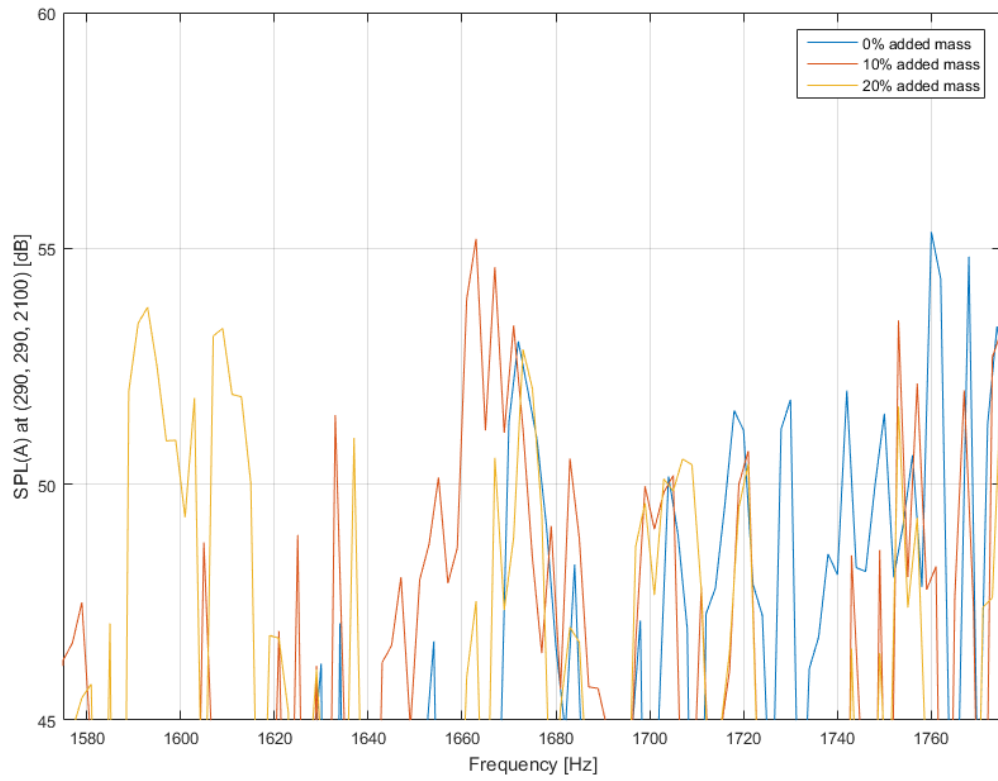
Figure 5.55: Generator SPL(A) at (290,290,2100) with added mass

# 6    Conclusion

The vibro-acoustic simulation is a fast and efficient tool to analyse the behaviour of the fluid-structure coupled system.  Changes can be quickly realised and investigated regarding different settings and solution methods.

The first verification example has indicated an accordance to the analytical solution, while the modified system has shown the similarity between the different absorbing boundary conditions. The influence of the boundary reflection could be impaired by the cavity's different construction; whereby a spherical hull is the fluid's optimal body for open domain problems. The use of PML could not be realised due to the strict setup, but is a possible alternative for further studies.

Detailed investigations were held on the cylindrical principle model, as it showed the influence of the system's eigenmodes regarding the radiation of sound into the acoustic domain. The applied constructive modifications resulted in a great improvement on the radiated sound pressure, if the influence of the added mass and added stiffness to the system was distinct, meaning a great shift in the frequency of the dominant peak for the added mass or a major damping effect on the displacement amplitude for the added stiffness. Varying the thickness in the regions of highest displacement at the part's outer shell, e.g by the addition of fitted patches, or adding point masses can support the reduction of the sound pressure without adding too much weight to the system. The use of a well-designed tuned mass damper can help to reduce the SPL for lower eigenfrequencies, but is counterproductive for higher modes. The detailed model of the power train confirmed the carried out improvements, as well as the use of the cylindrical model as a simplification of the power train. The recorded frequency response of the sound pressure clearly marks the sound emitting frequencies.

In the course of the upcoming research project X-Energy the presented model of the power train can be improved by creating the support of the power train within the wind turbine cabin. With the creation of the cabin's outer shell the influence of the power train's sound radiation for a point outside the cavity could be analysed. The implementation of the manufacturer's model of a power train could help to reduce the sound radiation in a more specific way, before enhancing and validating the model.

# 7 Literature

[1] A.J. Pretlove: Free Vibrations of a Rectangular Panel Backed by a Closed Rectangular Cavity. In: Journal of Sound and Vibration, S. 197–209

[2] 14.8. Mode-Superposition Method, ANSYS Inc., ANSYS 17.0 Help ANSYS Help System/Mechanical APDL/Theory Reference /14. Analysis Tools

[3] 8.3. Propagation, Radiation, and Scattering of Acoustic Pressure Waves, ANSYS Inc., ANSYS 17.0 Help ANSYS Help System/Mechanical APDL/Theory Reference /8.Acoustics

[4] 8.4. Acoustic Fluid-Structural Interaction (FSI), ANSYS Inc., ANSYS 17.0 Help ANSYS Help System/Mechanical APDL/Theory Reference /8.Acoustics

[5] ANSYS Mechanical APDL Acoustic Analysis Guide, ANSYS Inc., Theory Reference /Acoustic Analysis Guide

[6] AACTx_R170_L_01_Introduction to Acoustics, ANSYS Inc., Bestandteil der ANSYS ACT Acoustics Extension 2014

[7] AACTx_R170_L_03_Harmonic Analyses, ANSYS Inc., Bestandteil der ANSYS ACT Acoustics Extension 2014

[8] Baumann, B., Stein, U. u. Wolff, M.: Physik für Ingenieure. Bachelor Basics ; mit 21 Tabellen. Wilburgstetten: Schlembach 2011

[9] Beranek, L. L. (Hrsg.): Noise and vibration control engineering. Principles and applications. A Wiley Interscience publication. New York u.a.: Wiley 1992

[10] Franck, A.: Finite-Elemente-Methoden, Lösungsalgorithmen und Werkzeuge für die akustische Simulationstechnik. Techn. Hochsch., Diss.--Aachen, 2008. Aachener Beiträge zur technischen Akustik, Bd. 9. Berlin: Logos-Verl. 2009

[11] Frank Ihlenburg: Computational Methods for Vibroacoustic Simulations. Hamburg 2014

[12] Technische Schwingungslehre, Frank Ihlenburg, 2014

[13] Teilvorhabenbeschreibung Vibroakustik. Vibroakustische Optimierung der Haupttriebstrangkomponenten einer Windenergieanlage (VakuOm), Frank Ihlenburg u. Thomas Grätsch, 2016

[14] Howard, C. Q. u. Cazzolato, B. S.: Acoustic analyses using Matlab and Ansys. Boca Raton, Florida: CRC Press 2015

[15] Leissa, A. W.: Vibration of plates. Woodbury, NY: American Institute of Physics 1993

[16] Lerch, R., Sessler, G. u. Wolf, D.: Technische Akustik. Grundlagen und Anwendungen. Berlin, Heidelberg: Springer Berlin Heidelberg 2009

[17] M. Fischer u. L. Gaul: Fast BEM–FEM mortar coupling for acoustic–structure interaction. In: International Journal for Numerical Methods in Engineering, S. 1677–1690

[18] Möser, M.: Technische Akustik. VDI-Buch. Berlin, Heidelberg: Springer Vieweg 2015

[19] Möser, M. u. Kropp, W.: Körperschall. Physikalische Grundlagen und technische Anwendungen. Berlin, Heidelberg: Springer-Verlag Berlin Heidelberg 2010

[20] Ryan Bemrose: Louder Sounds Better, Microsoft Developer Blog 2007. https://blogs.msdn.microsoft.com/audiofool/2007/02/07/louder-sounds-better, abgerufen am: 20.08.2016

[21] Wagner, S., Bareiß, R. u. Guidati, G.: Wind Turbine Noise. Berlin, Heidelberg: Springer 1996

[22] Wikibooks.org: Acoustics/Fundamentals of Psychoacoustics, 2012. https://en.wikibooks.org/wiki/Acoustics/Fundamentals_of_Psychoacoustics, abgerufen am: 20.08.2016

# 8 Appendix

## 8.1 Guide to ACT Acoustics in ANSYS Workbench

This guide shows the main functions of the ACT Acoustics Extension and their set-up in the rectangular plate on cavity example examined in this work. The ACT Acoustics Extension is a free extension, which can be downloaded in the ANSYS Customer Portal. All the here presented content is implemented in ANSYS Mechanical APDL. A detailed guideline can be found in the help section of the program.

### 8.1.1 Installing the Extension



Figure 8.2: Installing the Extension
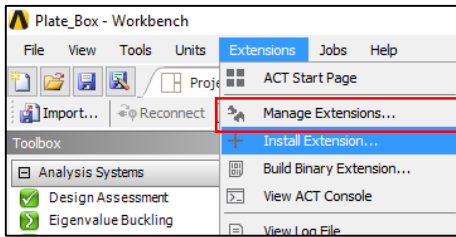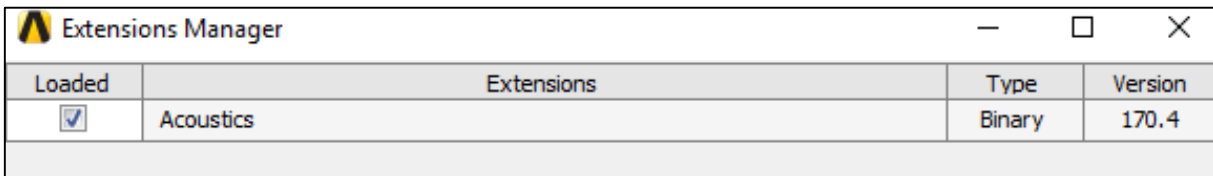
Once downloaded from the customer portal the extension can be easily installed by using Install Extension under Extensions. After the installation the extension can be found under Manage Extensions. The extension has to be picked manually at every new project.



Figure 8.1: Inside the Extensions Manager

### 8.1.2 Setting up the FSI Example

Considering the rectangular plate on cavity example the flexible plate is attached to the left of the rectangular cavity. Both have structural steel assigned as material. As this cannot be true for the acoustic fluid an Acoustic Body has to be applied to the cavity, which overwrites the pre-assigned properties to acoustic relevant properties.
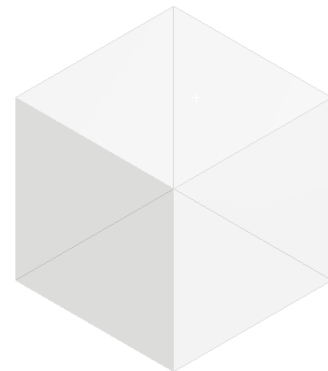


Figure 8.3: Rectangular Plate on Cavity Example



Figure 8.4: Selecting the Acoustic Body

| Details of "Acoustic Body" | |
|---|---|
| **Scope** | |
| Scoping Method | Named Selection |
| Named Selection | Cavity_Body |
| **Definition** | |
| Behavior | Compressible |
| Frequency Dependency | No |
| Mass Density | 1.2041E-09 [kg mm^-1 mm^-1 mm^-1] |
| Sound Speed | 343240 [mm sec^-1] |
| Dynamic Viscosity | 0 [MPa sec] |
| Bulk Viscosity | 0 [MPa sec] |
| Thermal Conductivity | 0 [W mm^-1 C^-1] |
| Specific Heat Cp | 0 [J kg^-1 C^-1] |
| Specific Heat Cv | 0 [J kg^-1 C^-1] |
| Reference Pressure | 2E-11 [MPa] |
| Reference Static Pressure | 0.101325 [MPa] |
| Acoustic-Structural Coupled Body Options | Program Controlled Uncoupled |
| | Program Controlled Uncoupled |
| | Program Controlled Coupled |
| | Uncoupled With Symmetric Algorithm |
| | Coupled With Symmetric Algorithm |

Figure 8.5: Details of the Acoustic Body

The scope of the acoustic domain can be selected by direct geometric selection or a prepared named selection. The main properties of the acoustic fluid can be defined in the Acoustic Body. The most important of this settings are already pre-defined by the acoustic fluid air. The reference pressure values are important for the further researches (e.g. for the evaluation of the SPL) and should better not be changed, if there is no need for it. Under Acoustic-Structural Coupled Body Options the symmetric and unsymmetric matrix formulation can be chosen VERWEIS AUF FLUID-STRUCTURE-INTERACTION. In case of a FSI problem it is very important to use either Program Controlled Coupled or Coupled With Symmetric Algorithm for the fluid element layer on the FSI Interface.
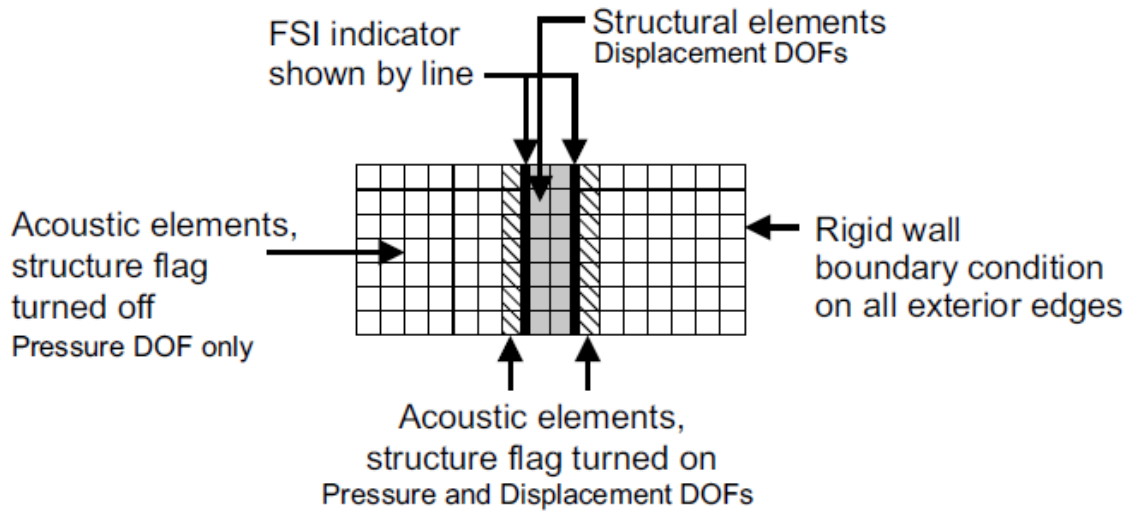


Figure 8.6: Setting of the FSI [14]

As coupled associated elements uses four DOF per knot it is recommended to use another fluid body with the uncoupled tag right behind it, to minimize the computational times with just one DOF per element knot (s. chapter 3.3). The coupling between the two domains is therefore implemented at the first layer of the acoustic domain. As long as not indicated by an additional boundary condition the two acoustical bodies are regarded as one acoustic domain.
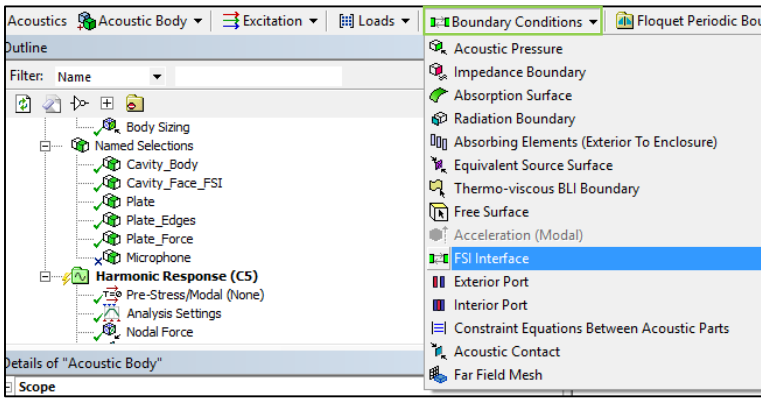
Figure 8.7: Selecting the FSI Interface

Setting the FSI Interface is important for non-solid structures, such as shell structures, which are in contact with the acoustic fluid. The FSI Interface for solid structures is set up automatically.

The related faces are the ones of the Acoustic body and not the faces of the structure! They can be picked manually, which can be difficult for some inner faces, by using the FSI Interface under Boundary Conditions or automatically by using the Automatically Create FSI Condition According to Contacts Tool under Tools in the Acoustics Tool Bar.
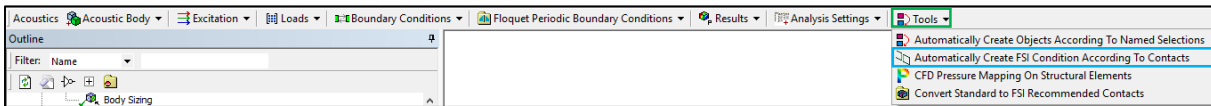


Figure 8.8: Picking the FSI Interface Tool
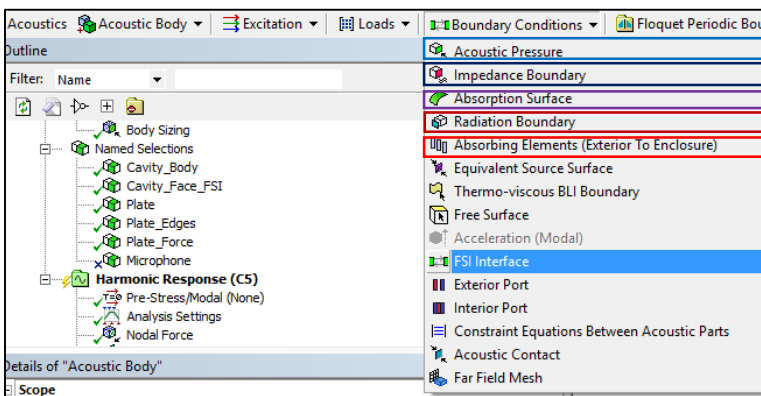


Figure 8.9: Selecting the Boundary Conditions

Without applying a boundary condition to the outer faces of the model the Neumann Boundary Condition (sound-hard boundary) is automatically set up to the system. As its sound reflecting behaviour is often unwanted absorbing boundary conditions, such as the Robin Boundary (Impedance Boundary and Radiation Boundary) can be selected from the Acoustics Tool Bar under Boundary Conditions. If an absorption coefficient is known the Absorption Surface can be used.

While the Robin boundary conditions can be used on every surface the Absorbing Elements (2.2.4) (s. Figure 4.9) can only be used on a sphere. It is important to specify the origin and radius of the sphere as well as forcing the elements to lie on this sphere, if not an error message will occur.



Figure 8.10: Setting up the Absorbing Elements

Figure 8.11: Analysis Settings of a Hamonic Analysis

In the analysis settings of the harmonic analysis the solution settings have to be defined. The requested frequency range can be inserted by a linear scale, logarithmic scale and in octave bands. The solution interval defines the steps within the frequency span.

The solution method can be chosen between the direct method and modal superposition. The use of Variational technology, meaning a mixture of both solution methods, is not recommended.

Some results need the General Miscellaneous and the Ansys MAPDL DB to be activated for their post-processing.

Modal damping can be applied by inserting a constant damping ratio $D$ or using Rayleigh Damping by setting the stiffness $\beta$ and/or mass coefficient $\alpha$.
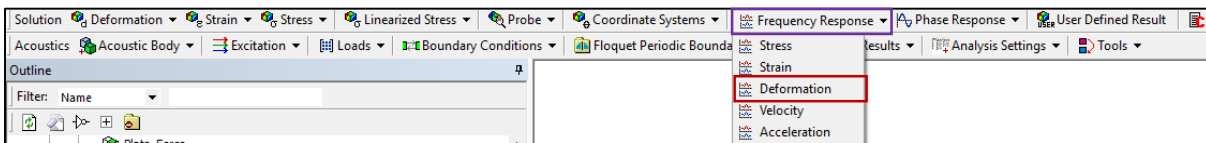


Figure 8.12: Selecting the frequency response for the deformation of the structure



Figure 8.13: Setting up the frequency response

As result the frequency response of displacement at the driving point and the acoustic response of a point in the cavity are of interest.

Therefore, the Frequency Response of the Deformation is used from the Solution Toolbar. We are interested in the deformation in the y-direction. The y-axis of the chart is logarithmic to clearly show the peaks of the response.
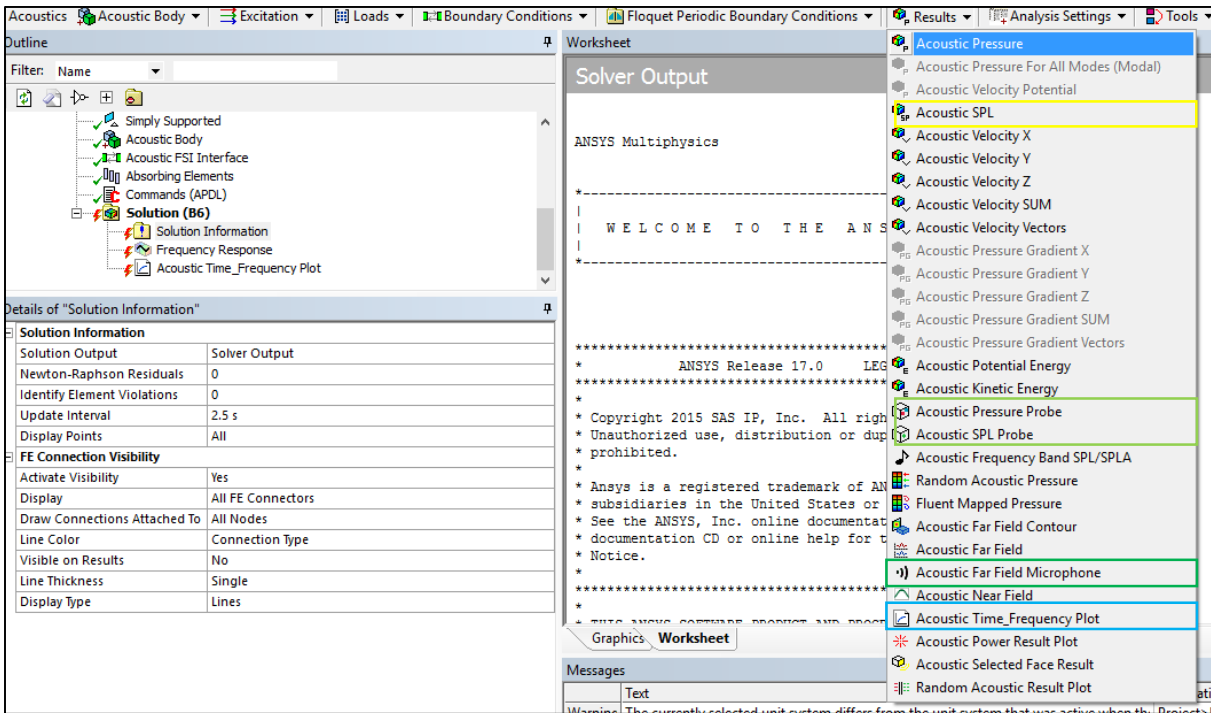
Figure 8.14: Results for Harmonic Analysis of the ACT Acoustic Extension

In the acoustic domain we are interested in the results in the far field, especially a point somewhere in the acoustic domain, which is not close to the acoustic source. When measuring the SPL at a point in the acoustic domain microphones are being used. In a similar way the far field microphone provides the possibility to enter a point by Spherical or Cartesian coordinates and evaluate the acoustic pressure, SPL or acoustic power at this point within the requested frequency range.



Figure 8.15: Far Field Microphone

As the FEA evaluates the acoustic pressure at every knot and not in-between, the program automatically searches the nearest knot.

The far field microphone is regrettably error-prone and is sometimes not working at all, e.g. after an unexpected error during the post-processing. The Acoustic-Time-Frequency-Plot offers the same bandwidth of results, but need a knot to be specified before, e.g. predefined in the worksheet of a named selection.



Figure 8.16: Point defined in the worksheet of a named selection

| Details of "Acoustic Pressure" | |
|---|---|
| **Scope** | |
| Scoping Method | Geometry Selection |
| Geometry | All Bodies |
| Sub Scope By | Layer |
| Layer | Entire Section |
| Position | Top/Bottom |
| **Definition** | |
| Type | User Defined Result |
| Expression | = PRES |
| Input Unit System | Metric (mm, kg, N, s, mV, mA) |
| Output Unit | Pressure |
| By | Frequency |
| ☐ Frequency | Last |
| Sweeping Phase | 0. ° |
| Coordinate System | Global Coordinate System |
| Identifier | |
| Suppressed | No |
| **Integration Point Results** | |
| Display Option | Averaged |
| Average Across Bodies | No |

Figure 8.17: Settings of Acoustic Pressure

Apart from the frequency responses we can look at the acoustic pressure, SPL and displacement at specific frequencies. The acoustic probe tools can deliver us the value of a knot at a specific frequency.

The frequency can be inserted directly and the nearest solution set will be displayed. We can also insert a solution set instead of a frequency. The advantage of this method is that we actually know the frequency it represents.

### 8.1.3    Setting the Mode-Superposition Method

The mode superposition method can be set as the solution method of a FSI problem, if absorbing boundary conditions are not required and other damping methods, apart from modal damping, are not considered.

| Details of "Analysis Settings" | |
|---|---|
| **Options** | |
| Frequency Spacing | Linear |
| ☐ Range Minimum | 0. Hz |
| ☐ Range Maximum | 250. Hz |
| ☐ Solution Intervals | 250 |
| User Defined Frequencies | Off |
| Solution Method | Mode Superposition |
| Include Residual Vector | No |
| Cluster Results | No |
| Modal Frequency Range | Program Controlled |
| Store Results At All Frequencies | Yes |

Figure 8.18: Analysis Settings for Mode-Superposition

The mode superposition method is set in the analysis settings under solution method. The modal frequency range, along with the number of modes to find, can remain program controlled or set manually. Residual vectors can enhance the solution of the mode-superposition, but are not supported by the unsymmetric eigensolver and therefore cannot be used during modal-superposition of a system with FSI coupling in ANSYS.

| Details of "Acoustic Body" | |
|---|---|
| **Scope** | |
| Scoping Method | Geometry Selection |
| Geometry | 1 Body |
| **Definition** | |
| Behavior | Compressible |
| Frequency Dependency | No |
| ☐ Mass Density | 1.2041E-09 [kg mm^-1 mm^-1 mm^-1] |
| ☐ Sound Speed | 343240 [mm sec^-1] |
| ☐ Dynamic Viscosity | 0 [MPa sec] |
| ☐ Bulk Viscosity | 0 [MPa sec] |
| ☐ Thermal Conductivity | 0 [W mm^-1 C^-1] |
| ☐ Specific Heat Cp | 0 [J kg^-1 C^-1] |
| ☐ Specific Heat Cv | 0 [J kg^-1 C^-1] |
| ☐ Reference Pressure | 2E-11 [MPa] |
| ☐ Reference Static Pressure | 0.101325 [MPa] |
| Acoustic-Structural Coupled Body Options | Program Controlled Coupled |

Figure 8.19: Setting of the Acoustic Body for Mode-Superposition

As only the unsymmetric MAPDL solver can be used within the mode-superposition method, the Acoustic-Structural Coupled Body Options has to be changed to Program Controlled Coupled within the acoustic body details.

| Results ▼ | Analysis Settings ▼ | Tools ▼ |
|---|---|---|
| | ⚛ Scattering Controls | |
| | ⚒ Linear Perturbation Process | |
| | ⚛ Unsymmetric Harmonic Mode Superposition | |
| | ⚛ Unsymmetric Mode Extraction For Downstream MSUP Harmonic Analysis | |
| | ⚛ Unsymmetric Mode Extraction For Downstream Spectrum Analysis | |
| | ● FSI Spectrum Analysis | |
| | ⊞ One Way Coupling Analysis (ASI File) | |
| | ⬚ Scale FSI Matrices for Modal | |
| | ⊟ Local Output Controls | |

Figure 8.20: Unsymmetric Harmonic Mode Superposition

At last the Unsymmetric Harmonic Mode Superposition has to be selected from the Analysis Settings of the Acoustics Toolbar in case of the bi-directional coupling between the fluid and the structure.

Without this setting or an equivalent MAPDL command the solver is not set properly and will create an error message while the evaluation of the mode-superposition.

## 8.2     ANSYS Mechanical ADPL Scripts

The use of the Ansys Workbench is a quite comfortable way of solving a problem using ANSYS, but in case of the acoustic analysis it requires an additional extension. Another way to solve an acoustic problem is the use of mechanical ADPL, often referred as Classic ANSYS. It offers all the possibilities of the program; of which many are not implemented into the workbench.

The interface is obsolescent and it is quite complicated to build and analyse the model using the available tools. Therefore, it is more efficient to write a script using the mechanical ADPL language and read it into the program.

With the use of MAPDL the two main examples are been created parallel to their counterparts in ANSYS Workbench. Because of the more user friendly interface regarding changes of the model the Workbench gained priority.

### 8.2.1     MAPDL Rectangular Plate on Rectangular Cavity

```
FINISH
/CLEAR

! Pre-Processing

/PREP7

! Material properties of fluid in cavity

speedair  = 344                          ! Speed of Sound of air [m/s]
dens_air  = 1.21                         ! Density of Air [kg/m^3]

! Material properties of flexible plate

platedens        = 7900                  ! Density [kg/m^3]
plate_E  = 210e9                         ! Youngs modulus [Pa]
plate_mu         = 0.32                  ! Poissons Ratio [-]

! Dimensions of the cavity

box_x = 1                                ! Length [m]
box_y = 1                                ! Width [m]
box_z = 1                                ! Height [m]

! Thickness of the plate.

plate_t = 0.01                           ! Thickness [m]
```

```
! Defining the Fluid Element (with FSI)

ET,1,FLUID30,,1                         ! Element type Fluid 30 with 4 DOF
MP,SONC,1,speedair                      ! Material Property Speed of Sound
MP,DENS,1,dens_air                      ! Material Property Density
MP,MU,1,0.00                            ! Material Property Damping
R,1,20e-6                               ! Real Constant for Reference pressure
                                        ! 20uPa
! Defining the Fluid Element (without FSI)

ET,2,FLUID30,,0                         ! Element Type Fluid 30 with 1 DOF
MP,SONC,2,speedair
MP,DENS,2,dens_air
MP,MU,2,0.00
R,2,20e-6


! Defining the Shell Element for the structure


R,3,plate_t                            ! Defining Plate Thickness as Real
                                        ! Constant


ET,3,SHELL181                          ! Element Type Shell 181
SECTYPE,,SHELL
SECDATA,plate_t,
MP,EX,3,plate_E                        ! Material Property Young's Module
MP,DENS,3,platedens                    ! Material Property Density
MP,NUXY,3,plate_mu                     ! Material Property Poisson's Ratio


! Create the acoustic cavity

BLOCK,0,box_x,0,box_y,0,-box_z

! Meshing

ESIZE,0.05                             ! Set element size

TYPE,1
REAL,1
MAT,1
VMESH,ALL                              ! Volume Meshing

NSEL,S,LOC,Z,0                         ! Selecting the Face for Plate
TYPE,3
REAL,3
MAT,3
ESURF,ALL


ESEL,S,TYPE,,3                         ! Change all the elements touching the
                                        ! plate to FSI

NELEM
ENODE
ESEL,R,TYPE,,1
TYPE,2
REAL,2
MAT,2
EMODIF,ALL
SF,ALL,FSI,1
```

```
ESEL,S,TYPE,,2                                  ! Constrain the Displacement DOF for the
                                                ! other fluid elements
NELEM
NSEL,U,LOC,Z,0
D,ALL,UX
D,ALL,UY
D,ALL,UZ

! Setting the Simply Supported Boundary at the Edges of the plate

ESEL,S,TYPE,,3
NSLE,S,1
NSEL,R,EXT
D,ALL,UZ
NSEL,S,LOC,Z,0
NSEL,R,LOC,X,0
D,ALL,UX
NSEL,S,LOC,Z,0
NSEL,R,LOC,Y,0
D,ALL,UY

ALLSEL
EPLOT

! Apply force to the plate

f_node=NODE(0.20000,0.3000,0.0)
F,f_node,FZ,1

! Solution

/SOLU
ANTYPE,3
HROPT,FULL                                      ! Direct Solution
HROUT,ON
LUMPM,0                                         ! Lumped Matrix Off
EQSLV,FRONT,1e-006,                             ! Specifying the Solver
PSTRES,0
HARFRQ,1,250,                                   ! Requested Frequency Range
NSUBST,249,                                     ! Number of Substeps
KBC,1                                           ! Load Step is Stepped
SAVE
SOLVE
SAVE

! Post-Processing

/POST26
LINES,100000

FILE,'file','rst','.'
PRCPLX,1
/gropt,logy,1

! Retrieve the displacement at the drive point on the plate

NSOL,2,f_node,UZ
```

```
! Retrieve the pressure at a point inside the cavity

p_node=NODE(0.2,0.3,-0.5)
NSOL,3,p_node,PRES

! Plot the drive point displacement

/AXLAB,X,Frequency [Hz]
/AXLAB,Y,Displacement [m]

PLVAR,2

! Export the drive point displacement

/OUTPUT,d_node,txt
PRVAR,2
/OUTPUT

! Export the pressure inside the cavity

/OUTPUT,p_node,txt
PRVAR,3
/OUTPUT
```

## 8.2.2 MAPDL Cylinder in Air

```
FINISH
/clear
/batch
/title, Acoustic Analysis of a thin walled zylinder
/nopr

! Pre-Processing

/prep7                                  ! Model creation preprocessor

E = 0.25                                ! Enclosure Thickness [m]

R1 = 0.25                               ! Radius Cylinder [m]
R2 = R1 + E                             ! Radius Fluid Enclosure [m]

L1 = 2                                  ! Length Cylinder [m]
L2 = L1+2*E                             ! Length Fluid Enclosure [m]

! Building the model

CYLIND,0,R1,-L1/2,L1/2,0,180            ! CYLIND, RAD1, RAD2, Z1, Z2, THETA1, THETA2
CYLIND,0,R2,-L2/2,L2/2,0,180           ! Creating upper half of the body

VSBV,2,1,,DELETE,DELETE                ! New body get volume number 3, so volume number
                                        ! 1 and 2 are free again

AROTAT,2,7,5, , , ,1,6,360,4 ,         ! Creating surface for the cylinder

CYLIND,0,R1,-L1/2,L1/2,-180,0          ! Creating lower half of the body
BLOCK,-R2,R2,-R2,,-L2/2,L2/2           ! BLOCK, X1, X2, Y1, Y2, Z1, Z2

VSBV,2,1,,DELETE,DELETE                ! New body get volume number 5, so volume number
                                        ! 4 and 2 are free again

VADD,3,4                                ! Boolean addition for fluid body

Lambda1 = 0.172                         ! Wave length Air [m]
Lambda2 = 1.686                         ! Wave length Solid [m]

! Setting the Element Size

N1 = 6                                  ! Air Elements per Wave length
N2 = 30                                 ! Sturcture Elements per Wave length

H1 = Lambda1/N1                         ! Element Size Air
H2 = Lambda2/N2                         ! Element Size Structure

! Material properties of fluid in cavity

speedair  = 344                         ! Speed of Sound of air [m/s]
dens_air  = 1.21                        ! Density of Air [kg/m^3]
```

```
! Material properties of cylinder

Cylinderdens = 7900                    ! Density [kg/m^3]
cylinder_E       = 210e9               ! Youngs modulus [Pa]
cylinder_mu      = 0.32                ! Poissons Ratio [-]



! Thickness of the clyinder.

cylinder_t = 0.01                      ! Thickness [m]

! Defining the Fluid Element (with FSI)

ET,1,FLUID221,,1                       ! Element type Fluid 221 with 4 DOF
MP,SONC,1,speedair                     ! Material Property Speed of Sound
MP,DENS,1,dens_air                     ! Material Property Density
MP,MU,1,0.002                          ! Material Property Damping
R,1,20e-6                              ! Real Constant for Reference pressure
                                       ! 20uPa


! Defining the Fluid Element (without FSI)

ET,2,FLUID221,,0                       ! Element Type Fluid 221 with 1 DOF
MP,SONC,2,speedair
MP,DENS,2,dens_air
MP,MU,2,0.002
R,2,20e-6


! Defining the Shell Element for the structure

R,3,cylinder_t                        ! Defining Plate Thickness as Real
                                       ! Constant

ET,3,SHELL181                         ! Element Type Shell 181
SECTYPE,,SHELL
SECDATA,cylinder_t,
MP,EX,3,cylinder_E                    ! Material Property Young's Module [Pa]
MP,DENS,3,cylinderdens                ! Material Property Density [kg/m^3]
MP,NUXY,3,cylinder_mu                 ! Material Property Poisson's Ratio [-]
MP,MU,1,0.002                         ! Material Property Damping

! Meshing

TYPE,1                                ! Meshing Fluid with FLUID221 Elements, as Fluid30
                                       ! Elements causes an Error

MAT,1
VSEL,S,,,1
ESIZE,H1
VMESH, ALL
NSEL,S,LOC,Z,-L1/2,L1/2              ! Applying the FSI
CSYS,1
NSEL,R,LOC,X,0,R1
SF,ALL,FSI
CSYS,0
ALLSEL, ALL
NSEL,S,EXT
SF,ALL,INF                           ! Radiation Boundary
```

A-13

```
ALLSEL, ALL

TYPE,3                              ! Meshing Solid
MAT,3
FLST,5,12,5,ORDE,12                 ! List the areas to mesh
FITEM,5,4
FITEM,5,5
FITEM,5,9
FITEM,5,10
FITEM,5,13
FITEM,5,14
FITEM,5,15
FITEM,5,16
FITEM,5,17
FITEM,5,18
FITEM,5,19
FITEM,5,20
ASEL,S,,,P51X                       ! Selecting the listet areas
ESIZE,H2
AMESH,ALL
ALLSEL,ALL
f_node=NODE(R1,0,L1/2)
F,f_node,FX,1

FINISH

! Solution

/SOLU
ANTYPE,3
HROPT,FULL                          ! Direct Solution
HROUT,ON
LUMPM,0                             ! Lumped Matrix Off
EQSLV,FRONT,1e-006,                 ! Specifying the Solver
PSTRES,0
HARFRQ,100,2000,                    ! Requested Frequency Range
NSUBST,9,                           ! Number of Substeps
KBC,1                              ! Load Step is Stepped
SAVE
SOLVE
SAVE

! Post-Processing

/POST26
LINES,100000

FILE,'file','rst','.'
PRCPLX,1
/gropt,logy,1

! Retrieve the displacement at the drive point on the plate

NSOL,2,f_node,UX
```

```
! Retrieve the pressure at a point inside the cavity

p_node=NODE(0.3,0,-0.3)
NSOL,3,p_node,PRES

! Plot the drive point displacement

/AXLAB,X,Frequency [Hz]
/AXLAB,Y,Displacement [m]

PLVAR,2

! Export the drive point displacement

/OUTPUT,d_node,txt
PRVAR,2
/OUTPUT

! Export the pressure inside the cavity

/OUTPUT,p_node,txt
PRVAR,3
/OUTPUT
```

## 8.3    Matlab Rectangular Plate on Rectangular Cavity (after Howard [14])

```
clc
clear all

% Dimensions of the cavity

cavity.len_x = 1;   % [m]
cavity.len_y = 1;   % [m]
cavity.len_z = 1;   % [m]

cavity.volume = cavity.len_x .* cavity.len_y .* cavity.len_z;   % [m^3]

% Parameters of the fluid

fluid.density   = 1000;     % [kg/m^3] density of the gas
fluid.speed     = 1481;     % [m/s] speed of sound of the gas

% Dimensions of the plate

plate.len_x = cavity.len_x;         % [m]
plate.len_y = cavity.len_y;         % [m]
plate.thick = 0.01;                 % [m]

surfacearea = plate.len_x .* plate.len_y;

% Material properties of Steel

plate.density   = 7900;     % [kg/m^3] density
plate.E         = 2.1e11;   % [Pa] Youngs modulus
plate.mu        = 0.3;      % [no units] Poissons Ratio

% Define location of acoustic source

speaker.loc_x=0.1;
speaker.loc_y=0.1;
speaker.loc_z=0.1;
speaker.vol_velocity=0;

% Define the location of the microphone

mic.loc_x=0.2;
mic.loc_y=0.3;
mic.loc_z=0.5;

% Define the point load on the plate

force.loc_x  = 0.2;
force.loc_y  = 0.3;
force.amp    = 1;      % amplitude of the force
```

```matlab
% Define location of accelerometer

accel.loc_x = force.loc_x;
accel.loc_y = force.loc_y;

% Define the number of structural and acoustic modes to use

nstrmodes  =  100;    % number of structural modes to use
ncavmodes  =  200;    % number of acoustic modes to use

% Define the analysis frequency range

freq_vect = [1:250];                % [Hz]
end_freq = freq_vect(length(freq_vect));

% Calculate the resonance frequencies of the cavity

n_max = 50;

fprintf('===Start calculation of the resonance frequencies of the cavity\n');

mode_index=[];
for ii=0:n_max
   for jj = 0:n_max
     for kk = 0:n_max
        mode_index = [ mode_index ; ii jj kk ];
     end;
   end;
end;

% Calculate the resonance frequencies of the cavity

res_freq = sqrt(   (mode_index(:,1) / cavity.len_x).^2 +   ...
           (mode_index(:,2) / cavity.len_y).^2 +   ...
           (mode_index(:,3) / cavity.len_z).^2 );

res_freq = res_freq .* fluid.speed ./ 2;   % [Hz]

% sort the resonance frequencies

temp=sortrows([res_freq mode_index],1);
res_freq = temp(:,1);
mode_index = temp(:,2:4);

% Use only first 1:ncavmodes

cavity.res_freq = res_freq(1:ncavmodes);
cavity.mode_index = mode_index(1:ncavmodes,:);
```

```matlab
% Calculate the modal volume

epsilon_modal_volume = zeros(size(cavity.mode_index));
index2change = find(cavity.mode_index(:,1)==0);
epsilon_modal_volume(index2change,1) = 1;
index2change = find(cavity.mode_index(:,1)>0);
epsilon_modal_volume(index2change,1) = 0.5;
index2change = find(cavity.mode_index(:,2)==0);
epsilon_modal_volume(index2change,2) = 1;
index2change = find(cavity.mode_index(:,2)>0);
epsilon_modal_volume(index2change,2) = 0.5;
index2change = find(cavity.mode_index(:,3)==0);
epsilon_modal_volume(index2change,3) = 1;
index2change = find(cavity.mode_index(:,3)>0);
epsilon_modal_volume(index2change,3) = 0.5;

cavity.modalvolume = cavity.volume        ...
       .* epsilon_modal_volume(:,1)   ...
       .* epsilon_modal_volume(:,2)   ...
       .* epsilon_modal_volume(:,3);

% Evaluate the mode shapes at the microphone locations

cavity.phi_eval = ...
   cos(cavity.mode_index(:,1)*pi*mic.loc_x.'/cavity.len_x) .*   ...
   cos(cavity.mode_index(:,2)*pi*mic.loc_y.'/cavity.len_y) .*   ...
   cos(cavity.mode_index(:,3)*pi*mic.loc_z.'/cavity.len_z);

% Evaluate the mode shapes at the acoustic source location

speaker.phi_eval = ...
   cos(cavity.mode_index(:,1)*pi*speaker.loc_x.'/cavity.len_x) .*   ...
   cos(cavity.mode_index(:,2)*pi*speaker.loc_y.'/cavity.len_y) .*   ...
   cos(cavity.mode_index(:,3)*pi*speaker.loc_z.'/cavity.len_z);

fprintf('===End of calculation of the resonance frequencies of the cavity \n');

% Calculate the resonance frequencies of the plate

n_max = 50;

fprintf('===Start calculation of the resonance frequencies of the plate\n');

str_mode_index=[];
for ii=1:n_max
  for jj = 1:n_max
      str_mode_index = [ str_mode_index ; ii jj ];
  end;
end;
```

```matlab
% Calculate the resonance frequencies of the plate

D = plate.E .* plate.thick.^3 ./ (12.*(1 - plate.mu.^2));

res_freq =  1./(2.*pi) .*  ...
        sqrt(D ./ plate.density ./ plate.thick ) .*  ...
        (  (str_mode_index(:,1).*pi ./ plate.len_x).^2 +  ...
           (str_mode_index(:,2).*pi ./ plate.len_y).^2  );

% sort the resonance frequencies

temp=sortrows([res_freq str_mode_index],1);
res_freq = temp(:,1);
str_mode_index = temp(:,2:3);

% use only first 1:nstrmodes

plate.res_freq = res_freq(1:nstrmodes);
plate.mode_index = str_mode_index(1:nstrmodes,:);

% Calculate the modal mass of the plate
plate.modalmass =   plate.density       ...
            .* plate.thick     ...
            .* plate.len_x     ...
            .* plate.len_y     ...
            ./ 4 * ones(1,nstrmodes);

% Calculate the force load vector in terms of modal participation

force_modal = - force.amp .*  ...
    sin(plate.mode_index(:,1).*pi.*force.loc_x ./ plate.len_x) .*  ...
    sin(plate.mode_index(:,2).*pi.*force.loc_y ./ plate.len_y);

% Calculate speaker acoustic load vector in terms of modal participation

Q_speaker =    speaker.vol_velocity      ...
            * speaker.phi_eval;

% Calculate the mode shapes at the accelerometer locations

plate.psi_eval =   ...
        sin(plate.mode_index(:,1)*pi*accel.loc_x.'/ plate.len_x) .* ...
        sin(plate.mode_index(:,2)*pi*accel.loc_y.'/ plate.len_y);

fprintf('===End of calculation of the resonance frequencies of the plate\n');

% Calculate the coupling coefficients matrix (Bij)

C_nm = zeros(ncavmodes,nstrmodes);
for nn_cav=1:ncavmodes
  for mm_plate=1:nstrmodes
```

```matlab
% This was the equation from the paper in Bokil,

    if (   ...
       (cavity.mode_index(nn_cav,1)~=plate.mode_index(mm_plate,1)) &   ...
       (cavity.mode_index(nn_cav,2)~=plate.mode_index(mm_plate,2)) ),   ...

% For the system under investigation here, the flexible plate is mounted at $z=0$.

        C_nm(nn_cav,mm_plate) =                   ...
            (1./pi.^2)   ...
            * (                   ...
              plate.mode_index(mm_plate,1)   ...
              .* plate.mode_index(mm_plate,2)   ...
              )          ...
            .*( (-1).^(cavity.mode_index(nn_cav,1) + plate.mode_index(mm_plate,1) ) -1 ) ...
            .*( (-1).^(cavity.mode_index(nn_cav,2) + plate.mode_index(mm_plate,2) ) -1 ) ...
            ./ (   ...
               (cavity.mode_index(nn_cav,1).^2 - plate.mode_index(mm_plate,1).^2)   ...
              .*(cavity.mode_index(nn_cav,2).^2 - plate.mode_index(mm_plate,2).^2) ...
              );
    end;
  end;
end;

% Pre-calculate some matrices before entering the frequency loop.

C_11_temp  = diag((plate.res_freq*2*pi).^2 .* plate.modalmass.');
C_12       = surfacearea*C_nm.';
C_21_temp  = surfacearea*C_nm;
C_22_temp1 = diag(cavity.modalvolume        ...
         .* (2*pi*cavity.res_freq).^2   ...
         / (fluid.density*fluid.speed.^2));
C_22_temp2 = diag(cavity.modalvolume        ...
         / (fluid.density*fluid.speed.^2));

% Execute the big frequency loop

for ii=1:length(freq_vect),

  omega = 2*pi*freq_vect(ii);

  load_vec = [              ...
        force_modal;          ...
        Q_speaker*(1j*omega)  ...
      ];

  LHS    = [  C_11_temp-diag(plate.modalmass.')*(omega.^2) C_12  ; ...
         (omega.^2)*C_21_temp                   C_22_temp1-omega.^2*C_22_temp2  ];

  small_q(:,ii) = inv(LHS)*load_vec;
end;

disp('End of calculations')
```

```matlab
% Separate the modal participation factors

struct_q = small_q(1:nstrmodes,:);
acoust_q = small_q(nstrmodes+1:nstrmodes+ncavmodes,:);

% Calculate some acoustic and structural results

sq_struct_q=struct_q.^2;
sq_acoust_q=acoust_q.^2;

sum_sq_struct_q=sum(sq_struct_q);
sum_sq_acoust_q=sum(sq_acoust_q);

matlab_ape=1/(4*fluid.density*fluid.speed^2)*cavity.modalvolume.'*abs(acoust_q.^2);
matlab_pressure = cavity.phi_eval.' * acoust_q;
matlab_sq_p= matlab_pressure.^2;

matlab_displacement = plate.psi_eval.' * struct_q;

% Plot the acoustic presure at the microphone

figure
set(gca,'fontsize',16);
p1h=semilogy(freq_vect,abs(matlab_pressure));
set(p1h,'linewidth',2);
xlabel('Frequency [Hz]');
ylabel('Pressure [Pa]');
title('Acoustic Pressure at a Point in the Cavity');
grid

% Plot the displacement at the accelerometer

figure
set(gca,'fontsize',16);
p2h=semilogy(freq_vect,abs(matlab_displacement));
set(p2h,'linewidth',2);
xlabel('Frequency [Hz]');
ylabel('Displacement [m]');
title('Plate Displacement at Drive Point');
grid
```